Comparative Bacterial Genomics and Fish Vaccinology: Genomic and Phenotypic Analysis of *Vibrio anguillarum* Isolated from Lumpfish (*Cyclopterus lumpus*) and Vaccine Evaluation in Sablefish (*Anoplopoma fimbria*) Against *Aeromonas salmonicida*

by

© Jose Vasquez Solis de Ovando

A thesis submitted to the

School of Graduate Studies

in partial fulfillment of the requirements for the degree of

Master of Science

Aquaculture

Faculty of Science

Memorial University of Newfoundland

2020

St. John's, Newfoundland & Labrador, Canada

ABSTRACT

Although aquaculture is the fastest growing food-producing industry in the world, it is negatively impacted by parasites and infectious diseases. Bacterial infections are the most important diseases of emergent Canadian aquaculture species such as lumpfish (*Cyclopterus lumpus*) and sablefish (*Anoplopoma fimbria*). *Aeromonas salmonicida* and *Vibrio anguillarum*, both Gram-negative pathogens, are the most prevalent infectious diseases agents affecting lumpfish aquaculture in the North Atlantic, meanwhile *A. salmonicida* is the most common pathogen in the sablefish aquaculture industry in the Pacific coast. Comparative genomic analysis of *V. anguillarum* and *A. salmonicida* isolates from lumpfish and sablefish outbreaks, respectively, can provide insights into bacterial evolution and virulence, and contribute to effective vaccine design programs. Currently, there are no commercial vaccines available specifically for lumpfish against *V. anguillarum*, and for sablefish against *A. salmonicida*. Therefore, the objectives of this study were to: ***i***) analyze the genome and phenotype of *V. anguillarum* strain J360 isolated from infected lumpfish (**Chapter 2**); and ***ii***) develop an infection model for atypical *A. salmonicida* strain J410 in sablefish to evaluate commercial vaccines and an autogenous vaccine (**Chapter 3**).

GENERAL SUMMARY

The global human population, and its demand for food, is growing. Aquaculture is one of the fastest growing food production sectors and could help to meet this demand. However, the aquaculture industry faces a number of challenges, including climate change, predators, and infectious diseases (including parasites, bacteria, and viruses). This research focuses on bacterial pathogens of two Canadian aquaculture species. The lumpfish (*Cyclopterus lumpus*), which is used as "cleaner fish" for sea lice biocontrol in the Atlantic salmon industry in the North Atlantic region, and sablefish (*Anoplopoma fimbria*) known as "black cod", which is an emerging aquaculture species in British Columbia and other Pacific coastal areas. *Vibrio anguillarum* and *Aeromonas salmonicida* are the causative agents of vibriosis and furunculosis in lumpfish, and the latter pathogen is the biggest disease issue in sablefish. In this study the genome and the phenotype of *V. anguillarum* strain J360 isolated from an outbreak in lumpfish was analyzed (**Chapter 2**); and an infection model for atypical *A. salmonicida* strain J410 was developed in sablefish to evaluate commercial vaccines and an autogenous vaccine (**Chapter 3**).

ACKNOWLEDGEMENTS

I would like to thank my supervisor, Dr. Javier Santander for his time, patience, dedication, and for supporting my professional and personal goals. I would also like to thank the Marine Microbial Pathogenesis and Vaccinology Lab members for their support during my research, Dr. Jillian Westcott for her guidance, patience, and her willingness to help me as a co-supervisor, as well as the members of my M.Sc. supervisory committee, Drs. Kurt Gamperl and Matthew Rise. Finally, I would like to thank Mr. Danny Boyce and the staff of the Dr. Joe Brown Aquatic Research Building, as well as the staff of the Cold-Ocean Deep-Sea Research Facility, for their technical support. This research was supported through modules J.3. and J.5.1. of the Ocean Frontiers Institute (a grant funded through the Canada First Excellence Research Fund program), and though Dr. J. Santander's NSERC Discovery grant.

TABLE OF CONTENTS

ABSTRACT…….....i

GENERAL SUMMARY……ii

ACKNOWLEDGEMENTS…….iii

LIST OF TABLES…….....x

LIST OF FIGURES……...xi

LIST OF ABBREVIATIONS……..……xii

LIST OF APPENDICES……xiii

CO-AUTHORSHIP STATEMENT……...xiv

CHAPTER 1: General Introduction…….1

1.1 Introduction…...…….……...…….....1

1.2 The Canadian Aquaculture Industry……..……...……...1

1.3 Lumpfish (*Cyclopterus lumpus*) Aquaculture ……..…….....3

1.4 Sablefish (*Anoplopoma fimbria*) Aquaculture…….4

1.5 Impact of Infectious Diseases on Aquaculture…..……...5

1.6 Comparative Genomics as a Tool for Vaccine Development…….6

1.7 Research Rationale.…….9

1.8 General Objective…….....9

1.9 Specific Objectives……....9

1.10 References...…...……11

CHAPTER 2: Comparative Genomic and Phenotypic Analysis of *Vibrio anguillarum* J360 Isolated from Cultured Lumpfish (*Cyclopterus lumpus*) in Newfoundland, Canada……...17

2.1 Abstract…….18

2.2 Introduction……...19

2.3 Materials and Methods……..……21

2.3.1 Bacterial culture conditions……21

2.3.2 *V. anguillarum* isolation……..…..21

2.3.3 Matrix-assisted laser desorption/ionization – time of flight (MALDI-TOF) mass spectrometry and serotypification analysis….....22

2.3.4 Biochemical, enzymatic, and physiological characterization…….....22

2.3.5 Siderophores synthesis……...24

2.3.6 Fish holding……...…….24

2.3.7 Infection assay in lumpfish…….....25

2.3.8 DNA extraction and sequencing…….25

2.3.9 Genome assembly, annotation, and mapping…….26

2.3.10 Whole genome comparison and phylogeny analysis…..…….26

2.3.11 Multi-locus sequence analysis of *V. anguillarum* housekeeping gene…..……...27

2.3.12 Genomic island and antibiotic resistance gene analysis……30

2.3.13 Syntenic analysis of *V. aguillarum* J360 large plasmid.……30

2.3.14 Statistical analyses……31

2.3.15 Ethics statements.……..……..…..31

2.4 Results……...31

2.4.1 Phenotypic, biochemical and enzymatic characterization……..31

2.4.2 MALDI-TOF and agglutination analysis…….……..33

2.4.3 Infection assay in lumpfish...……..……33

2.4.4 *V. anguillarum* J360 genome sequencing, assembly and annotation……..34

2.4.5 Whole genome alignment, phylogeny and synteny.....38

2.4.6 Multi-locus sequence analysis (MLSA) and phylogeny…….39

2.4.7 Distribution of genes associated with pathogenesis and environmental adaptation in *V. anguillarum* J360…….……..40

2.4.8 Genomic Islands (GIs)……41

2.4.9 *V. anguillarum* large plasmid analysis……..……..43

2.5 Discussion…….53

2.6 Conclusion……62

2.7 References…….63

CHAPTER 3: *Aeromonas salmonicida* Infection Kinetics and Protective Immune Response to Vaccination in Sablefish (*Anoplopoma fimbria*)…….70

3.1 Abstract…….71

3.2 Introduction……...72

3.3 Materials and Methods……..……74

3.3.1 Bacterial strains, media and reagents……..……74

3.3.2 Bacterin preparation…….……..75

3.3.3 Ethics statement……..……76

3.3.4 Fish origin and holding conditions…….76

3.3.5 Determination of the LD_{50} of *A. salmonicida* J410 in *A. fimbria*…..77

3.3.6 Tissue sampling and analysis……..……...77

3.3.7 Histopathology…..…….78

3.3.8 Sablefish immunization using a common garden experiment……..79

3.3.9 Challenge of immunized sablefish…..…….79

3.3.10 Sablefish IgM purification……80

3.3.11 Immunohistochemistry……....81

3.3.12 Confocal microscopy and immune fluorescence visualization……82

3.3.13 Direct enzyme linked immunosorbent assay (dELISA)……82

3.3.14 Statistical analyses……84

3.4 Results……...85

3.4.1 LD_{50} determination and *A. salmonicida* infection kinetics in sablefish…..……85

3.4.2 Expression of *A. salmonicida*, IgM and CD10 in *A. salmonicida* infected sablefish tissues……..……..86

3.4.3 Vaccine challenge…...……...86

3.4.4 IgM titers in immunized sablefish……..87

3.5 Discussion…….92

3.6 Conclusions…….100

3.7 References……...101

4. SUMMARY……...……..108

5. APPENDICES…….110

LIST OF TABLES

Table 2-1. Geographic origin and host species of *Vibrio anguillarum* isolates…..……28

Table 2-2. Phenotypic characteristics of *V. anguillarum* J360……..…….……36

Table 2-3. Summary of genome: two chromosomes and one plasmid ……..45

Table 2-4. Genome RAST annotation summary…….45

Table 2-5. Prokaryotic genome annotation summary…….46

Table 2-6. Predicted genes associated to subsystems on pathogenesis and environmental adaption……..48

Table 3-1. Summary table for the infection and vaccination model for sablefish (*Anoplopoma fimbria*)……88

LIST OF FIGURES

Figure 2-1. Bacterial growth and physiological characteristics of *V. anguillarum* J360...35

Figure 2-2. Pathogenicity and virulence of *V. anguillarum* J360..…….....37

Figure 2-3. *V. anguillarum* J360 genome visualization…..……...42

Figure 2-4. Phylogenetic and comparative genomic analysis of *V. anguillarum* J360..…….....47

Figure 2-5. Comparative genome synteny between *V. anguillarum* J360 and *V. anguillarum VIB43*…….....51

Figure 2-6. *V. anguillarum* J360 genomic islands (GIs)..……...52

Figure 3-1. *A. salmonicida* infection assay …….…….....89

Figure 3-2. Detection of *A. salmonicida*, IgM and CD10 in *A. salmonicida* infected sablefish tissues.....90

Figure 3-3. Challenge of immunized sablefish.…….94

Figure 3-4. Non-specific binding of immunoglobulins to *A. salmonicida* VapA protein…….95

Figure 3-5. Post-challenge IgM levels is sablefish as quantified by dELISA…..……...96

LIST OF ABBREVIATIONS

°C	Degrees centigrade
µl	Microliter
ANOVA	Analysis of variance
CDRF	Cold-Ocean and Deep-Sea Research Facility
CFU	Colony forming unit
DAPI	4′, 6-diamidino-2-phenylindole
dpc	Days post-challenge
dpi	Days post-infection
dpv	Days post-vaccination
FACS	Fluorescence-activated cell sorting
FITC	Fluorescein isothiocyanate
GG	Genomes gaps
h	Hour
HPR	Horseradish peroxidase
Ig	Immunoglobulins
IHC	Immunohistochemistry
ip	Intraperitoneal
ISs	Insertion sequences
JBARB	Dr. Joe Brown Aquatic Research Building
l	Liter
LCBs	Locally collinear blocks
LD_{50}	Median lethal dose
mg	Milligram
min	Minute
ml	Milliliter
MLSA	Multi-locus sequence analysis
ncRNA	Non-coding RNAs
O.D.	Optical density
PBS	Phosphate buffered saline
RPS	Relative survival percentage
SEM	Standard error of the mean
TSA	Tryptic Soy Agar
TSB	Tryptic Soy Broth media
wpi	Weeks post-immunization

LIST OF APPENDICES

Appendix I. Housekeeping genes used for MLSA.…….....110

Appendix II. Enzymatic profile of *V. anguillarum* J360 using the API ZYM system….112

Appendix III. Enzymatic profile of *V. anguillarum* J360 using API20NE……..113

Appendix IV. Enzymatic profile of *V. anguillarum* J360 using API20E…….114

Appendix V. Evolutionary taxa relationship of *V. anguillarum* chromosome-I and chromosome-II…….115

Appendix VI. Average nucleotide identity (ANI) comparison of *V. anguillarum* whole genome alignment…….116

Appendix VII. Phylogenetic analysis of *V. anguillarum* using Multi-Locus Sequence Analysis (MLSA).……117

Appendix VIII. Comparative whole genome alignment close-up view between *V. anguillarum* J360 and *V. anguillarum* VIB43……..118

Appendix IX. Comparative analysis of *V. anguillarum* J360 large plasmid pVaJ360-I...119

Appendix X. *V. anguillarum* VIB43 genomic islands (GIs)…….....120

Appendix XI. Flow cytometry based bacterial cell-counting……...121

Appendix XII. *A. salmonicida* LD_{50} experimental design……...122

Appendix XIII. *A. fimbria* immunization common garden experimental design…….122

CO-AUTHORSHIP STATEMENT

The research described in this thesis was conducted by Jose Ignacio Vasquez Solis de Ovando with guidance from Dr. Javier Santander. Jose Vasquez was responsible for conducting the experiments, collecting, and analyzing the data, and writing the thesis. Several other individuals were instrumental in the completion of this research. They include Ph.D. candidates, Trung Cao[1], Setu Chakraborty[1], Ahmed Hossain[1], Hajarooba Gnanagobal[1], and MSc. Student My Dang[1] who collaborated on the experiments in Chapter 2. Additionally, Jennifer Monk[3], Danny Boyce[3], and Dr. Nicole O'Brien[4] provided technical support for the research conducted in Chapter 2. Regarding Chapter 3 research, Dr. Katherine Valderrama[1] collaborated in the experiments related to *Aeromonas salmonicida*, Michael Ness[6] was an industrial collaborator who provided *A. salmonicida* isolates, and Dr. Kurt Gamperl[2] was a departmental collaborator. Co-authorship in terms of Chapter 3, also includes Ph.D. candidate Robine H. J. Leeuwis[2], who provided technical support for the experiments related to sablefish and the immunology assays. Briony Campbell[7] worked for our industrial collaborator (Golden Eagle Sable Fish). Drs. Robert Gendron[5] and Kenneth Kao[5] provided technical support for the experiments involving histology and immunohistochemistry assays.

All the chapters were written by Jose Vasquez Solis de Ovando, with suggestions, recommendations and edits provided by Drs. Javier Santander and Jillian Westcott. A manuscript has been submitted to the journal to *BMC Genomics* based on Chapter 2, and another has been accepted in the journal *Fish and Shellfish Immunology* based on the work presented in Chapter 3. Below are the citations for these papers.

Ignacio Vasquez[1], Trung Cao[1], Setu Chakraborty[1], Hajarooba Gnanagobal[1], Jillian D. Westcott[4], Jennifer Monk[3], Danny Boyce[3], Javier Santander[1*] (2020). Comparative Genomics Analysis of *Vibrio anguillarum* J360 Isolated from Infected Lumpfish (*Cyclopterus lumpus*) in Newfoundland, Canada. *Microorganisms. (Submitted)*

Ignacio Vasquez[1], Trung Cao[1], Ahmed Hossain[1], Katherinne Valderrama[1], Hajarooba Gnanagobal[1], My Dang[1], Robine H. J. Leeuwis[2], Michael Ness[6], Briony Campbell[7], Robert Gendron[5], Kenneth Kao[5], Jillian Westcott[4], A. Kurt Gamperl[2], Javier Santander[1*]. (2020). *Aeromonas salmonicida* Infection Kinetics and Protective Immune Response to Vaccination in Sablefish (*Anoplopoma fimbria*). *Fish & Shellfish Immunology*, *104*, 557-556.

[1]Memorial University, Marine Microbial Pathogenesis and Vaccinology Laboratory, Department of Ocean Sciences, 0 Marine Lab Road, St. John's, NL A1K 3E6, Canada

[2]Memorial University, Fish Physiology Laboratory, Department of Ocean Sciences, 0 Marine Lab Road, St. John´s, NL A1K 3E6, Canada

[3]Memorial University, Dr. Joe Brown Aquatic Research Building (JBARB), Department of Ocean Sciences, 0 Marine Lab Road, St. John's, NL A1K 3E6, Canada

[4]Memorial University, Fisheries and Marine Institute, 155 Ridge Road, St. John's, NL A1B 5R3, Canada

[5]Memorial University, Faculty of Medicine, 300 Prince Philip Drive, St. John's, NL A1B 3V6, Canada.

[6]Zoetis, 100 Strathcona Way, Campbell River, BC V9H 1W4, Canada

[7]Golden Eagle Sable Fish, 335 Walkers Hook Rd, Salt Spring Island, BC V8K 1P5, Canada

1. CHAPTER 1: General Introduction

1.1 Introduction

The global human population was ~7.6 billion people in 2017, and it continues to increase annually by 1.2% (FAO, 2017). The Food and Agriculture Organization (FAO) estimated that global agricultural production, including aquaculture, would need to increase by at least 60% by 2050, relative to 2006 levels, to feed the world's predicted population of ~9.6 billion people (FAO, 2009). Aquaculture has the fastest global growth rate of all food-producing sectors, and currently accounts for over 50% of seafood consumed worldwide (FAO, 2018). Moreover, global fish production peaked at approximately 171 million tonnes in 2016 (between wild fisheries and aquaculture), with aquaculture contributing approximately 80 million tonnes (FAO, 2018). Since 1961, the annual growth of finfish consumption has been twice that of population growth (FAO, 2018). As a food-producing sector, the aquaculture industry has a high socio-economic impact (FAO, 2018). For instance, in 2016 it was reported that 18.7 million people in the world were working as fish farmers and this number would increase between 3-4 fold if secondary and post-harvest employment are included (FAO, 2016). Given the contribution of the aquaculture sector to global food security, the sustainable development of this industry is key to achieve the future demands of the world's population (FAO, 2009, 2017, 2018).

1.2 The Canadian Aquaculture Industry. The Canadian aquaculture industry began in the 1970's, and during the last 50 years has played an important social and economic role. In 2018, the economic contribution (or "gross value added") of the Canadian

aquaculture industry reached CAD $5.16 billion, increasing by 58.4% from 2005 and creating 26,000 jobs for Canadians through the food production value chain (CAIA, 2018; DFO, 2017a). More than 60% of Canada's aquaculture production is exported, this is primarily to the United States but includes shipments to more than 20 other countries worldwide (DFO, 2017b). About 45 different species of finfish, shellfish and marine algae are commercially cultivated across Canada. However, production is largely based on five high-volume species, including Atlantic salmon (*Salmo salar*), rainbow trout (*Oncorhynchus mykiss*), blue mussel (*Mytilus edulis*), oyster (*Crassostrea virginica*) and clams (*Ruditapes phillippinarum*), where the mainly production is Atlantic salmon about 64% of total aquaculture production in Canada (DFO, 2019a). In Canada, the aquaculture industry is focused on the Pacific and Atlantic coasts, with British Columbia accounting for about 54% of total production volume, followed by New Brunswick (17%), Nova Scotia (8.2%), Newfoundland and Labrador (7.4%), and Prince Edward Island (5.6%) (DFO, 2019a). However, aquaculture occurs in all Canadian provinces and the Northwest territories, and several other finfish species are produced such as coho salmon (*Oncorhynchus kisutch*), chinook salmon (*Oncorhynchus tshawytscha*), white sturgeon (*Acipenser transmontanus*), tilapia (*Oreochromis niloticus*), and sablefish (*Anoplopoma fimbria*) (DFO, 2020). All these species contributed approximately 149,418 tonnes towards Canada's finfish production in 2018 (DFO, 2019b).

1.3 Lumpfish (*Cyclopterus lumpus*) Aquaculture. Even though aquaculture is the fastest growing food production sector globally (FAO, 2017), parasitic diseases like sea lice

(*Lepeophtheirus salmonis, Caligus elongatus,* etc.) afflict the global Atlantic salmon industry (DFO, 2019c; Jackson et al., 2018; Stentiford et al., 2017). Sea lice represent one of the greatest health challenges faced by the Canadian Atlantic salmon aquaculture industry (DFO, 2019c; Nilsen et al., 2017; Powell et al., 2017). Sea lice are an ectoparasitic copepods that compromises the fish's (hosts) immune system and causes great damage to the fish's skin. This can result in increased susceptibility to viral and bacterial infections, and significant losses and high treatment costs (Brooker et al., 2018; Mustafa et al., 2001). Several pest control strategies have been developed over the years, including technologies involving physical removal (e.g., brushes, water jets, osmolarity and heat-shock treatments, etc.), feed additives, selective breeding and chemotherapeutants, but the latter are losing their efficacy due to evolved parasite resistance (Aaen et al., 2015; Torrissen et al., 2013).

The use of 'cleaner fish", such the ballan (*Labrus bergylta*), corkwing (*Crenilabrus melops*), rock cook (*Centrolabrus exoletus*) and goldsinny (*Ctenolabrus rupestris*) (Blanco Gonzalez & de Boer, 2017; Deady et al., 1995) wrasses, and the lumpfish (*Cyclopterus lumpus*), have been widely adopted as a natural method of sea lice control in Atlantic salmon aquaculture (Imsland et al., 2018; Powell et al., 2017). Cleaner fish species actively remove sea lice from salmon's skin, and have been used to delouse farmed Atlantic salmon in sea cages for several decades (Bjordal, 1991; Powell et al., 2017). The lumpfish (*C. lumpus*) is native to the North Atlantic Ocean, performs well at cold temperatures, and is currently the most commonly farmed and utilized cleaner fish species in the North Atlantic region (Boyce et al., 2018). Commercial production of lumpfish has grown in the last few

years in the North Atlantic region (Powell et al., 2017), including Newfoundland, Canada (Boyce et al., 2018).

1.4 Sablefish (*Anoplopoma fimbria*) Aquaculture. The sablefish, originally described by Pallas in 1814 (Amaoka, 1984; FAO, 2019), and commonly referred to as "Black Cod", is a deep-sea fish found in the Pacific Ocean as far north as the Bering Sea, and as far south as Japan and California. Adult sablefish live on the continental shelf and slope at depths of approximately 1,500 meters. Decreases in wild sablefish stocks due to predators (e.g. whales) and environmental conditions (Hanselman et al., 2018; Liu et al., 2005), as well as increasing consumer demands (Sonu, 2014), and a high market value (Wiedenhoft, 2017), have positioned sablefish farming as an emerging aquaculture industry in Canada. However, limited information related to current culture methods and production values are available. Sablefish aquaculture began in 1984 on the North Pacific coast (USA and Canada), where they were reported to grow well in marine sea-cages at < 6°C (Gores et al., 1984) and reach 3-4 kg in 2 years; as one of the fastest known growth rates of all teleost species (Kendall & Matarese, 1987). Golden Eagle Sable Fish (Salt Spring Island, British Columbia) is one of the world's few commercial sablefish producers, the largest in Canada, and the only international supplier of cultured sablefish. Current production capacity is approximately 500,000 (20 g), with the fish reared from eggs to fingerlings in a land-based hatchery, and then transferred to sea cages to grow to market size (2-4 kg) (Chettleburgh, 2016). Consistent larval survival has been identified as one of the major challenges to the aquaculture production of sablefish. A better understanding of nutritional requirements at

multiple life stages, including broodstock (to produce quality eggs) and larval stages (to enhance growth and development), and improved understanding of genetic selection within the species, have also been identified as key factors to improving the consistency of larval survival (Chettleburgh, 2016). However, disease has also become an issue, with the most serious disease being furunculosis caused by *Aeromonas salmonicida*. More than 74% of Canada's cultured sablefish are exported to Japan. Other key markets include the United States, the United Kingdom (DFO, 2017; FAO, 2019), South Korea and China (FIS, 2020). Exported sablefish (frozen) to South Korea, Japan and China reached a total value of 6,151 tonnes in 2020, with an associated market price of $9.40 USD/Kg (FIS, 2020).

1.5 Impact of Infectious Diseases on Aquaculture. Common pathogens afflicting the Canadian aquaculture industry include, but are not limited to, Infectious Salmon Anaemia virus (ISAV) and various bacterial pathogens such as *Moritella viscosa* (causative agent of winter ulcer), *Renibacterium salmoninarum* (causative agent of bacterial kidney disease), *Vibrio anguillarum* (causative agent of vibriosis) and *Aeromonas salmonicida* (causative agent of furunculosis) (Brooker et al., 2018; Nilsen et al., 2017; Powell et al., 2017; Stentiford et al., 2017). Due to their adaptability and wide host range, these pathogens affect the aquaculture industry worldwide (Frans et al., 2011; Hickey & Lee, 2018; Lafferty et al., 2015). Bacterial diseases are the primary challenge for lumpfish (Brooker et al., 2018; Powell et al., 2017) and cultured sablefish (Arkoosh & Dietrich, 2015) during sea cage culture. Common bacterial pathogens affecting lumpfish and sablefish are *V. anguillarum* and *A. salmonicida* (Arkoosh et al., 2018; Liu et al., 2005).

V. anguillarum, a Gram-negative bacterium, is the causative agent of vibriosis, a fatal disease impacting marine finfish aquaculture worldwide (Egidius, 1987; Naka & Crosa, 2011; Naka et al., 2011). Globally, mortality due to *V. anguillarum* has reached as high as 100% (Austin et al., 2005; Frans et al., 2011), and lumpfish deployed in sea cages for sea lice management are facing significant health problems as a result of this bacterium (Brooker et al., 2018; Powell et al., 2017). For example, lumpfish frequently show signs of systemic bacterial infection, including skin lesions, gill haemorrhages and bacterial aggregations in the lymphoid organs (head kidney, spleen, liver, etc.) (Powell et al., 2017). Several *V. anguillarum* outbreaks have also been reported in lumpfish aquaculture in Norway and Scotland (Brooker et al., 2018; Marcos-Lopez et al., 2013; Powell et al., 2017), as well as in Newfoundland, Canada (Vasquez et al., 2018).

In the case of sablefish, once the farmed juveniles are moved to sea cages to reach market size, they are naturally exposed to infectious bacterial diseases (Krkošek, 2017). Currently, the most common pathogen isolated from infected farmed sablefish in British Columbia is *A. salmonicida* subspecies *mausocida* (Arkoosh et al., 2018), but *V. anguillarum* outbreaks have also been reported (Liu et al., 2005).

1.6 Comparative Genomics as a Tool for Vaccine Development. Globally, vaccination has become the most cost-effective method for controlling infectious diseases in commercial aquaculture (Pastoret, 1999). Since the 1940s, fish vaccination has been used for preventing bacterial and viral diseases (Snieszko & Friddle, 1949). Over 26 licensed commercial fish vaccines are currently available worldwide for use in a variety of cultured fish species (Gudding & Van Muiswinkel, 2013; Ma et al., 2019). The majority of licensed

vaccines currently in use are comprised of heat- or formalin-inactivated bacterial pathogens, and the most efficient administration routes for large-scale fish vaccination are immersion or injection. Vaccines are prepared with or without adjuvants, such as mineral oils (e.g. incomplete or complete (dried *M. tuberculosis* added) Freund's adjuvant), which are added mainly to enhance the immune response of the vaccinated fish (Gudding & Van Muiswinkel, 2013; Sudheesh & Cain, 2017; Tafalla et al., 2013). Over the last decade, the main focus of vaccine development has been the search for new technologies, and advancements in adjuvants which improve vaccine effectiveness (Tafalla et al., 2013). Modern vaccine research and development has targeted specific pathogen components using approaches for the utilization of live-attenuated, subunit or recombinant DNA, and RNA particle vaccines that contain novel antigens (Kim et al., 2016). Live-attenuated vaccines are based on attenuated virulence, or the use of natural low virulence of viruses or bacteria through physical or chemical processes, passage in culture media, or genetic manipulation. Attenuated vaccines have been reported to be more immunogenic than killed bacteria due to their ability to proliferate, to gain entry into the host and to stimulate cellular responses associated with innate and adaptive immune responses (Adams, 2019; Liu et al., 2018). DNA vaccines consist of an expression plasmid that carries a specific gene that codes for a desired antigenic protein that is produced in high quantities within bacterial cells. The gene of interest is flanked by promoter and termination elements that facilitate the expression. DNA vaccines that are able to strongly stimulate the adaptive immune responses are usually constructed to be multivalent, and provide protection or cross-protection by using genes coding for multiple antigens in the plasmid design (Adams, 2019; Levine & Sztein, 2004). RNA vaccines are distinguished by their translational capacity:

conventional non-amplifying mRNA that only carries a specific antigen and self-amplifying mRNA (replicons) that possesses a replicase binding site and a specific antigen. An advantage of their use is their rapid development and safety, because RNA is non-infectious and degraded by normal cellular processes without the risk of mutagenesis (Adams, 2019; Pardi et al., 2018).

One of the most beneficial technologies for the improvement of vaccines has been comparative bacterial genomics, which utilizes genome-sequenced data to answer biological questions about bacterial evolution, physiology and pathogenesis (Fraser et al., 2000; Prentice, 2004). Furthermore, genomics and related studies (e.g., classic microbiology, molecular microbiology and host-pathogen interactions) can provide a better understanding of pathogenesis, the host immune response, and aspects of the pathogen-host interaction that are important to prevent infectious diseases, based on the development of a prompt humoral response by the host to specific antigens (García-Angulo et al., 2014; Seib et al., 2009; Weinstock, 2000). Comparative bacterial genomic approaches contribute directly to novel vaccines and drug design, and these can be used to control and prevent infectious diseases based on the screening of antigens/targets that are present in a pathogenic strain but conserved through several strains of the same species, mostly focus on genes that encode for surface-exposed or secreted proteins. (Fraser et al., 2000; García-Angulo et al., 2014; Prentice, 2004; Seib et al., 2009; Weinstock, 2000)

1.7 Research Rationale.

There are currently no specific commercial vaccines available for lumpfish against *V. anguillarum* or for sablefish against *A. salmonicida*. Comparative genomic studies of *V. anguillarum* and *A. salmonicida* isolates from cultured lumpfish and sablefish outbreaks, respectively, may provide novel insights regarding bacterial evolution and virulence, and they may contribute to the development of effective vaccine design programs for each species. As such, the overall objective of this research was to analyze the genome and phenotype of *V. anguillarum* isolated from infected cultured lumpfish and develop an infection model for atypical *A. salmonicida* in sablefish to evaluate commercial vaccines and an autogenous vaccine.

1.8 GENERAL OBJECTIVE

To analyze the genome and phenotype of *Vibrio anguillarum* isolated from *Cyclopterus lumpus* and evaluate commercial vaccines and an autogenous vaccine in *Anoploploma fimbria* against *Aeromonas salmonicida*, respectively.

1.9 SPECIFIC OBJECTIVES

1. To analyze the genome and phenotype of *V. anguillarum* strain J360 isolated from infected cultured lumpfish (**Chapter 2**)
2. To develop an infection model for atypical *A. salmonicida* strain J410 in sablefish to evaluate commercial vaccines and an autogenous vaccine (**Chapter 3**).

1.10 References

Aaen, S., Helgesen, K., Bakke, M., Kaur, K., Horsberg, T. (2015). Drug resistance in sea lice: a threat to salmonid aquaculture. *Trends in Parasitology, 31*(2), 72-81. doi:10.1016/j.pt.2014.12.006

Adams, A. (2019). Progress, challenges and opportunities in fish vaccine development. *Fish and Shellfish Immunology, 90*, 210-214. doi:10.1016/j.fsi.2019.04.066

Amaoka, K. (1984). Anoplopomatidae. In H. Masuda, K. Amaoka, C. Araga, T. Uyeno and T. Yoshino (eds.). *The Fishes of the Japanese Archipelago* (320 p). Tokai Univ. Press, Tokyo, Japan.

Arkoosh, M., Dietrich, J., Rew, M., Olson, W., Young, G., Goetz, F. (2018). Exploring the efficacy of vaccine techniques in juvenile sablefish, *Anoplopoma fimbria*. *Aquaculture Research, 49*(1), 205-216. doi:10.1111/are.13449

Arkoosh, M. & Dietrich, J. (2015). Pathogenicity of members of the vibrionaceae family to cultured juvenile sablefish. *Journal of Aquatic Animal Health, 27*(2), 96-103. doi:10.1080/08997659.2015.1019159

Austin, B., Austin, D., Sutherland, R., Thompson, F., Swings, J. (2005). Pathogenicity of vibrios to rainbow trout (*Oncorhynchus mykiss,* Walbaum) and *Artemia nauplii*. *Environmental Microbiology, 7*(9), 1488-1495. doi:10.1111/j.1462-2920.2005.00847.x

Bjordal, A. (1991). Wrasse as cleaner fish of farmed salmon. *Progress in Underwater Science, 16*, 17-29.

Blanco Gonzalez, E., & de Boer, F. (2017). The development of the Norwegian wrasse fishery and the use of wrasses as cleaner fish in the salmon aquaculture industry. *Fisheries Science, 83*(5), 661-670. doi:10.1007/s12562-017-1110-4

Boyce, D., Ang, K., & Prickett, R. (2018). Cunner and lumpfish as cleaner fish species in Canada. *In J.W. Treasurer* (Ed). *Cleaner fish biology and aquaculture applications* (451 pp) Sheffield, UK.

Brooker, A., Papadopoulou, A., Gutierrez, C., Rey, S., Davie, A., Migaud, H. (2018). Sustainable production and use of cleaner fish for the biological control of sea lice: recent advances and current challenges. *Veterinary Record, 183*(12), 383. doi:10.1136/vr.104966

Canadian Aquaculture Industry Association, (CAIA). (2018). Benefits to Canadian Index-Canadian Aquaculture Alliance. Retrieved from http://www.aquaculture.ca/benefits-to-canadians-index

Chettleburgh, P. (2016). New life for Canadian black cod hatchery. *Hatchery international*. Retrieved from https://www.hatcheryinternational.com/new-life-for-canadian-black-cod-hatchery-1736/

Deady, S., Varian, S., Fives, J. (1995). The use of cleaner-fish to control sea lice on two Irish salmon (*Salmo salar*) farms with particular reference to wrasse behaviour in salmon cages. *Aquaculture, 131*(1), 73-90. doi:https://doi.org/10.1016/0044-8486(94)00331-H

Department of Fisheries and Oceans Canada, DFO. (2017a). *Value Added | Fisheries and Oceans Canada*. Retrieved from http://www.dfo-mpo.gc.ca/stats/aqua/aqua-val-eng.htm

Department of Fisheries and Oceans Canada, DFO. (2017b). *Canadian Aquaculture R & D Review*. Retrieved from http://dfo-mpo.gc.ca/aquaculture/sci-res/rd2017/health-eng.html

Department of Fisheries and Oceans Canada, DFO. (2019a). *Aquaculture Development Strategy 2016-2019*. Retrieved from https://www.dfo-mpo.gc.ca/aquaculture/collaboration/ccfam-eng.html

Department of Fisheries and Oceans Canada, DFO. (2019b). *Aquaculture Production and Value*. Retrieved from http://www.dfo-mpo.gc.ca/stats/aqua/aqua18-eng.htm

Department of Fisheries and Oceans Canada, DFO. (2019c). *Managing diseases and parasites*. Retrieved from http://www.dfo-mpo.gc.ca/aquaculture/protect-protege/parasites-eng.html

Department of Fisheries and Oceans Canada, DFO. (2020). *Aquaculture farmed species profiles*. Retrieved from http://www.dfo-mpo.gc.ca/aquaculture/farmed-elevage/listing-eng.htm

Egidius, E. (1987). Vibriosis: Pathogenicity and pathology. A review. *Aquaculture, 67*(1), 15-28. doi:https://doi.org/10.1016/0044-8486(87)90004-4

Food and Agriculture Organization of the United Nations, FAO. (2009). *How to feed the world 2050*. Retrieved from http://www.fao.org/fileadmin/templates/wsfs/docs/expert_paper/How_to_Feed_the_World_in_2050.pdf

Food and Agriculture Organization of the United Nations, FAO. (2016). *The state of world fisheries and aquaculture 2016: contributing to food security and nutrition for all*. Retrieved from http://www.fao.org/3/a-i5555e.pdf

Food and Agriculture Organization of the United Nations, FAO. (2017). *GLOBEFISH - Information and Analysis on World Fish Trade*. Retrieved from http://www.fao.org/in-action/globefish/news-events/details-news/en/c/897130/

Food and Agriculture Organization of the United Nations, FAO. (2018). *State of Fisheries and Aquaculture in the world*. Retrieved from www.fao.org/state-of-fisheries-aquaculture

Food and Agriculture Organization of the United Nations, FAO. (2019). *Fisheries and Aquaculture Department, Species Fact Sheets*. Retrieved from http://www.fao.org/fishery/species/3341/en

Fish Information Service, FIS. (2020). Black cod (sablefish) imports: USA and Canada. *Fish Information & Services*. Retrieved from https://www.fis.com/fis/worldnews/worldnews.asp?monthyear=&day=6&id=107115&l=e&special=0&ndb=0

Frans, I., Michiels, C., Bossier, P., Willems, K., Lievens, B., Rediers, H. (2011). *Vibrio anguillarum* as a fish pathogen: virulence factors, diagnosis and prevention. *Journal of Fish Diseases, 34*(9), 643-661. doi:10.1111/j.1365-2761.2011.01279.x

Fraser, C., Eisen, J., Fleischmann, R., Ketchum, K., Peterson, S. (2000). Comparative genomics and understanding of microbial biology. *Emerging Infectious Diseases, 6*(5), 505-512. doi:10.3201/eid0605.000510

García-Angulo, V., Kalita, A., Kalita, M., Lozano, L., Torres, A. (2014). Comparative genomics and immunoinformatics approach for the identification of vaccine candidates for enterohemorrhagic *Escherichia coli* O157:H7. *Infection and Immunity, 82*(5), 2016-2026. doi:10.1128/IAI.01437-13

Gores, K., & Prentice, E. (1984). Growth of sablefish (*Anoplopoma fimbria*) in marine net-pens. *Aquaculture, 36*(4), 379-386. doi:10.1016/0044-8486(84)90330-2

Gudding, R., & Van Muiswinkel, W. (2013). A history of fish vaccination: science-based disease prevention in aquaculture. *Fish and Shellfish Immunology, 35*(6), 1683-1688. doi:10.1016/j.fsi.2013.09.031

Hanselman, D., Rodgveller, C., Fenske, K., Shotwell, S., Echave, K., Malecha, P., Lunsford, C. (2018). Assessment of the Sablefish stock in Alaska. Retrieved from https://www.afsc.noaa.gov/refm/stocks/plan_team/2018/sablefish.pdf

Hickey, M., & Lee, J. (2018). A comprehensive review of *Vibrio (Listonella) anguillarum*: ecology, pathology and prevention. *Reviews in Aquaculture, 10*(3), 585-610. doi:10.1111/raq.12188

Imsland, A., Hanssen, A., Nytrø, A., Reynolds, P., Jonassen, T., Hangstad, T., Elvergard, T., Urskog, T., Mikalsen, B. (2018). It works! Lumpfish can significantly lower sea lice infestation in large-scale salmon farming. *Biology open, 7*(9), bio036301. doi:10.1242/bio.036301

Jackson, D., Moberg, O., Stenevik Djupevag, E., Kane, F., Hareide, H. (2018). The drivers of sea lice management policies and how best to integrate them into a risk management strategy: An ecosystem approach to sea lice management. *Journal of Fish Diseases, 41*(6), 927-933. doi:10.1111/jfd.12705

Kendall, A., & Matarese, A. (1987). Biology of eggs, larvae and epipelagic juvinales of sablefish, *Anoplopoma fimbria*, in relation to their potential use in management. *Marine Fisheries Review*. Retrieved from https://spo.nmfs.noaa.gov/sites/default/files/pdf-content/MFR/mfr491/mfr4911.pdf

Kim, H., Lee, Y., Kang, S., Han, B., Choi, K. (2016). Recent vaccine technology in industrial animals. *Clinical and Experimental Vaccine Research, 5*(1), 12-18. doi:10.7774/cevr.2016.5.1.12

Krkošek, M. (2017). Population biology of infectious diseases shared by wild and farmed fish. *Canadian Journal of Fisheries and Aquatic Sciences, 74*(4), 620-628. doi:10.1139/cjfas-2016-0379

Lafferty, K., Harvell, C., Conrad, J., Friedman, C., Kent, M., Kuris, A., Powell, E., Rondeau, D., Saksida, S. (2015). Infectious diseases affect marine fisheries and aquaculture economics. *Annual Review of Marine Science, 7*(1), 471-496. doi:10.1146/annurev-marine-010814-015646

Levine, M., & Sztein, M. (2004). Vaccine development strategies for improving immunization: the role of modern immunology. *Nature Immunology, 5*(5), 460-464. doi:10.1038/ni0504-460

Liu, X., Jiao, C., Ma, Y., Wang, Q., & Zhang, Y. (2018). A live attenuated *Vibrio anguillarum* vaccine induces efficient immunoprotection in Tiger puffer (*Takifugu rubripes*). *Vaccine, 36*(11), 1460-1466. doi:10.1016/j.vaccine.2018.01.067

Liu, Y., Volpe, J., Sumaila, U. (2005). Ecological and economic impact assessment of Sablefish aquaculture in British Columbia. Retrieved from https://open.library.ubc.ca/collections/52383/items/1.0074787

Ma, J., Bruce, T., Jones, E., Cain, K. (2019). A Review of Fish Vaccine Development Strategies: Conventional Methods and Modern Biotechnological Approaches. *Microorganisms, 7*(11), 569. doi:10.3390/microorganisms7110569

Marcos-Lopez, M., Donald, K., Stagg, H., McCarthy, U. (2013). Clinical *Vibrio anguillarum* infection in lumpsucker *Cyclopterus lumpus* in Scotland. *Veterinary Records, 173*(13), 319. doi:10.1136/vr.101763

Mustafa, A., Rankaduwa, W., Campbell, P. (2001). Estimating the cost of sea lice to salmon aquaculture in eastern Canada. *The Canadian veterinary journal = La revue veterinaire canadienne, 42*(1), 54-56. Retrieved from https://www.ncbi.nlm.nih.gov/pmc/PMC1476418/

Naka, H., & Crosa, J. (2011). Genetic Determinants of Virulence in the Marine Fish Pathogen *Vibrio anguillarum*. *Fish Pathology, 46*, 1-10. doi:10.3147/jsfp.46.1

Naka, H., Dias, G., Thompson, C., Dubay, C., Thompson, F., & Crosa, J. (2011). Complete genome sequence of the marine fish pathogen *Vibrio anguillarum* harboring the pJM1 virulence plasmid and genomic comparison with other virulent strains of *V. anguillarum* and *V. ordalii*. *Infectious Immunity, 79*(7), 2889-2900. doi:10.1128/IAI.05138-11

Nilsen, A., Nielsen, K., Biering, E., Bergheim, A,. (2017). Effective protection against sea lice during the production of Atlantic salmon in floating enclosures. *Aquaculture, 466* 41-50pp. doi:https://doi.org/10.1016/j.aquaculture.2016.09.009

Pardi, N., Hogan, M., Porter, F., Weissman, D. (2018). mRNA vaccines - a new era in vaccinology. *Nat Rev Drug Discov, 17*(4), 261-279. doi:10.1038/nrd.2017.243

Pastoret, P. (1999). Veterinary vaccinology. *Comptes Rendus de l'Académie des Sciences - Series III - Sciences de la Vie, 322*(11), 967-972. doi:https://doi.org/10.1016/S0764-4469(00)87194-2

Powell, A., Treasurer, J., Pooley, C., Keay, A., Lloyd, Imsland, A., Garcia de Leaniz, C. (2017). Use of lumpfish for sea-lice control in salmon farming:challenges and opportunities. *Reviews in Aquaculture, 0*, 1-20. doi:doi: 10.1111/raq.12194

Prentice, M. (2004). Bacterial comparative genomics. *Genome biology, 5*(8), 338-338. doi:10.1186/gb-2004-5-8-338

Seib, K., Dougan, G., Rappuoli, R. (2009). The key role of genomics in modern vaccine and drug design for emerging infectious diseases. *PLoS genetics, 5*(10), e1000612-e1000612. doi:10.1371/journal.pgen.1000612

Snieszko, S., & Friddle, S. (1949). Prophylaxis of furunculosis in brook trout (*Salvelinus Fontinalis*) by oral immunization and sulfamerazine. *The Progressive Fish-Culturist, 11*(3), 161-168. doi:10.1577/1548-8640(1949)11[161:POFIBT]2.0.CO;2

Sonu, S. (2014). Supply and market for sablefish in Japan. *NOAA technical memoramdum.* Retrieved from https://www.st.nmfs.noaa.gov/Assets/commercial/market-news/sablefishSupplyMarket2014.pdf

Stentiford, G., Sritunyalucksana, K., Flegel, T., Williams, B., Withyachumnarnkul, B., Itsathitphaisarn, O., Bass, D. (2017). New Paradigms to help solve the global aquaculture disease crisis. *PLoS Pathogens, 13*(2), e1006160. doi:10.1371/journal.ppat.1006160

Sudheesh, P., & Cain, K. (2017). Prospects and challenges of developing and commercializing immersion vaccines for aquaculture. *International Biology Review, 1*(1). doi:10.18103/ibr.v1i1.1313

Tafalla, C., Bøgwald, J., & Dalmo, R. (2013). Adjuvants and immunostimulants in fish vaccines: current knowledge and future perspectives. *Fish and Shellfish Immunology, 35*(6), 1740-1750. doi:10.1016/j.fsi.2013.02.029

Torrissen, O., Jones, S., Asche, F., Guttormsen, A., Skilbrei, O., Nilsen, F., Horsberg, T., Jackson, D. (2013). Salmon lice--impact on wild salmonids and salmon aquaculture. *Journal of Fish Diseases, 36*(3), 171-194. doi:10.1111/jfd.12061

Vasquez, I., Cao, T., Chakraborty, S., Gnanagobal, H., Westcott, J., Boyce, D., Santander, J. (2018). *Characterization and Draft Genome of Vibrio anguillarum J360 Isolated from an Outbreak in Lumpfish (Cyclopterus lumpus).* Paper presented at the 8th International Symposium on Aquatic Animal Health, Charlottetown, Prince Edward Island, Canada.

Weinstock, G. (2000). Genomics and bacterial pathogenesis. *Emerging Infectious Diseases, 6*(5), 496-504. doi:10.3201/eid0605.000509

Wiedenhoft, H. (2017). Advances in US sablefish aquaculture. *Aquaculture North America.* Retrieved from https://www.aquaculturenorthamerica.com/advances-in-us-sablefish-aquaculture-hits-snag-1584/

2. CHAPTER 2: Comparative Genomic and Phenotypic Analysis of *Vibrio anguillarum* J360 Isolated from Cultured Lumpfish (*Cyclopterus lumpus*) in Newfoundland, Canada

The research described in Chapter 2 has been submitted to *Microorganisms* as:

Ignacio Vasquez[1], Trung Cao[1], Setu Chakraborty[1], Hajarooba Gnanagobal[1], Jillian D. Westcott[4], Jennifer Monk[3], Danny Boyce[3], Javier Santander[1*] (2020). Comparative Genomic Analysis of *Vibrio anguillarum* J360 Isolated from Infected Lumpfish (*Cyclopterus lumpus*) in Newfoundland, Canada.

2.1 Abstract

Vibrio anguillarum is a Gram-negative marine pathogen causative agent of vibriosis in a wide range of hosts, including invertebrates and teleosts. Lumpfish (*Cyclopterus lumpus*), a native fish of the North Atlantic Ocean, utilized as cleaner fish to control sea lice (*Lepeophtheirus salmonis*) infestations in the Atlantic salmon (*Salmo salar*) aquaculture industry. *V. anguillarum* is one of the most frequent bacterial pathogens affecting lumpfish. Here, we described the phenotype and genomic characteristics of *V. anguillarum* strain J360 isolated from infected cultured lumpfish in Newfoundland, Canada. Koch's postulates determined in naïve lumpfish showed lethal acute vibriosis in lumpfish. *V. anguillarum* J360 genome showed to be composed of two chromosomes and two plasmids with a total genome size of 4.56 Mb with 44.85% G+C content. Phylogenetic and comparative analyses showed that *V. anguillarum* J360 is closely related to *V. anguillarum* strain VIB43, isolated in Scotland, with a 99.8% of genome identity. Differences in the genomic organization were identified and associated to insertion sequence elements (ISs). Additionally, *V. anguillarum* J360 does not possess a pJM1-like plasmid, typically present in virulent isolates from the Pacific Ocean, suggesting that acquisition of this extrachromosomal element the virulence of *V. anguillarum* J360 or other Atlantic isolates could increase.

2.2 Introduction

Vibrio spp. are naturally ubiquitous in aquatic and marine environments (Pruzzo et al., 2005). Some members of this genus cause infections in humans after exposition to contaminated water, such as *Vibrio cholerae*, the causative agent of cholera, and after consumption of raw contaminated seafood, such as *V. parahaemolitycus*, *V. alginolyticus*, and *V. vulnificus* (Baker-Austin et al., 2018; Baker-Austin et al., 2010; Pruzzo et al., 2005). Other members of *Vibrio* spp., such as *V. splendidus*, *V. nereis*, *V. harveyi*, *V. damsela*, *V. tubiashi* and *V. anguillarum* are pathogens of aquatic organisms including cultured fish species (Frans et al., 2011; Gram et al., 1999). *V. anguillarum* is a Gram-negative marine pathogen, which causes vibriosis in a wide range of cultured and wild invertebrate and teleost hosts, but is also present in brackish and fresh water (Holm et al., 2015; Li et al., 2013; Naka et al., 2011).

The lumpfish (*Cyclopterus lumpus*), a native fish of the North Atlantic Ocean, is utilized as a cleaner fish to control sea lice (*Lepeophtheirus salmonis*) infestations in the Atlantic salmon (*Salmo salar*) aquaculture industry (Brooker et al., 2018; Imsland et al., 2014; Powell et al., 2017). The lumpfish performs well in cold environments (~6-12°C), and removes nearly to 90% of the sea lice at sea-cages (with a feeding rate of 0.3 sea lice per day) (Barrett et al., 2020; Brooker et al., 2018; McEwan et al., 2019). Lumpfish have been reported to be up to 64% more efficacious with respect to sea lice removal when compared to other cleaner fish species, such as various wrasse species like ballan (*Labrus bergylta*), corkwing (*Crenilabrus melops*), rock cook (*Centrolabrus exoletus*) and goldsinny (*Ctenolabrus rupestris*) wrasses (McEwan et al., 2019; Powell et al., 2017). In addition, these wrasses used as cleaner fish species (not including lumpfish) exhibit a

reduce activity during winter, because they enter into a hypometabolic state (similar to hibernation) (Sayer et al., 1996; Costa et al., 2013), and this eventually decreases sea lice removal efficiency (Blanco Gonzalez & de Boer, 2017; Deady et al., 1995).

V. anguillarum is one of the most frequent pathogens affecting lumpfish in sea-cages (Brooker et al., 2018; Powell et al., 2017). In lumpfish, *V. anguillarum* causes a hemorrhagic septicemia, which is characterized by skin lesions, gill hemorrhages, and bacterial aggregations in lymphoid organs (Breiland et al., 2016; Marcos-Lopez et al., 2013; Powell et al., 2017). In Atlantic Canada, *V. anguillarum* is frequent (Fisheries and Land Resources, 2020), but it has not been reported in lumpfish.

Currently, 23 serotypes of *V. anguillarum* have been described, and serotypes O1, O2 and O3 are the most frequent serotypes causing outbreaks in teleosts (Holm et al., 2018; Pedersen et al., 1999; Sørensen & Larsen, 1986). The *V. anguillarum* genome consists of two chromosomes and a large virulence plasmid is present in some isolates (Naka et al., 2011). Several virulent strains of *V. anguillarum* from different geographic locations and fish species have been sequenced (Holm et al., 2018), including *V. anguillarum* M3 (Li et al., 2013), *V. anguillarum* NB10 (Holm et al., 2015) and *V. anguillarum* 775 (Naka et al., 2011). *V. anguillarum* is more frequently reported in warm water fish, and several of these genomes have been sequence, assembled, and annotated, and although virulent strains of *V. anguillarum* have been isolated from cold water environments, only a few of these isolates have been described (Holm et al., 2018).

In this study, we describe the complete genome of a *V. anguillarum* strain J360 isolated from an outbreak in cultured lumpfish in Newfoundland, Canada, and compared

its genome to other known *V. anguillarum* strains. We determined that *V. anguillarum* J360 produces an acute vibriosis in lumpfish, does not harbor virulence plasmids, is closely related to *V. anguillarum* strains isolated from the Atlantic coasts, and distantly related to *V. anguillarum* strains isolated from the Pacific coasts. *V. anguillarum* J360 also showed high similarity to a *V. anguillarum* isolated from sea bass (*Dicentrarchus labrax*) in Scotland. Comparative analysis suggested that insertion sequence elements play a key role in *V. anguillarum* evolution.

2.3 Materials and Methods

2.3.1 Bacterial culture conditions.

A single colony of *V. anguillarum* J360 was grown routinely in 3 ml of Trypticase Soy Broth (TSB, Difco, Franklin Lakes, NJ, USA) supplemented up to 2% NaCl at 15ºC in a 16 mm diameter glass tube and placed in a roller drum shaker (TC7; New Brunswick Scientific, USA) for 24 h. When required, the cultured media was supplemented with 100 µM of $FeCl_3$, 100 µM of 2,2 dipyridyl, or of 1.5% bacto-agar (Difco). CAS plates were used for the siderophores secretion assay (Louden et al., 2011). Blood agar plates (0.5% salmon blood) were used to evaluate hemolytic activity. Bacterial cells were harvested at mid-log phase, at an optical density (O.D. 600 nm) of ~0.7 (~ 4.1×10^8 CFU/ml), washed three times with phosphate buffered saline (PBS; 136 mM NaCl, 2.7 mM KCl, 10.1 mM Na_2HPO_4, 1.5 mM KH_2PO_4 (pH 7.2) (Wood, 1983) at 4,200 × *g* for 10 min at room temperature. Bacterial O.D. was monitored using a Genesys 10 UV spectrophotometer (Thermo Spectronic, Thermo Fischer Scientific, USA).

2.3.2 V. anguillarum isolation.

V. anguillarum strain J360 was isolated from the head kidney of infected lumpfish in Newfoundland, Canada. Fish with classic vibriosis clinical signs were netted and immediately euthanized with an overdose of MS-222 (400 mg/l) (Syndel Laboratories, BC, Canada). Tissue samples were collected and placed into sterile homogenized bags (Nasco whirl-pak®, USA). The infected tissues were weighed and homogenized in PBS up to a final volume of 1 ml. One hundred microliters of the homogenized tissue suspension were plated onto TSA plates and incubated at 15°C for 48 h. Isolated colonies were selected and purified for further analysis. Bacterial stocks were preserved at -80°C in a 10% glycerol and 1% peptone solution.

2.3.3 Matrix-assisted laser desorption/ionization – time of flight (MALDI-TOF) mass spectrometry and serotypification analysis.

Serotypification and MALDI-TOF was performed at the University of Prince Edward Island, Canada. The MALDI Biotyper RTC was performed according to the MALDI Biotyper 3.1 user manual and parameter settings as previously published (Cameron et al., 2017).

2.3.4 Biochemical, enzymatic, and physiological characterization.

V. angillarum J360 growth curves were conducted in triplicate at 15ºC, 28ºC, and under rich and iron limited conditions according to established protocols (Connors et al.,

2019). Briefly, a single colony of *V. angillarum* J360 was inoculated in 3 ml of TSB and grown in a roller drum shaker for 24 h at 15ºC. Three hundred microliters of cells at mid-log phase (O.D. 600nm ~0.7) were added to 30 ml of fresh TSB into 250 ml flasks and incubated for 48 h at 15ºC or 28°C with aeration (180 rpm) in an orbital shaker. Bacterial growth was monitored until O.D. 600 nm was ~ 2.0 ± 0.3 (~ 8×10^8 CFU/ml). The growth of *V. anguillarum* J360 under iron limited conditions was determined using three different 2,2 dipyridyl concentrations (100, 150, 250µM). Controls consisted of non-supplemented TSB. The doubling time was estimated using the O.D. values, and the equation $g = b - B$, where b was the O.D. value at the end of the time interval and B was the O.D. value at the beginning of the time interval.

The biochemical profile of *V. anguillarum* J360 was characterized using API20E, API20NE and APY ZYM systems (BioMerieux, Marcy-l'Etoile, France) according to manufacturer's instructions. The strips were incubated at 15°C for 48 h, and the results were analyzed using APIweb (BioMerieux). *V. anguillarum* J360 growth was also tested at different temperatures (4°C, 15°C, 28°C and 37°C) and different concentrations of NaCl (0%, 0.5% and 2%). Motility, hemolysin on TSA 5% salmon blood, siderophores synthesis, catalase activity and oxidase activity were evaluated using standard methods (Myhr et al., 1991). Antibiograms of *V. anguillarum* J360 were determined for tetracycline (10 mg/ml), oxytetracycline (30 mg/ml), ampicillin (10 mg/ml); sulfamethoxazole (STX) (25 mg/ml), chloramphenicol (30 mg/ml), colistin sulphate (10 mg/ml), and oxalinic acid (2 mg/ml) using standard methods (Myhr et al., 1991; Ramasamy et al., 2018).

2.3.5 Siderophores synthesis.

V. anguillarum J360 was grown under conditions previously described. Bacterial cells were harvested at mid-log phase, at an O.D. 600 nm of ~0.7 (~4.1×10^8 CFU/ml), washed three times with phosphate buffered saline (PBS; 136 mM NaCl, 2.7 mM KCl, 10.1 mM Na_2HPO_4, 1.5 mM KH_2PO_4 (pH 7.2) (Wood, 1983) at 4,200 × *g* for 10 min at room temperature, and resuspended in 1 ml of PBS. An inoculum of 300 µl of bacteria were added to 3 ml of TSB media and TSB media supplemented with 100 µM of $FeCl_3$ or 100 µM of 2,2 dipyridyl. *V. anguillarum* J360 was grown at 15°C for 24 h with aeriation. After the incubation period, the cells were harvested at mid-log phase, washed twice with PBS, and resuspended in 100 µl of PBS. Then, 5 µl of the concentrated bacterial pellet was inoculated onto CAS agar plates (Louden et al., 2011) and incubated at 15°C or 28°C for 48 h.

2.3.6 Fish Holding.

Fish were maintained at the Dr. Joe Brown Aquatic Research Building (JBARB) at MUN under the animal protocol #18-1-JS. Lumpfish were reared under optimal conditions, the fish were acclimated to ~8-10°C in 500 l tanks supplied with 95-110% air saturated and UV treated filtered flow-through seawater, and an ambient photoperiod. Biomass density was maintained at 6.6 kg/m^3. The fish were fed daily using a commercial diet (Skretting – Europa 15; crude protein (55%), crude fat (15%), crude fiber (1.5%), calcium (3%), phosphorus (2%), sodium (1%), vitamin A (5000 IU/kg), vitamin D (3000 IU/kg) and vitamin E (200 IU/kg) at 0.5% of their body weight per day.

2.3.7 Infection assay in lumpfish.

Naïve cultured lumpfish (weight = ~55 g) were transferred from the JBARB to the AQ3 biocontainment Cold-Ocean and Deep-Sea Research Facility (CDRF) for infection assays. Fish were separated into three 500 l tanks containing 60 fish per dose and acclimated for 2 weeks under previously described conditions. The infections were done according to established protocols (Chakraborty et al., 2019). Briefly, fish were anesthetized with 40 mg of MS-222 (Syndel Laboratories, BC, Canada) per liter of sea water, and intraperitoneally infected with 100 μl of 10^6, or 10^7 CFU per dose of *V. anguillarum* J360. Control group (n=60) was mock infected with PBS. Mortality was monitored daily until 30 days post-infection. Samples of liver, spleen and head kidney were taken from moribund fish to re-isolate the pathogen.

2.3.8 DNA Extraction and Sequencing.

V. anguillarum J360 was grown under conditions previously described. Bacterial cells were harvested at mid-log phase at an O.D. 600 nm of ~0.7 (~ 4.1×10^8 CFU/ml) and washed three times with PBS. DNA extraction was performed using the Wizard DNA extraction High Molecular Weight Kit (Promega, USA). DNA integrity and purity were evaluated by gel electrophoresis (agarose gel 0.8%) (Sambrook & Russell, 2001) and spectrophotometry using a Genova-Nano spectrophotometer (Jenway, UK). Libraries and sequencing were done by Genome Quebec (QC, Canada) using PacBio RS II and Miseq Illumina sequencers.

2.3.9 Genome assembly, annotation, and mapping.

PacBio reads were assembled at Genome Quebec using Celera Assembler (August 2013 version). Annotation was done using the Rapid Annotation Subsystem Technology pipeline (RAST) (http://rast.nmpdr.org/) (Aziz et al., 2008). The two *V. anguillarum* J360 chromosomes, and large plasmid, were submitted to National Center for Biotechnology Information (NCBI) and re-annotated using the NCBI Prokaryotic Genome Annotation Pipeline.

To detect small plasmids, the Illumina reads were trimmed using CLC Genomics Workbench v20.0 (CLC Bio) and examined for quality using FastQC version 12 (Andrews, 2010). High quality Illumina reads were assembled using the CLC Genomics Workbench *de novo* tool and aligned to the reference *V. anguillarum* J360 chromosomes and large plasmid using the genome finishing module tools with defaults parameters. Illumina sequences that did not align with the chromosomes or large plasmid were analyzed and annotated using the previously described methods. The whole genome of *V. anguillarum* J360 was mapped using DNA plotter software (Carver et al., 2009).

2.3.10 Whole genome comparison and phylogeny analysis.

The genomes utilized are listed in Table 1. Whole genomes were aligned to calculate the average nucleotide identity (ANI) using the CLC Genomic Workbench v20 (CLC Bio) whole genome analysis tool with default parameters (Min. initial seed length = 15; Allow mismatches = yes; Min. alignment block = 100). A minimum similarity (0.8) and a minimum length (0.8) were used as parameters for CDS identity. A comparative heat map was constructed using the heat map tool with default parameters (Euclidean distance

method and complete cluster linkages). Phylogenetic analysis was performed in two different software CLC Genomic workbench v20.0 and MEGA X (Kumar et al,2018) with same parameters for robustness comparison purposes, using the extracted alignment from ANI analysis. Evolutionary history was calculated using the Neighbor-Joining method (Saitou & Nei, 1987) with a bootstrap consensus of 500 replicates, and evolutionary distance was computed using Jukes-Cantor method (Juke & Cantor, 1969). *Photobacterium damselae* 91-197 (AP018045/6) chromosomes were utilized as an outgroup (Teru et al., 2017). Whole genome dot plots between closely related strains were constructed using the CLC Genomic Workbench v20.0, whole genome analysis tool to visualize and further analyze genomic differences. Comparative alignment analysis represents homologous regions, translocations, and inversions within the two bacterial genomes for chromosome-I and for chromosome-II. Homologous regions identified as locally collinear blocks (LCBs), represent conserved regions which do not present genomic rearrangements, and genomic gaps (GGs) were identified as un-matched regions. Analysis was performed using the progressive Mauve v20150206 (Darling et al., 2004).

2.3.11 Multi-locus sequence analysis of V. anguillarum housekeeping genes.

Multi-locus sequence analysis (MLSA) was used to infer the phylogenetic history of *V. anguillarum* strains using reference genes including 16S ribosomal RNA subunit (*rrn*), cell-division protein (*ftsZ*), glyceraldehyde-3-phosphate dehydrogenase (*gapA*), gyrase beta subunit (*gyrB*), rod shape-determining protein (*mreB*), uridine monophosphate (UMP) kinase or uridylate kinase (*pyrH*), recombinase A (*recA*), RNA polymerase alpha

Table 2-1. Geographic origin and host species of *Vibrio anguillarum* isolates.

Species and Serotype	Geographic Origin/Host Species	Genome Size (bp)	Accession Numbers	References
V. anguillarum 775 / O1	USA, Pacific coast / *Oncorhynchus kisutch*	4,117,056	CP002284 / 5	(Naka et al., 2011)
V. anguillarum M3 / O1	China, Shandong / *Paralichthys olivaceus*	4,117,885	CP006699 / 700	(Li et al., 2013)
V. anguillarum NB10 / O1	Sweden, Baltic Sea / *Oncorhynchus mykiss*	4,373,835	LK021130 / 29	(Holm et al., 2015)
V. anguillarum VIB12 / O2	Greece / *Dicentrarchus labrax*	4,897,690	CP023310 / 11	(Holm et al., 2018)
V. anguillarum VIB43 / O1	Scotland, UK / *Dicentrarchus labrax*	4,407,865	CP023054 / 5	(Holm et al., 2018)
V. anguillarum CNEVA / O3	France / *Dicentrarchus labrax*	4,256,429	CP022103 / 4	(Holm et al., 2018)
V. anguillarum MHK3 / O1	China / Flounder	4,015,925	CP022468 / 9	-
V. anguillarum 425	China / Sea bass	4,373,373	CP020533 / 4	-
V. anguillarum 87-9-116 / O1	Finland / *Salmo salar*	4,338,125	CP021980 / 1	(Holm et al., 2018)
V. anguillarum JLL237 / O1	Denmark /	4,286,989	CP022101 / 2	(Holm et al., 2018)

V. anguillarum ATCC-68554 / O1	*Oncorhynchus mykiss* USA, Pacific coast / *Oncorhynchus kisutch*	4,141,906	CP023209 / 8	(Holm et al., 2018)
V. anguillarum 90-11-286	Denmark / Farm-water sample	4,342,224	CP011460 / 1	(Rasmussen et al., 2016)
V. anguillarum S3 / O1	Denmark / *Oncorhynchus mykiss*	4,272,973	CP022099/ 100	(Holm et al., 2018)
V. campbelli ATCC 25920	USA, Hawaii / Seawater isolate	5,178,103	CP015863 / 4	(Gomez-Gil et al., 2004)
V. fluvialis ATCC 33809	Bangladesh / *Homo sapiens*	4,827,733	CP014034 / 5	(Lee et al., 1981)
V. parahaemolyticus ATCC 17802	Japan / Seawater isolate	5,152,461	CP014046 / 7	(Fujino et al., 1965)
V. tasmaniensis LGP32	France / *Crassostrea gigas*	4,974,818	FM954972 / 3	(Le Roux et al., 2009)
Photobacterium damselae 91-197	USA /Hybrid Striped Bass (*Morone sp*.)	4,293,175	AP018045 / 6	(Teru et al., 2017)

subunit (*rpoA*), and topoisomerase I (*topA*) genes sequences. Only genes from complete genomes were considering for the MLSA. Sequences were aligned using CLC Genomic Workbench v20.0 (CLC Bio). Concatenation of locus sequences was made using Sequence Matrix software v1.7.8 (Vaidya et al., 2011). Phylogenetic analysis was performed using the two software above mentioned with same parameters. Evolutionary history was estimated using Neighbor-Joining method (Saitou & Nei, 1987) with a bootstrap consensus of 500 replicates, and evolutionary distance was computed using Jukes-Cantor method (Juke & Cantor, 1969). The gene loci and accession numbers are listed in Appendix I.

2.3.12 Genomic island and antibiotic resistance gene analysis.

Detection of genomic islands (GIs) was conducted using IslandViewer v.4 pipeline (https://www.pathogenomics.sfu.ca/islandviewer/browse/), which integrates IslandPath-DIMOB, SIGH-HMM and IslandPick analysis tools into a single analysis (Bertelli et al., 2017). Analysis was performed for both chromosomes and both plasmids.

2.3.13 Syntenic analysis of V. anguillarum J360 large plasmid.

Genomic comparisons of virulent and non-virulent plasmids between *V. anguillarum* species were performed using the whole genome alignment tool of CLC Genomics Workbench v20.0 with default parameters. Plasmids used in this analysis were: p292-VIB12 (CP023312); p15-VIB43 (CP023056); pVaM3 (CP006701); pJM1

(AY312585), p67vangNB10 (LK021128) and p65-ATCC 68554 (CP023210). Plasmids were aligned to calculate the ANI. A comparative heat map was constructed using the heat map tool with default parameters (Euclidean distance method and complete cluster linkages).

2.3.14 Statistical analysis.

Fish survival percentages were arcsine transformed ($\sqrt{survival\ rate\ ratio}$). A one-way ANOVA, followed by a Tukey's post hoc test, was used to determine significant differences ($P < 0.05$). All statistical analyses were performed using GraphPad Prism 6 (GraphPad Software, California, USA).

2.3.15 Ethics statement.

All animal protocols required for this research were approved by the Institutional Animal Care Committee and the Biosafety Committee at Memorial University of Newfoundland (MUN). Animal assays were conducted under protocols #18-01-JS #18-03-JS, and biohazard license L-01.

2.4 Results

2.4.1 Phenotypic, biochemical, and enzymatic characterization.

V. anguillarum strain J360 was capable of growth in Tryptic Soy Broth (TSB) and Luria Bertani (LB) media up to 30ºC (Table 2-1). The doubling time for *V. anguillarum*

J360 in TSB supplemented with 2% NaCl at 15°C was 2 h (Fig. 2-1A) and 1 h at 28°C (Fig. 2-1B). *V. anguillarum* J360 did not grow at 37ºC, in TCBS selective media at 15 and 28°C, or in the absence of NaCl. *V. anguillarum* J360 was shown to be motile and capable of synthesizing type I fimbria, oxidase and catalase (Table 2-2). The antibiogram analysis showed that *V. anguillarum* J360 is ampicillin resistant and susceptible to tetracycline, oxytetracycline, sulfamethoxazole, chloramphenicol, colistin sulphate, oxalinic acid and O-129 (Table 2-2).

V. anguillarum J360 growth was evaluated under iron limited conditions at 15°C in TSB media with different 2,2 dipyridyl concentrations (100, 150, 250 µM). *V. anguillarum* J360 was able to grow in the presence of high concentrations of 2,2 dipyridyl. The doubling time at 100 µM of 2,2 dipyridyl was 3 h (Fig. 2-1C), however, it was increased to 4 h ($O.D._{600}$ ~0.7) and 5h ($O.D._{600}$ ~0.2) at 150 and 250 µM of 2,2 dipyridyl, respectively (Fig. 2-1C). To evaluate siderophores secretion the lowest concentration of 2,2 dipyridyl (100 µM) was used. *V. anguillarum* J360 grown under iron-enriched or iron-limited conditions were plated on CAS plates and incubated at 15°C and 28°C for 48 h. No siderophores secretion was observed in the cells grown under iron-enriched conditions. Additionally, there was no significant differences in the size of the halo for siderophores secretion between non-supplemented TSB and supplemented TSB with 100 µM of 2,2 dipyridyl at 28°C (Fig. 2-1D). Nonetheless, a small difference in halo increased diameter was observed for siderophores secretion under iron-limited condition at 15°C (Fig. 2-1D). Hemolytic activity was evaluated on blood agar plates at 28°C and 15°C. *V. anguillarum* J360 hemolytic activity was observed only at 28°C (Fig. 2-1E).

The biochemical and enzymatic profiles indicate that *V. anguillarum* J360 is able to synthetize alkaline phosphatase, esterase (C_4), esterase lipase (C_8), lipase (C_{14}), leucine, valine and cysteine arylamidase, and acid phosphatase (Appendix II). *V. anguillarum* J360 reduces nitrates and glucose, produces indole from tryptophan, produces urease, β-galactosidase, arginine hydrolase, esculinase and gelatinase, and is able to utilize arabinose, mannose, mannitol, N-acetyl-glucosamine and maltose (Appendix III and IV). The API20NE profile indicated that the isolate was *V. fluvialis*, with 99.7% probability (Appendix III).

2.4.2 MALDI-TOF and agglutination analysis.

The MALDI-TOF mass spectrometry score for *V. anguillarum* was 1.96, indicating that there was a low confidence for identification. The *V. anguillarum* agglutination test was positive for the O2 serotype and negative for the O1 serotype.

2.4.3 Infection assay in lumpfish.

Naïve cultured lumpfish (~55 g) were intraperitoneally (ip) infected with *V. anguillarum* J360 to evaluate its virulence (Fig. 2-2A and B). Two groups of 60 lumpfish were injected with $1x10^6$ CFU/dose and $1x10^7$ CFU/dose, respectively. The control group was mock infected with PBS, and mortality was monitored until 30 days post-infection (dpi). Mortality began at 2 dpi and reached 100% in both doses at 10 dpi (Fig. 2-2C). Vibriosis clinical signs were observed at 5 dpi, including hemorrhage over the lateral lines,

dorsal and/or caudal fins, ventral sucker, vent, mouth, and the operculum. Additionally, infected fish exhibited exophthalmia (Fig. 2-2B).

2.4.4 V. anguillarum J360 genome sequencing, assembly, and annotation.

V. anguillarum genomic DNA sequenced by PacBio resulted in five contiguous sequences (contigs). The larger contigs corresponded to circularized chromosome-I (3,320,860 bp), chromosome-II (1,171,281 bp), and a large plasmid pVaJ360-I (56,630 bp) with a coverage assembly of 211, 167, and 36 times, respectively. The plasmid profile of *V. anguillarum* J360 indicated that there was also a small plasmid (Fig. 2-3A). Using Illumina reads, we were able to assemble pVaJ306-II (11,995 bp) with a coverage of 226 times. The *V. anguillarum* J360 genome was submitted to NCBI under the BioProject (PRJNA485045) and BioSample (SAMN09781303). The complete genome of *V. angullarum* J360 possesses 2 chromosomes [chromosome-I (NZ_CP034672) and chromosome-II (NZ_CP034673)], a large plasmid pVaJ360-I (NZ_CP034674) and a small plasmid pVaJ360-II (MT050454), and has an estimated total length of 4.55 Mb and a G+C content of 44.6% (Fig. 2-3B and Table 2-3). RAST pipeline annotation predicted a total of 441 subsystems and 3,149 coding sequences (CDS) for chromosome-I; a total of 88 subsystems and 1,143 CDSs for chromosome-II; a total of 2 subsystems and 96 CDSs for the large plasmid pVaJ360-I; and a total of 24 CDS in a single subsystem and 1 total RNAs

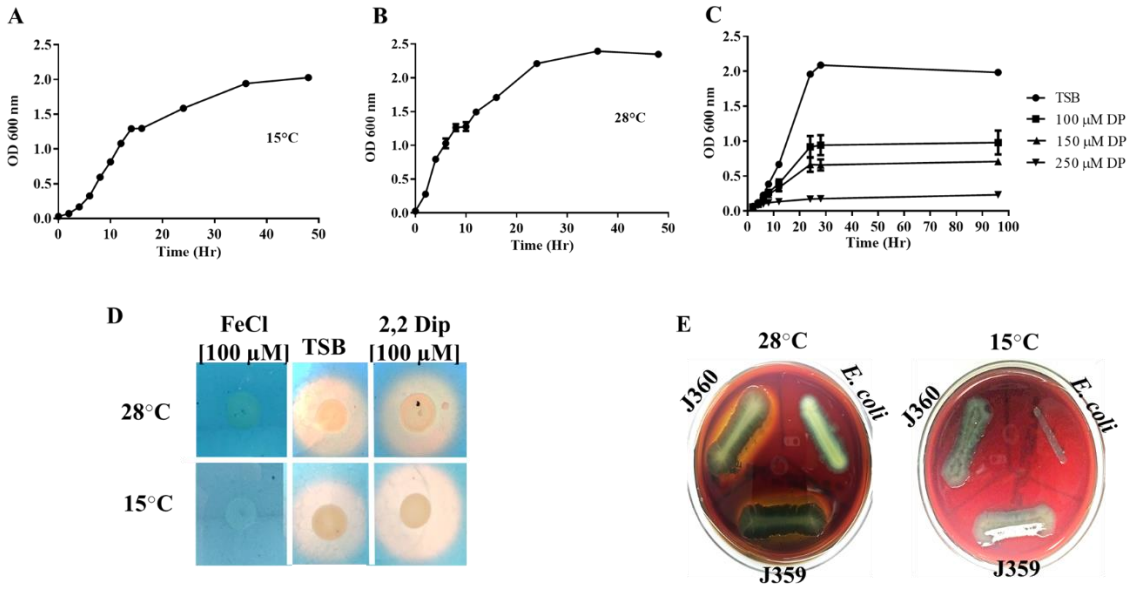

Figure 2-1. Bacterial growth and physiological characteristics of *V. anguillarum* J360. **A.** *V. anguillarum* J360 growth in TSB at 15°C for 48 h. Independent triplicates were utilized; **B.** *V. anguillarum* J360 growth in TSB at 28°C for 48 h. Independent triplicates were utilized; **C.** *V. anguillarum* J360 growth under iron limited conditions (TSB supplemented with 100, 150 and 250 µM of 2,2 dipyridyl). **D.** Siderophores synthesis on CAS agar plates from *V. anguillarum* J360 grown under iron enriched conditions (TSB supplemented with 100 µM of $FeCl_3$), standard culture conditions (TSB), and iron limited conditions (TSB supplemented with 100 µM of 2,2 dipyridyl [DIP or Dip]). The yellow reaction around the *V. anguillarum* J360 colony indicates that it is positive for siderophore synthesis. **E.** *V. anguillarum* J360 hemolysin activity assay on sheep blood agar plates incubated at 15°C and 28°C for 48 h. *V. anguillarum* J359 corresponds to a clone of *V. anguillarum* J360.

Table 2-2. Phenotypic characteristics of *V. anguillarum* J360.

Characteristic	*Vibrio anguillarum* J360
Grown at:	
4°C	+
15°C	+
28°C	+
37°C	-
LB NaCl 0%	-
LB NaCl 0.5%	+
LB NaCl 2%	+
Plate Count Agar 50% seawater	+
TCBS	-
Motility	+
Fimbria Type I	+
Siderophore synthesis	+
Catalyze	+
Oxidase	+
Antibiogram:	
Tetracycline (10 mg/ml)	31 (Susceptible)
Oxytetracycline (30 mg/ml)	34 (Susceptible)
Ampicillin (10 mg/ml)	0 (Resistant)
Sulfamethoxazole (25 mg/ml)	33 (Susceptible)
Chloramphenicol (30 mg/ml)	35 (Susceptible)
Colistin sulphate (10 mg/ml)	15 (Susceptible)
Oxalinic acid (2 mg/ml)	39 (Susceptible)
O-129	39 (Susceptible)

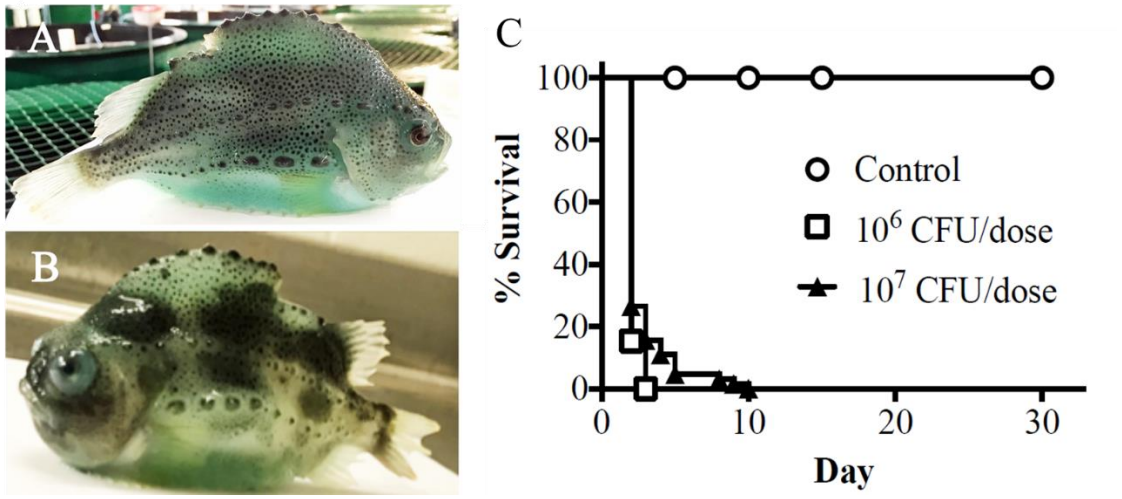

Figure 2-2. Pathogenicity and virulence of *V. anguillarum* J360. A. Healthy lumpfish cultured at the Dr. Joe Brown Aquatic Research Building (JBARB). **B.** Lumpfish infected with *V. anguillarum* J360 (5 days post-infection at 10ºC). **C.** Lumpfish survival after intra-peritoneal infection with *V. anguillarum* J360.

sequence for the small plasmid pVaJ360-II (Table 2-4). The NCBI Prokaryote Genome Annotation pipeline showed a total of 4,371 genes predicted, a total of 10 (5S), 9 (16S) and 9 (23S) rRNAs, 105 tRNAs and 4 ncRNAs for the whole genome (Table 2-5).

2.4.5 Whole genome alignment, phylogeny and synteny.

Phylogenetic analysis of *Vibrio* spp. was performed using only complete genome sequences (Table 2-1). Phylogenetic analysis of chromosome-I showed that there are three clusters with three or more strains, whereas *V. tasmaniensis*, *V. parahaemolyticus* and *V. campbellii* clustered together as one and *V. fluvialis* clustered separately. In contrast, *V. anguillarum* species were represented by two clusters plus *V. anguillarum* strains CNEVA, MHK3, VIB12, NB10 and 8-9-116 that clustered separately. *V. anguillarum* J360 was closely related to *V. anguillarum* VIB43 isolated from Scotland, UK (Fig. 2-4A, Table 2-1). Phylogenetic analysis of chromosome-II indicated four clusters, whereas non-*V. anguillarum* species cluster together, and *V. fluvialis* clustered separately (Fig. 2-4B). Similar to chromosome-I, *V. anguillarum* J360 chromosome-II was closely related to *V. anguillarum* VIB43 (Fig. 2-4B). Same results were observed in the phylogenetic analysis using MEGA X for chromosome-I (Appendix V-A) and chromosome-II (Appendix V-B). The heat maps indicated that there was high identity between *V. anguillarum* J360 and *V. anguillarum* VIB43 alignments of chromosome-I (Fig. 2-4C) and chromosome-II (Fig. 2-4D), respectively. The ANI analysis for whole genome alignment indicates a 99.95% for chromosome-I (Appendix VI-A) and an 99.93% for chromosome-II of genome identity (Appendix VI-B) that support previous observed results. Dot plot visualization matches

between *V. anguillarum* J360 and the closest related strain, *V. anguillarum* VIB43, showed that there was high similarity within the genome. However, two reversion events and genomic gaps (GGs) were identified (Fig. 2-5A and B). The whole genome alignment identified several Locally Collinear Blocks (LCBs), described as conserved segments free from genomic rearrangements (Darling, 2004). The comparative alignment analysis of each chromosome showed 5 LCBs in chromosome-I (Fig. 2-5C) and 2 LCBs in chromosome-II (Fig. 2-5D). Additionally, the LCBs identified in both chromosomes are conserved, and in agreement with the reversion events and GGs identified in the dot plot analysis (Fig. 2-5 and Appendix VIII).

2.4.6 Multi-locus sequence analysis (MLSA) and phylogeny.

We also utilized MLSA to contrast these results with the whole genome analyses. MLSA was computed using the nine housekeeping genes listed in Appendix I. Gene sequences were aligned, concatenated, and analyzed. The phylogenetic analysis showed that there were 5 clusters with at least 2 strains, whereas *V. anguillarum* J360 clustered alone. This analysis indicated that *V. anguillarum* J360 is closely related to *V. anguillarum* NB10, which clustered with *V. campbelli* and *V. tasmaniensis,* and is distantly related to *V. anguillarum* 775 and *V. anguillarum* M3 (Appendix VII-A). Same results were observed using MEGA X software (Appendix VII-B).

2.4.7 Distribution of genes associated with pathogenesis and environmental adaptation in V. anguillarum J360.

Gene distribution within the *V. anguillarum* J360 chromosomes was determined for virulence and environmental adaptation related genes (Table 2-6). Genes associated to iron homeostasis were identified, including ferrous and ferric transport, and regulatory mechanisms. In chromosome-I genes like ferric iron uptake transcriptional regulator (*fur*), *tonB1, tonB2,* and *feoABC* uptake system were identified. Hemolysis activity-related genes like heme transport (DYL72_00770, DYL72_02835), TonB-dependent hemoglobin receptors (DYL72_17445, DYL72_00730, DYL72_20920), and heme transporters (CcmB and CcmD) were distributed in both chromosomes. Furthermore, five hemolysin encoding genes (DYL72_01800, DYL72_07805, DYL72_12295, DYL72_17765) were found distributed in both chromosomes, including a thermolabile hemolysin (DYL72_17760) in chromosome-II.

Toxin-antitoxin associated genes were also identified. We found that *V. anguillarum* J360 possesses five different type II toxin-antitoxin system protein families, such as RelBE/ParDE/DinJ, Txe/YoeB, PhD/YefM, YafQ and a prevent-host-death system located in chromosome-II. Also, a toxin precursor gene (*rtxA*), a serine/threonine-protein kinase gene (*hipA*), and 4 toxin genes (DYL72_00035, DYL72_00045, DYL72_14975, DYL72_14985) were found in chromosome-I, and an antibiotic resistance gene *ampC* was found in chromosome-II.

Metalloprotease coding genes were found in both chromosomes, including a CPBP family intermembrane metalloprotease (DYL72_00295), a *sprT* family zinc-dependent metalloprotease (DYL72_09830) gene, and 3 metalloprotease genes (*pmbA*, *tldD* and *ftsH*)

are present in chromosome-I. Additionally, a M6 family domain that possesses metallopeptidase activity was found in chromosome-I. Motility genes were found in chromosome-I, except for flagellar motor brake proteins that were found in chromosome-II. Chemotaxis genes were found on both chromosomes, including 17 genes in chromosome-I and 16 genes in chromosome-II that encode for methyl-accepting chemotaxis proteins. Four copies of *cheV* and 5 copies of *cheW* were also found, and these are involved in phosphorylation-dependent excitation and methylation-dependent adaptation, respectively. We identified 5 type IV pilus associated genes in chromosome-I, and type VI secretion system related genes in both chromosomes, including 6 copies of *tssI*, and 2 operons encoding *tssBCEFG* and *tssKJHFE2*. Two secretion system families were identified, including the Hcp type VI secretion system family effector and DotU family type IV and type VI secretion system related proteins. A single quorum-sensing associated gene was found in chromosome-II, which is a quorum-sensing autoinducer synthase. Transcriptional regulators were found in chromosome-I, such as *lysR*, *cysB*, *nhaR* and *hfq*, and *luxR* was present in both chromosomes.

2.4.8 Genomic Islands (GIs).

Twenty-one putative GIs were identified within the chromosomes; 15 GIs in chromosome-I and 6 GIs in chromosome-II, respectively (Fig. 2-6; Supplementary File 1 and 2). The GIs size ranged from 5 kb to 73.4 kb with a total of 724 genes. The largest genomic island (GI15) (Fig. 2-6) consisted of 147 genes (predicted by at least one of the

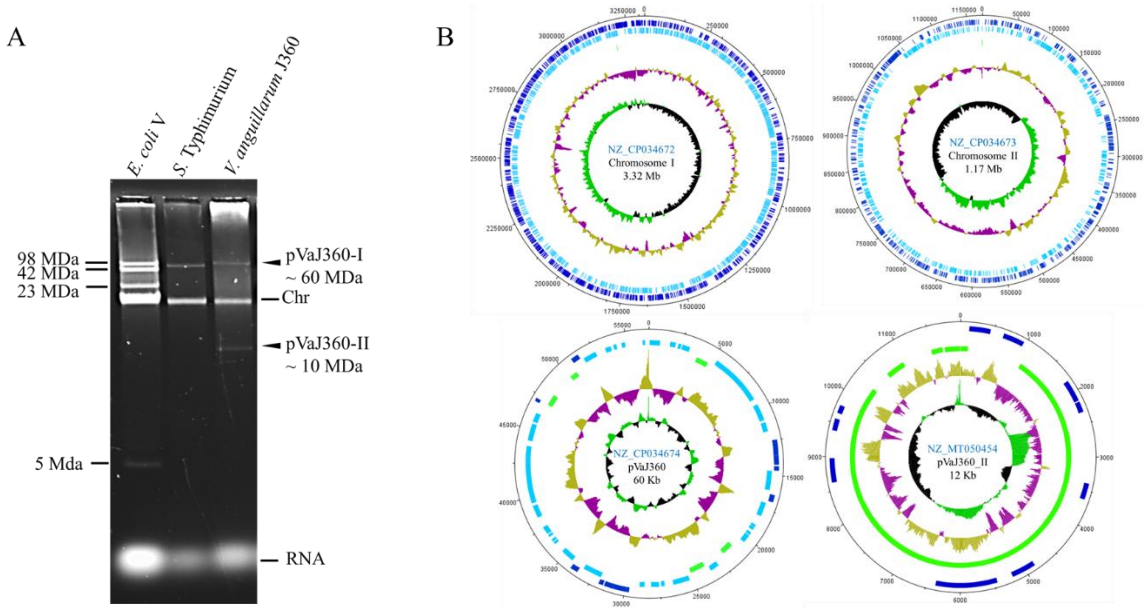

Figure 2-3. *V. anguillarum* J360 genome visualization. A. *V. anguillarum* J360 plasmid profile in 0.5% agarose using nucleic acid alkaline extraction; *E. coli* V and *S.* Typhimurium UK-1 (χ3761) were used as markers; Chr: chromosomal band; **B.** Genome map of *V. anguillarum* strain J360. Chromosome I, chromosome II, large plasmid pVaJ360-I (~ 60 MDa) and small plasmid pVaJ360-II (~10 MDa) were mapped using DNA plotter. Blue bars represent forward genes, light blue bars represent reverse genes, and green bars represent pseudogenes and miscellaneous_features. Gold (high) and violet (low) represent G+C content percent. Green (high) and black (low) represent G+C skew plot.

three software used, see method section), and was flanked by two site-specific integrase genes and a zinc ribbon-domain protein.

Genes encoding for integrases, porins, transposases, and iron transport were found among the GIs. Genes such as phosphonate C-P lyases, associated with the cleavage of carbon-phosphorus compounds for organic phosphorus reservoir in marine bacteria (Villarreal-Chiu et al., 2012), zinc ribbon domain proteins, AbrB/MazE/SpoVT DNA-binding domains, a ParA domain, for a GCN5-related N-acetyltransferase (GNAT) associated with regulatory post-transcriptional acetylation (Favrot et al., 2016), two site-specific integrases, and a MasF transcriptional regulator related to toxin/anti-toxin systems (Supplementary File 1) were identified in these GIs. GI5 is the smallest genomic island identified in *V. anguillarum* J360 (Fig. 2-6) and possesses five unique genes which encode for acetyltransferase, acyltransferase, formyltransferase, asparagine synthase, and one hypothetical protein (Supplementary File 1).

2.4.9 V. anguillarum large plasmid analysis.

The plasmid profile indicates that *V. anguillarum* J360 harbors one large plasmid and one small plasmid (Fig. 2-3A). The large plasmid pVaJ360-I (~60 kb) has genes that encode for integrases, DNA-binding proteins, peptidases, site-specific integrases, resolvase, mobile elements, and pro-phages. Comparative analysis showed that pVaJ360-I is not related to *V. anguillarum* virulent plasmids such as pJM1 (strain 775) and p65 (strain ATCC-68554), pJM1-like plasmid, p67 (strain NB10) and p15 (strain VIB43) (Appendix

IX-A). The ANI analysis of these plasmids demonstrated that pVaJ360-I does not has percentage of identity with pJM1 or pJM1-like plasmids (Appendix IX-B), suggesting that pVaJ360 is not a virulent plasmid.

The small plasmid pVaJ360-II (~12 kb) has only 10 CDSs that encode for hypothetical proteins, transposases, mobile elements, a transcriptional regulator LysR, a tRNA Glu, and additionally 14 miscellaneous-features. BLASTn analysis indicates that this plasmid has no similarities with the pJM1 or pJM1-like plasmids described above.

Table 2-3. Summary of genome: two chromosome and two plasmids.

Labels	Size (Mb)	Topology	RefSeq ID	INSDC Identifier
Chromosome 1	3.32	Circular	NZ_CP034672	CP034672
Chromosome 2	1.17	Circular	NZ_CP034673	CP034673
Plasmid pVaJ360	0.06	Circular	NZ_CP034674	CP034674
Plasmid pVaJ360_II	0.012	Circular	NZ_MT050454	MT050454

*** INSDC; International Nucleotide Sequence Database Collaboration**

Table 2-4. Genome RAST annotation summary.

	Chromosome 1	Chromosome 2	Plasmid pVaJ360	Plasmid pVasJ360_II
Genome Size	3,320,860 bp	1,172,081 bp	56,630 bp	11,995 bp
G+C Content	44,6%	44.1%	43.7%	47%
Number of Subsystems	441	88	2	1
Number of Coding Sequences	3149	1143	96	24
Number of RNAs	129	5	-	1

Table 2-5. Prokaryotic genome annotation summary.

Attribute	Data Provided
Annotation Pipeline	NCBI prokaryotic Genome Annotation pipeline
Annotation Method	Best placed reference protein set; GeneMarks v4.6
Genes (total)	4,371
CDSs (total)	4,234
Genes (coding)	3,966
Genes (RNA)	137
rRNAs	10, 9, 9 (5S, 16S, 23S)
Complete rRNAs	10, 9, 9 (5S, 16S, 23S)
tRNAs	105
ncRNAs	4
Pseudogenes (total)	268
Pseudogenes (ambiguous residues)	0 of 268
Pseudogenes (frameshifted)	105 of 268
Pseudogenes (incomplete)	163 of 268
Pseudogenes (internal stop)	45 of 268
Pseudogenes (multiple problems)	41 of 268

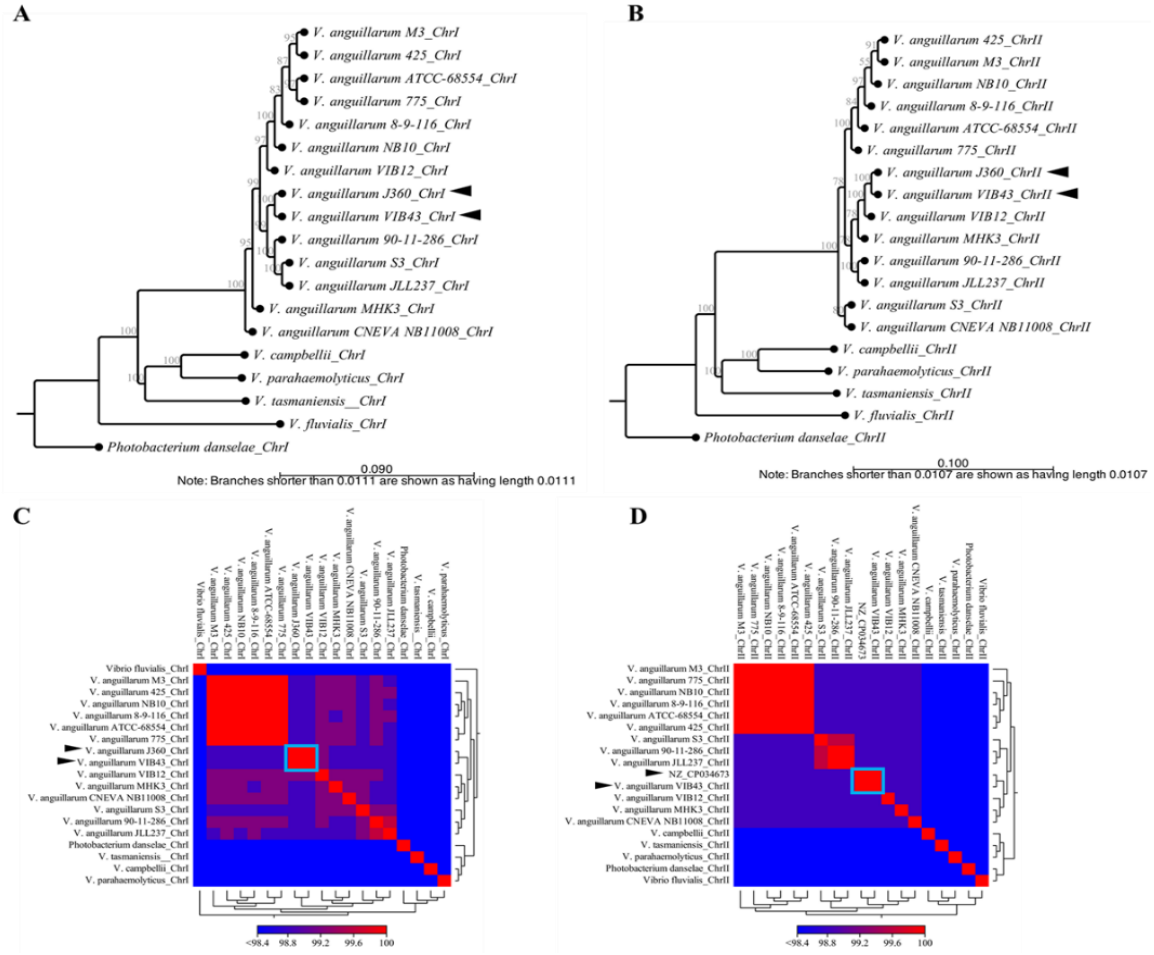

Figure 2-4. Phylogenetic and comparative genomic analysis of *V. anguillarum* J360. **A.** Phylogenetic history of *V. anguillarum* J360 chromosome-I; **B.** Phylogenetic history of chromosome-II. Evolutionary history was inferred using Neighbor-Joining method, with a bootstrap consensus of 500 replicates for taxa analysis. Evolutionary distance was computed using Jukes-Cantor method. All ambiguous positions were removed for each sequence pair (pairwise deletion option). **C.** Heat map visualization of aligned sequences identity for *V. anguillarum* J360 chromosome-I; **D.** Heat map visualization of aligned sequences identity for *V. anguillarum* J360 chromosome-II; Whole genome alignments and the phylogenetic analysis involved 18 *Vibrio sp*. listed in Table 1. *Photobacterium damselae* 91-197 as an outgroup. Analysis was performed using CLC workbench v.20 (CLC Bio). Black arrows represent *V. anguillarum* J360 genome and *V. anguillarum* VIB43 as the closest related strain, light blue square represent percentage of identity between strains.

Table 2-6. Predicted genes associated with subsystems of pathogenesis and environmental adaption.

Gene Subsystem Category and Name	Presence/Absence of Gene in *V. anguillarum* J360. Chr 1	Chr 2	GenBank Accession N°
Iron transport and regulation			
iron-regulated protein A	X		DYL72_00705
tonB2, exbD2	X		DYL72_00755, DYL72_00745
tonB1, exbB, exbD1	X		DYL72_00260, DYL72_00265, DYL72_00270
fur	X		DYL72_03070
iron ABC transport permease	X		DYL72_00175, DYL72_00765
Heme transport			
Ton-B dependent hemoglobin receptor	X	X	DYL72_17445, DYL72_00730, DYL72_20920
hutXZ	X		DYL72_00735, DYL72_00740
heme ABC transporter protein	X		DYL72_00770, DYL72_02835
heme exporter protein *ccmBD*	X		DYL72_02830, DYL72_02840
Ferrous and ferric transport			
ferric ABC transporter	X		DYL72_00180
feoABC	X		DYL72_02945, DYL72_02940, DYL72_02935
Ferrichrome			
fhuACBD	X		DYL72_06770, DYL72_10590
Hemolysins			
hemolysin genes	X	X	DYL72_01800, DYL72_07805, DYL72_12295, DYL72_17765
thermolabile hemolysin		X	DYL72_17760
Toxin-associated genes			
toxins and pseudo genes	X		DYL72_00035, DYL72_00045, DYL72_14975, DYL72_14985
rtxA, hipA	X		DYL72_01180, DYL72_03440
type II toxin-antitoxin system RelBE/ParDE/DinJ family		X	DYL72_18560, DYL72_18565, DYL72_18715, DYL72_18750, DYL72_19140, DYL72_19250, DYL72_19960
type II toxin-antitoxin system prevent-host-death family antitoxin		X	DYL72_18805
Txe/YoeB family addiction module		X	DYL72_18810
type II toxin-antitoxin system Phd/YefM family antitoxin		X	DYL72_19255
type II toxin-antitoxin system YafQ family toxin		X	DYL72_19965
toxin-antitoxin system subunit antitoxin		X	DYL72_20370

Metalloproteases			
CPBP family intramembrane metalloprotease	X		DYL72_00295
pmbA, tldD, ftsH	X		DYL72_05300, DYL72_09550, DYL72_10735
SprT family zinc-dependent metalloprotease	X		DYL72_09830
M6 family metalloprotease domain-containing protein		X	DYL72_17780
Secreted enzymes			
phospholipase gene		X	DYL72_16230
lipase		X	DYL72_17465, DYL72_18050, DYL72_20375
Motility and chemotaxis			
fliRQPONMLKJIHGFE, fliSTD, fliL	X		DYL72_03140-DYL72_03205, DYL72_03225-DYL72_03235, DYL72_08330
motYA, motB	X		DYL72_12660, DYL72_00275, DYL72_12090
flhFAB	X		DYL72_02900, DYL72_02905, DYL72_03135,
flag, flaCA	X		DYL72_03240, DYL72_03670, DYL72_03675
flagellin	X		DYL72_03245, DYL72_03250, DYL72_03255
flgLKJIHGFEDCB, flgAMNP	X		DYL72_03685-DYL72_03735, DYL72_03750-DYL72_03765
flagellar basal -body protein	X		DYL72_03775
pomA	X		DYL72_12085
flagellar brake protein		X	DYL72_17355, DYL72_20195
methyl-accepting chemotaxis protein	X (17)	X (16)	
chemotaxis response regulator protein-glutamate methylesterase	X	X	DYL72_00595, DYL72_02870, DYL72_16590
cheD, cheW, cheA, cheV, cheY, cheX, cheC	X	X	, DYL72_00600, DYL72_00610, DYL72_00620, DYL72_01045, DYL72_02885, DYL72_09235, DYL72_20035
cheV2, cheW2, cheW3, cheA2, cheV3, cheD2, cheW4, cheW5, cheA3, cheV4	X	X	DYL72_02435, DYL72_02855, DYL72_02860, DYL72_02875, DYL72_03745, DYL72_16595, DYL72_16610, DYL72_16615, DYL72_16620, DYL72_21345
chemotaxis protein	X	X	DYL72_00635, DYL72_16275, DYL72_16460
chemotaxis protein methyltransferase	X		DYL72_03740

Type IV pilus			
pilQ, pilW, pilM, pilT, pilB	X		DYL72_05800, DYL72_01100, DYL72_05820, DYL72_09795, DYL72_10350
Type VI secretion system (T6SS)			
tssI, tssBCEFG, tssJ, tssK tssH, tssAM		X	DYL72_16415, DYL72_17000 - DYL72_17020, DYL72_17030, DYL72_17045, DYL72_17055, DYL72_17070, DYL72_17075, DYL72_17085, DYL72_21115,
tssI2, tssM2, tssKJHFE2, tssC2, tssI3, tssI4, tssI5, tssI6	X	X	DYL72_00885, DYL72_00895, DYL72_00900, DYL72_00930, DYL72_00940, DYL72_00945, DYL72_00955, DYL72_00960, DYL72_00975, DYL72_02685, DYL72_10015
tagHO		X	DYL72_17025, DYL72_17065
Hcp family type VI secretion system effector	X	X	DYL72_16420, DYL72_18695, DYL72_21120, DYL72_02690, DYL72_10010
type VI secretion system tube protein Hcp	X		DYL72_00965
DotU family type IV/VI secretion system protein	X	X	DYL72_17050, DYL72_00890
type VI secretion protein	X	X	DYL72_17080, DYL72_00950, DYL72_00970, DYL72_00985
type VI secretion system PAAR protein	X	X	DYL72_21095, DYL72_02650, DYL72_02660, DYL72_10045,
type VI secretion protein VasB-1	X		DYL72_00935
Quorum sensing			
quorum-sensing autoinducer synthase		X	DYL72_17995
Regulators			
transcriptional regulator *luxR*	X	X	DYL72_06050, DYL72_21285
transcriptional regulator *lysR*	X		DYL72_03060, DYL72_09990
transcriptional regulator XRE	X		DYL72_10570
cysB	X		DYL72_13470
nhaR	X		DYL72_10935
hfq	X		DYL72_09115

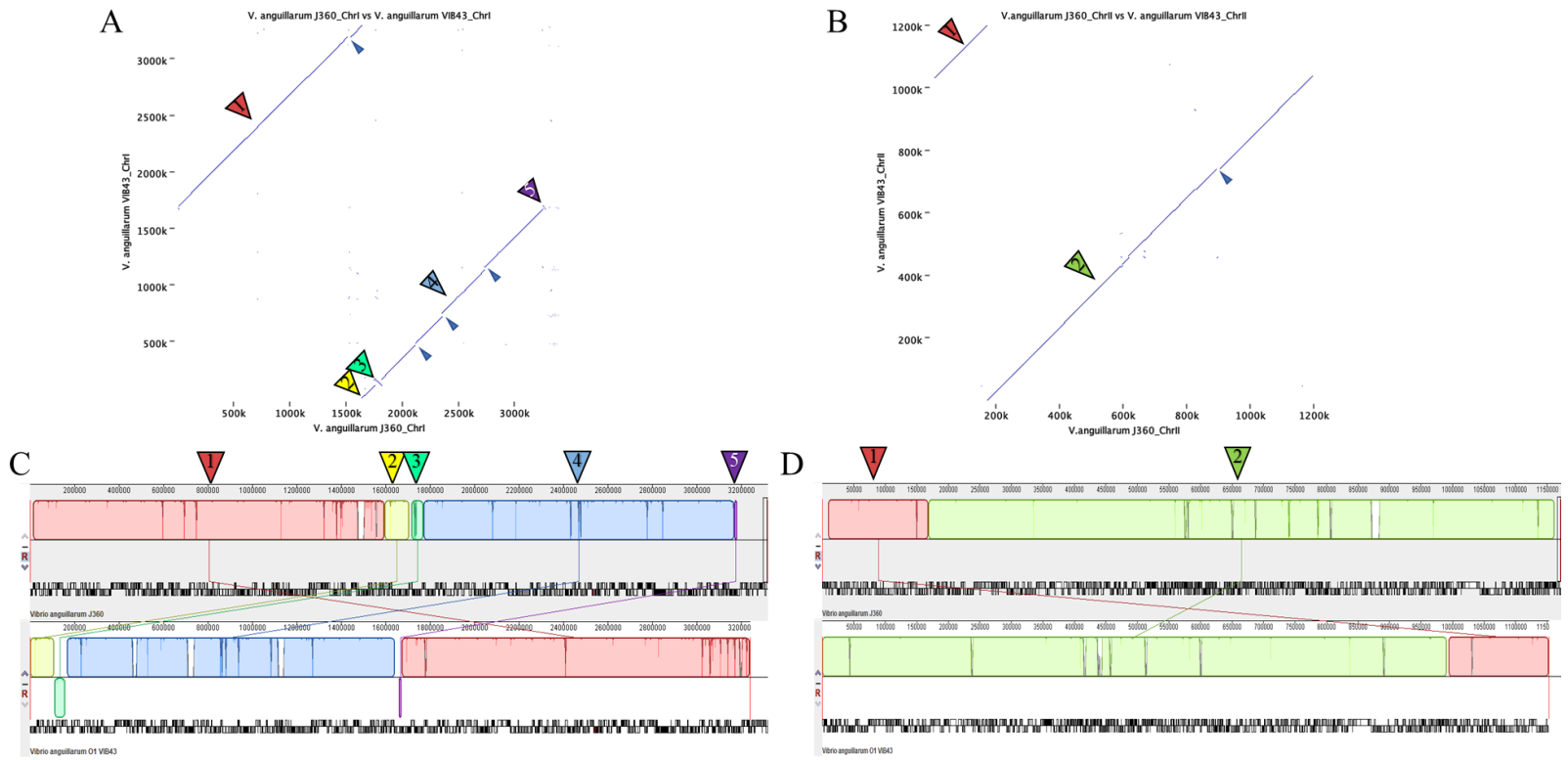

Figure 2-5. Comparative genome synteny between *V. anguillarum* J360 and *V. anguillarum* VIB43. A. Dot plot analysis for chromosome-I; **B.** Dot plot analysis for chromosome-II. Numerated arrows represent homologous regions and arrowheads represent inversions. Dot plots were computed using CLC Genomics Workbench v.20; **C.** Homologous regions identified as locally colinear blocks (LCBs) (numerated arrows) of chromosome-I; **D.** LCBs (numerated arrows) of chromosome-II**.**

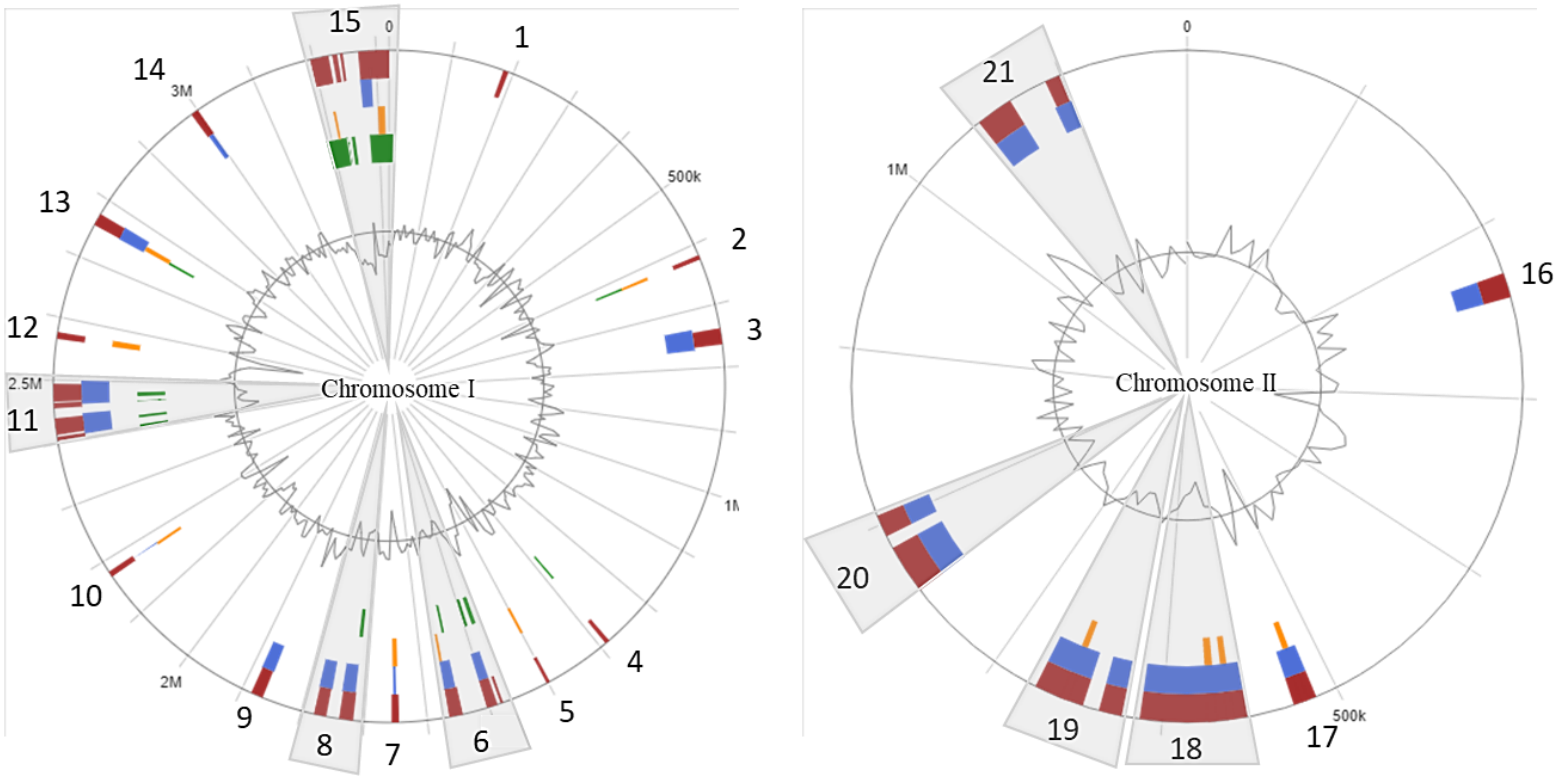

Figure 2-6. *V. anguillarum* J360 genomic islands (GIs). Genomic islands (GIs) detected in chromosome-I; Genomic islands (GIs) detected in chromosome-II. Red bars represent GIs detected using 3 different packages; blue bars represent the GIs detected with SIGI-HMM package; orange bars represent the GIs detected with the IslandPath-DIMOB package; green bars represent the GIs detected with the IslandPick package.

2.5 Discussion

Lumpfish in hatcheries and at cage sites frequently show signs of systemic bacterial infection, including skin lesions, gill hemorrhages, and bacterial aggregations in the lymphoid organs (i.e. spleen, liver, head kidney) (Powell et al., 2017). In the United Kingdom, Iceland and Norway, several bacterial outbreaks have been reported in lumpfish hatcheries and at cage sites, and the most frequent pathogen detected is *V. anguillarum* (Marcos-Lopez et al., 2013). Thus, it is not surprising that this pathogen was found to be present in Atlantic Canada.

V. anguillarum serotypes O1, O2 and O3 are the most prevalent strains among the 23 serotypes currently described (Pedersen et al., 1999; Sørensen & Larsen, 1986). Agglutination assays indicated that *V. anguillarum* J360 is O2, similar to other *V. anguillarum* strains isolated from lumpfish infections in the North Atlantic (Marcos-Lopez et al., 2013). The biochemical profile obtained using API20NE showed that *V. anguillarum* J360 was able to reduce sugars, urea and produce indole, suggesting a 99% possibility for *V. fluvialis* (Appendix III). Although the biochemical profile did not identify *V. anguillarum* J360, its phenotypic characterization is consistent with other *V. anguillarum* isolates (Myhr et al., 1991; Ramasamy et al., 2018), except that *V. anguillarum* J360 was positive for urease (Appendix III). This result is coincident with the presence of the urease encoding gene in chromosome-II (DYL2_19555). Also, *V. anguillarum* J360 was not able to grow in TCBS selective media suggesting susceptibility to bile salts (Table 2-2).

V. anguillarum J360 showed a thermo-inducible α-hemolysin activity at 28°C, but no hemolytic activity was observed at temperatures below 15°C (Fig. 2-1E). Hemolytic

activity is an important virulence factor for *V. anguillarum* (Li et al., 2011). For instance, severe hemorrhages are a typical clinical sign of *V. anguillarum* infection in fish, including lumpfish (Marcos-Lopez et al., 2013). Coincidently, in the current study, *V. anguillarum* J360 was shown to be highly virulent in lumpfish, and infected lumpfish displayed severe hemorrhagic clinical signs at 5 dpi (Fig. 2-2B), similar to other strains described in Marco-Lopez *et al*. (2013). Koch's postulates for *V. anguillarum* J360 showed that lumpfish infected with $1x10^6$ and $1x10^7$ CFU/dose reached 100% mortality within 10 dpi at 10ºC (Fig. 2-2C). Also, *V. anguillarum* was re-isolated from spleen, liver, and head-kidney, confirming Koch´s postulates. The original *V. anguillarum* outbreak in cultured lumpfish and the infection assays in the current study showed similar clinical signs (Fig. 2-2B). *V. anguillarum* hemolytic activity was evident during infection. However, the lumpfish is a cold-water fish typically cultured between 6-12ºC (Boyce et al., 2018). These results were contradicted with the *V. anguillarum* thermo-inducible hemolytic activity at 28ºC (See Fig. 1E). Perhaps, internal fish conditions (e.g. innate and adaptive immunity) triggered *V. anguillarum* hemolytic activity. These results suggest that its regulatory mechanisms need further analysis.

V. anguillarum J360 possesses two chromosomes, a large plasmid, and a small plasmid (Fig. 2-3 and Table 2-4). *Vibrio* spp. and *V. anguillarum* genomes selected for phylogenetic and comparative genomics analysis possess two chromosomes and one large plasmid (Table 2-1). Typically, serotype O1 harbors a virulent plasmid, called pJM1 or pJM1-like, and serotypes O2 and O3 possess a non-virulent large plasmid (Castillo et al., 2017; Steinum et al., 2016) or they do not harbor large plasmids (Holm et al., 2018; Rasmussen et al., 2016). *V. anguillarum* J360 is a O2 serotype that does not harbor a

virulence plasmid (Appendix IX), suggesting that this strain could increase its virulence if a virulence plasmid is acquired.

The total genome size *V. anguillarum* J360 is 4,561,566 bp (Table 2-4), which is larger than the currently available *V. anguillarum* genomes (Table 2-1). This may suggest that *V. anguillarum* J360 may have acquired genetic material through horizontal gene transfer and/or adapted to its lumpfish host or to environmental conditions in Atlantic Canada.

Phylogenetic distance based on the whole genome alignment analysis of chromosome-I and chromosome-II showed that *V. anguillarum* J360 is closely related to *V. anguillarum* VIB43, and distantly related to *V. anguillarum* VIB12 (Fig. 2-4A and B). Interestingly, *V. anguillarum* VIB43 and VIB12 were isolated from the same host species, sea bass (*Dicentrarchus labrax*), but from different locations. *V. anguillarum* VIB43 was isolated in Scotland and *V. anguillarum* VIB12 was isolated from the Mediterranean Sea (Holm et al., 2018). The ANI analysis between *V. anguillarum* J360 and *V. anguillarum* VIB43 showed a 99.93% of identity for chromosome-I and 99.95% for chromosome-II (Fig. 2-4 and Appendix VI), which suggest that these two strains share a common ancestor.

Additionally, the whole genome phylogenetic analysis showed that *V. anguillarum* J360 and VIB43 are not closely related to *V. anguillarum* 775, M3 and NB10, which is contradictory to previous MLSA studies that indicated that *V. anguillarum* VIB43 and VIB12 are closely related to those *V. anguillarum* strains (Castillo et al., 2017; Holm et al., 2018). The MLSA compute phylogenetic trees based on concatenated conserved sequences (Glaeser & Kämpfer, 2015; Steinum et al., 2016). In this study, we used nine housekeeping genes, including 16S rRNA, *ftsZ, gapA, gyrB, mreB, pyrH, recA, rpoA* and *topA* (Appendix

I). In contrast to the whole genome phylogenetic analysis, the MLSA showed that *V. anguillarum* J360 clusters alone, and the closest related strain is *V. anguillarum* NB10 isolated from rainbow trout (*Oncorhynchus mykiss*) in the Gulf of Bothnia, Sweden (Holm et al., 2015), and distantly related to *V. anguillarum* 775 and M3 strains (Appendix VII, Table 2-1). *V. anguillarum* M3 was isolated from Japanese flounder (*Paralichthys olivaceus*) in Shandong, China, and classified as closely related to *V. anguillarum* 775 isolated from Coho salmon (*Oncorhynchus kisutch*) in the Pacific Coast of the USA (Li et al., 2013; Naka et al., 2011). In contrast, MLSA phylogenetic analysis based only on 16S rRNA gene showed that *V. anguillarum* NB10 is closely related to *V. anguillarum* M3 (Holm et al., 2015).

In contrast to the MLSA analysis, the whole genome phylogenetic analysis of *V. anguillarum* strains it is in concordance with the geographic origin of the strain isolation. For instance, according to the whole genome phylogenetic analysis, *V. anguillarum* J360 and *V. anguillarum* VIB43, both isolated in the North Atlantic Ocean, are highly related, and closely related to *V. anguillarum* strains 90-11-286, S3, JLL237 isolated in Finland (Table 2-1, Fig. 2-4). Actually, these geographic locations are natural habitat for lumpfish populations (Whittaker et al., 2018).

In contrast to the whole genome phylogenetic analysis, the MLSA uses protein-coding genes, which evolved at a slow, but constant rate and this could have better resolution, especially at the species level (Glaeser & Kämpfer, 2015; Steinum et al., 2016). However, the selection and number of coding genes, alignment method, are variable for MLSA. We found that the phylogenetic analysis using whole genomes is more reliable than MLSA, and the robustness of our analyses was showed to be consistent with two different

software. In addition, whole genome analyses allow that homologous regions, deletion, translocation, and inversion events can be identified.

Genome alignment and synteny analysis between *V. anguillarum* J360 and *V. anguillarum* VIB43 showed a high similarity within the chromosome sequences, but reversions and unmatched regions were also observed (Fig. 2-5A and B). This suggests that homologous recombination events play an important role in *V. anguillarum* evolution, perhaps influenced by insertion sequence (IS) elements such as a chromosomal integrons or "super integrons" (SIs) described *Vibrio* spp. and several Gram-negative species (Holm et al., 2018). We determined that there are 5 LCBs in chromosome-I (Fig. 2-5C) and 2 LCBs in chromosome-II (Fig. 2-5D) shared between *V. anguillarum* J360 and VIB43. Further, analysis revealed that all the LCBs present in chromosome-I had small inversion events (Fig 2-5A and C). Also, we found that LCBs-1 and -4 have genome gaps (GGs) or unmatched regions in both strains (Fig. 2-5A and Appendix VIII-A). The GGs identified in the LCB-1 of *V. anguillarum* J360 chromosome-I are not present in *V. anguillarum* VIB43 LCB-1 (Appendix VIII-A). These identified GGs possess several genes that encode for IS families transposases (IS66, ISL3, IS3, IS5) and site-specific integrases previously described in the *V. anguillarum* VIB43 genome, and with high similarity to *V. anguillarum* NB10, 775 and ATCC-6855 genomes (Holm et al., 2018; Holm et al., 2015). We found that the unique GGs in LCB-1 of *V. anguillarum* J360 possess genes related to iron uptake and iron homeostasis (Appendix VIII-A), suggesting that these genes could be acquired by horizontal gene transfer.

In *V. anguillarum* J360 chromosome-II, two GGs were identified in LCB-1 and LCB-2 (Appendix VIII-B), and both GGs have an IS630-like element belonging to the

ISVa15 transposase family. This IS630-like element not present in *V. anguillarum* VIB43 LCBs. According to the description of Holm *et al.* (2018), ISVa3-ISVa20 are new insertion sequence (IS) elements in the *V. anguillarum* genomic repertory that are responsible for the divergency within strains. This suggests that *V. anguillarum* J360 and *V. anguillarum* VIB43 could be derived from a common ancestor and adapted to local environmental conditions and host species.

Pathogenesis-associated genes were found in both chromosomes, but chromosome-I harbor most of virulence genes and their respective transcriptional regulators (Table 2-6). No virulence associated genes were found in pVaJ360-I or pVaJ360-II. The *V. anguillarum* virulence plasmid pJM1 possesses intrinsic virulence genes associated with iron uptake, like anguibactin biosynthesis (*angA*-*angE*, *vabA*-*E*) and anguibactin transport (*fatA*-*fatD*) (Naka & Crosa, 2011; Naka et al., 2010; Naka et al., 2011). In contrast, all the *V. anguillarum* J360 iron homeostasis related genes are in its chromosomes. For instance, genes related to ferric-anguiobactin and siderophore uptake (e.g., *exbB* and *exbD2*, respectively) are present in chromosome-I. Comparative genomic analyses showed that the large virulent plasmids pJM1, P67-NB10 and p65-ATCC have high similarity (Figs. S5A-B). However, the large plasmid pVaJ360-I and the small plasmid pVaJ360-II of *V. anguillarum* J360 does not present similarity (Appendix IX-A) or identity (Appendix IX-B) with other reported plasmid sequences, nor does possess virulence associated genes. This suggests that *V. anguillarum* J360 does not harbor plasmid previously described in *V. anguillarum*, including serotype O2 strains (Castillo et al., 2017).

Hemolysins are important virulence factors for *V. anguillarum* species, and contribute to its attachment, tissue colonization and iron homeostasis, thus increasing its

pathogenicity (Hirono et al., 1996; Rock & Nelson, 2006). *V. anguillarum* J360 has 4 hemolysin genes, and these are consistent with the hemorrhagic clinical signs observed in lumpfish during the infection assays (Fig. 2-2B). In addition, a thermolabile hemolysin gene is present in chromosome-II, that can be related to the thermo-inducible hemolytic phenotype of *V. anguillarum* J360 (Fig. 2-1E).

The resistance of *V. anguillarum* J360 to ampicillin (Table 2-2) relates to the presence of a class C beta-lactamase (*ampC*) encoding gene in chromosome-II. Metalloproteases such as *pmbA*, *tldD* and *ftsH* genes, which are associated to carbon storage, hydrolysis of peptide bonds, and virulence, were also identified.

V. anguillarum J360 does not possess some of the virulence genes present in *V. anguillarum* strains isolated from the Pacific coasts, including the metalloproteases *empA* and *prtV* (Naka & Crosa, 2011; Naka et al., 2011). Nonetheless, *V. anguillarum* J360 harbors a M6 family metalloprotease (DYL72_17780) similar to the *prtV* gene, associated to gelatinase activity (Appendix III).

In addition, genes that encoded for secreted enzymes such as phospholipase and lipases were found in chromosome-II, which correlates with the lipase (C_{14}) positive phenotype observed in the enzymatic profile (Appendix III). *V. anguillarum* J360 possesses several genes associated with flagella and motility, such as the operons *fliRQPONMLKJIHGFE* (DYL72_03140-DYL72_03205), *flgLKJIHGFEDCB* (DYL72_03685-DYL72_03735) and *motYBA* (DYL72_12660, DYL72_00275, DYL72_12090) located in chromosome-I, which is consistent with the mot^+ phenotype of *V. anguillarum* J360 (Table 2-2).

Virulence factors present in other *V. anguillarum* genomes (e.g., *V. anguillarum* 775 and *V. anguillarum* M3) were not identified in *V. anguillarum* J360 genome. These include mannose-sensitive hemagglutinin type 4 pilus (MHSA) (Marsh & Taylor, 1999; Naka et al., 2011), *vstA-vstH* genes encoding for components of the Type VI secretion system (Weber et al., 2009) and *virA-virB* genes related to lipopolysaccharides synthesis (Naka & Crosa, 2011).

In concordance with the locations of the virulence factors, transcriptional regulators ending genes such as *luxR*, *lysR*, *cysB*, *nhaR* and *hfq* were mostly located in chromosome-I, and an additional copy of *luxR* was found in chromosome-II. LuxR belongs to a transcriptional activators family, that together with an N-(3-oxodecanoyl)-L-homoserine lactone (ODHL), mediates the signal transduction mechanisms of quorum-sensing genes such as *luxICDABE* operon (Milton et al., 1997). The duplication of *luxR* in *V. anguillarum* J360 suggests that quorum-sensing plays an important role in the biology of this strain.

Genomic Islands (GIs) have been identified in *V. anguillarum* species, for instance *V. anguillarum* NB10 possesses 29 GIs (Holm et al., 2015), *V. anguillarum* 775 possesses 10 GIs (Naka et al., 2011), *V. anguillarum* J360 has 21 GIs (Fig. 2-6). We found that GI-19 in chromosome-I (2,994,299..3,011,196 nt) of *V. anguillarum* NB10 (Holm et al., 2015) has homologous regions with *V. anguillarum* J360 GI-14 in chromosome-I (2,988,473..3,000,617 nt). Also, we determined that GI-25 (546,066..578,220 nt) and GI-26 (639,559..674,888 nt) in chromosome-II of *V. anguillarum* NB10 (Holm et al., 2015) share similar genetic context with GI-18 (552,330..612,508 nt) and GI-19 (622,682..673,456 nt) in chromosome-II of *V. anguillarum* J360, respectively. However, the low similarity between GIs of *V. anguillarum* J360 and *V. anguillarum* NB10 suggests

a relatively distant relationship, consistent with the whole genome phylogenetic analysis (Fig. 2-4).

In contrast, 19 GIs were identified in *V. anguillarum* VIB43 (Appendix X, Supplementary files 3 and 4), which showed high similarities with the GIs founded in *V. anguillarum* J360. For instances, GI-1, GI-4, and GI-12 present in *V. anguillarum* VIB43 chromosome-I (Appendix X), possess several homologous regions with GI-8, GI-10, and GI-3 of *V. anguillarum* J360 chromosome-I (Fig. 2-6), respectively (Supplementary files 1 and 3). In addition, GI-6 shared homologous regions with GIs 11 and 12, however all these regions are flanked by IS66 or IS66-like family transposases (ISVa9, ISVa15, ISVa11), suggesting that these regions are hot spots for recombination events (Supplementary files 1 and 3). GI-12 of *V. anguillarum* VIB43 and GI-3 of *V. anguillarum* J360 are highly conserved (Supplementary 1 and 3). Similar results were observed in chromosome-II. GI-15 and GI-16 of *V. anguillarum* VIB43 (Appendix X) showed several homologous regions with GI-16 and GI-17 of *V. anguillarum* J360 (Fig. 2-6), respectively (Supplementary files 2 and 4). GI-17 of *V. anguillarum* VIB43 have several homologous regions with GIs-18 and GI-19 of *V. anguillarum* J360 (Supplementary files 2 and 4). The homologous regions between GIs-17 of *V. anguillarum* VIB43, and GI-18 and GI-19 of *V. anguillarum* J360, encode for several virulence factors like lipocalin, Hcp tube protein (T6SS), interferase toxin, damage-inducible protein J, secretion proteins and toxins. These homologous regions are flanked by several ISs elements (Supplementary files 2 and 4), which indicates that this three GIs are genomic pathogenic islands, perhaps acquired through horizontal gene transference. These results support the hypothesis that this ISs elements (IS66, ISL3, IS3, IS5) are the responsible for the genomic gaps (GGs) and genomic rearrangements

previously mentioned, as well as support that 0.05-8% of genomic differences observed at the identity analyses.

2.6 Conclusion

In this study, the complete genome of *V. anguillarum* J360 serotype O2 isolated from infected cultured lumpfish in Newfoundland, Canada was reported. *V. anguillarum* J360 has a larger genome size (4,549,571 bp) as compared to other available *V. anguillarum* genomes. *V. anguillarum* J360 genome has genes related to antibiotic resistance, hemolysin activity, gelatinase and lipases that play a major role in virulence. *V. anguillarum* J360 was shown to be closely related to *V. anguillarum* VIB43 strain isolated in Scotland, UK, from sea bass. Comparative genomics revealed that five LCBs are shared between *V. anguillarum* J360 and *V. anguillarum* VIB43 chromosome-I, and two LCBs are shared in chromosome-II. Twenty-one genomic islands (GIs) were identified within the chromosomes of *V. anguillarum* J360. Similar GIs identified in *V. anguillarum* J360 were found in *V. anguillarum* VIB43 chromosomes, and this is consistent with the whole genome phylogenetic analysis. *V. anguillarum* J360 has virulence associated genes in both chromosomes but does not harbor a virulent plasmid.

2.7 References

Andrews, S. (2010). FastQC: a quality control tool for high throughput sequence data. Retrieved from http://www.bioinformatics.babraham.ac.uk/projects/fastqc.

Aziz, R., Bartels, D., Best, A., DeJongh, M., Disz, T., Edwards, R., Formsma, K., Gerdes, S., Glass, E., Kubal, M., Meyer, F., Olsen, G., Olson, R., Osterman, A., Overbeek, R., McNeil, L., Paarmann, D., Paczian, T., Parrello, B., Pusch, G., Reich, C., Stevens, R., Vassieva, O., Vonstein, V., Wilke, A., Zagnitko, O. (2008). The RAST Server: rapid annotations using subsystems technology. *BMC Genomics, 9*, 75. doi:10.1186/1471-2164-9-75

Baker-Austin, C., Oliver, J., Alam, M., Ali, A., Waldor, M., Qadri, F., Martinez-Urtaza, J. (2018). *Vibrio spp*. infections. *Nature Reviews Disease Primers, 4*(1), 8. doi:10.1038/s41572-018-0005-8

Baker-Austin, C., Stockley, L., Rangdale, R., Martinez-Urtaza, J. (2010). Environmental occurrence and clinical impact of *Vibrio vulnificus* and *Vibrio parahaemolyticus*: a European perspective. *Environmental Microbiology Reports, 2*(1), 7-18. doi:10.1111/j.1758-2229.2009.00096.x

Barrett, L., Overton, K., Stien, L., Oppedal, F., Dempster, T. (2020). Effect of cleaner fish on sea lice in Norwegian salmon aquaculture: a national scale data analysis. *International Journal for Parasitology*. doi:https://doi.org/10.1016/j.ijpara.2019.12.005

Bertelli, C., Hoad, G., Winsor, G., Brinkman, F., Laird, M., Lau, B., Williams, K. (2017). IslandViewer 4: expanded prediction of genomic islands for larger-scale datasets. *Nucleic Acids Research, 45*(W1), W30-W35. doi:10.1093/nar/gkx343

Blanco Gonzalez, E., & de Boer, F. (2017). The development of the Norwegian wrasse fishery and the use of wrasses as cleaner fish in the salmon aquaculture industry. *Fisheries Science, 83*(5), 661-670. doi:10.1007/s12562-017-1110-4

Breiland, M., Johansen, L., Mikalsen, H., Sae-Lim, P., Hansen, Ø., Mortensen, A. (2016). Susceptibility of 68 different lumpfish (*Cyclopterus lumpus*) families to *Vibrio ordalii* infection. Oral presentation at EAS 2016, Edinburgh, Scotland.

Brooker, A., Papadopoulou, A., Gutierrez, C., Rey, S., Davie, A., Migaud, H. (2018). Sustainable production and use of cleaner fish for the biological control of sea lice: recent advances and current challenges. *Veterinary Records, 183*(12), 383. doi:10.1136/vr.104966

Cameron, M., Barkema, H., De Buck, J., De Vliegher, S., Chaffer, M., Lewis, J., Keefe, G. (2017). Identification of bovine-associated coagulase-negative staphylococci by matrix-

assisted laser desorption/ionization time-of-flight mass spectrometry using a direct transfer protocol. *Journal of Dairy Science, 100*(3), 2137-2147. doi:10.3168/jds.2016-12020

Carver, T., Thomson, N., Bleasby, A., Berriman, M., Parkhill, J. (2009). DNAPlotter: circular and linear interactive genome visualization. *Bioinformatics, 25*(1), 119-120. doi:10.1093/bioinformatics/btn578

Castillo, D., Alvise, P., Xu, R., Zhang, F., Middelboe, M., Gram, L. (2017). Comparative genome analyses of *Vibrio anguillarum* strains reveal a link with pathogenicity traits. *mSystems, 2*(1). doi:10.1128/mSystems.00001-17

Chakraborty, S., Cao, T., Hossain, A., Gnanagobal, H., Vasquez, I., Boyce, D., & Santander, J. (2019). Vibrogen-2 vaccine trial in lumpfish (*Cyclopterus lumpus*) against Vibrio anguillarum. *Journal of Fish Diseases, 42*(7), 1057-1064. doi:10.1111/jfd.13010

Connors, E., Soto-Dávila, M., Hossain, A., Vasquez, I., Gnanagobal, H., Santander, J. (2019). Identification and validation of reliable *Aeromonas salmonicida* subspecies *salmonicida* reference genes for differential gene expression analyses. *Infection, Genetics and Evolution, 73*, 314-321. https://doi.org/10.1016/j.meegid.2019.05.011

Costa, I., Driedzic, W., Gamperl, K. (2013). Metabolic and cardiac responses of cunner (*Tautogolabrus adspersus*) to seasonal and acute changes in temperature. *Physiological & Biochemical Zoology*. 186: 233 – 244.

Darling, A., Mau, B., Blattner, F., Perna, N. (2004). Mauve: multiple alignment of conserved genomic sequence with rearrangements. *Genome Research, 14*(7), 1394-1403. doi:10.1101/gr.2289704

Deady, S., Varian, S., Fives, J. (1995). The use of cleaner-fish to control sea lice on two Irish salmon (*Salmo salar*) farms with particular reference to wrasse behaviour in salmon cages. *Aquaculture, 131*(1), 73-90. doi:https://doi.org/10.1016/0044-8486(94)00331-H

Favrot, L., Blanchard, J., Vergnolle, O. (2016). Bacterial GCN5-Related N-Acetyltransferases: From resistance to regulation. *Biochemistry, 55*(7), 989-1002. doi:10.1021/acs.biochem.5b01269

Fisheries and Land Resources. (2020). *Newfoundland and Labrador Aquatic Animal Reportable and Notifiable Diseases*. Fisheries and Aquaculture, Newfoundland and Labrador, Canada Retrieved from https://www.fishaq.gov.nl.ca/licensing/pdf/NL_Aquatic_Animal_Reportable_Notifiable_Diseases.pdf

Frans, I., Michiels, C., Bossier, P., Willems, K., Lievens, B., Rediers, H. (2011). *Vibrio anguillarum* as a fish pathogen: virulence factors, diagnosis and prevention. *Journal of Fish Diseases, 34*(9), 643-661. doi:10.1111/j.1365-2761.2011.01279.x

Fujino, T., Miwatani, T., Yasuda, J., Kondo, M., Takeda, Y., Akita, Y., Kotera, K., Okada, M., Nishimune, H., Shimizu, Y., Tamura, T., Tamura, Y. (1965). Taxonomic studies on the bacterial strains isolated from cases of "shirasu" food-poisoning (*Pasteurella parahaemolytica*) and related microorganisms. *Biken Japan, 8*(2), 63-71.

Glaeser, S., & Kämpfer, P. (2015). Multilocus sequence analysis (MLSA) in prokaryotic taxonomy. *Systematic and Applied Microbiology, 38*(4), 237-245. doi:https://doi.org/10.1016/j.syapm.2015.03.007

Gomez-Gil, B., Soto-Rodríguez, S., García-Gasca, A., Roque, A., Vazquez-Juarez, R., Thompson, F.L., Swings, J. (2004). Molecular identification of *Vibrio harveyi*-related isolates associated with diseased aquatic organisms. *Microbiology, 150*(6), 1769-1777. doi:https://doi.org/10.1099/mic.0.26797-0

Gram, L., Melchiorsen, J., Spanggaard, B., Huber, I., Nielsen, T. (1999). Inhibition of *Vibrio anguillarum* by *Pseudomonas fluorescens* AH2, a possible probiotic treatment of fish. *Applied Environmental Microbiology, 65*(3), 969-973. Retrieved from https://www.ncbi.nlm.nih.gov/pubmed/10049849

Hirono, I., Masuda, T., Aoki, T. (1996). Cloning and detection of the hemolysin gene of *Vibrio anguillarum. Microbial Pathogens, 21*(3), 173-182. doi:10.1006/mpat.1996.0052

Holm, K., Bækkedal, C., Söderberg, J., Haugen, P. (2018). Complete genome sequences of seven *Vibrio anguillarum s*trains as derived from PacBio sequencing. *Genome biology and evolution, 10*(4), 1127-1131. doi:10.1093/gbe/evy074

Holm K., Nilsson, K., Hjerde, E., Willassen, N., Milton, D. (2015). Complete genome sequence of *Vibrio anguillarum* strain NB10, a virulent isolate from the Gulf of Bothnia. *Standards in Genomic Sciences, 10*(1), 60. doi:10.1186/s40793-015-0060-7

Imsland, A., Reynolds, P., Eliassen, G, Hangstad, T., Foss A, Vikingstad E, Elvegård T. (2014). The use of lumpfish (*Cyclopterus lumpus* L.) to control sea lice (*Lepeophtheirus salmonis* Krøyer) infestations in intensively farmed Atlantic salmon (*Salmo salar* L.). *Aquaculture, 424*, 18-23. doi:doi: 10.1016/j.aquaculture.2013.12.033.

Jukes, T. & Cantor, C., (1969). Evolution of Protein Molecules. In *Mammalian Protein Metabolism*, Munro, H., (Ed.) Academic Press: pp 21-132.

Kumar, S., Stecher, G., Li, M., Knyaz, C., Tamura, K., (2018). MEGA X: Molecular Evolutionary Genetics Analysis across Computing Platforms. *Molecular biology and evolution, 35* (6), 1547-1549

Le Roux, F., Zouine, M., Chakroun, N., Binesse, J., Saulnier, D., Bouchier, C., Zidane, N., Ma, L., Rusniok, C., Lajus, A., Buchrieser, C., Medigue, C., Polz, M., Mazel, D. (2009). Genome sequence of *Vibrio splendidus*: an abundant planctonic marine species with a large genotypic diversity. *Environmental Microbiology, 11*(8), 1959-1970. doi:10.1111/j.1462-2920.2009.01918.x

Lee, J., Shread, P., Furniss, A., Bryant, T. (1981). Taxonomy and description of *Vibrio fluvialis* sp. nov. (synonym group F vibrios, group EF6). *Journal of Applied Bacteriology, 50*(1), 73-94. doi:10.1111/j.1365-2672.1981.tb00873.x

Li, G., Mo, Z., Li, J., Xiao, P., Hao B. (2013). Complete genome sequence of *Vibrio anguillarum* M3, a serotype O1 strain isolated from Japanese flounder in China. *Genome announcements, 1*(5), e00769-00713. doi:10.1128/genomeA.00769-13

Li, L., Mou, X., Nelson, D. (2011). HlyU is a positive regulator of hemolysin expression in *Vibrio anguillarum. Journal of Bacteriology, 193*(18), 4779. doi:10.1128/JB.01033-10

Louden, B., Haarmann, D., Lynne, A. (2011). Use of blue agar CAS assay for siderophore detection. *Journal of Microbiology & Biology Education, 12*(1), 51-53. doi:10.1128/jmbe.v12i1.249

Marcos-Lopez, M., Donald, K., Stagg, H., McCarthy, U. (2013). Clinical *Vibrio anguillarum* infection in lumpsucker *Cyclopterus lumpus* in Scotland. *Veterinary Records, 173*(13), 319. doi:10.1136/vr.101763

Marsh, J., & Taylor, R. (1999). Genetic and transcriptional analyses of the *Vibrio cholerae* mannose-sensitive hemagglutinin type 4 pilus gene locus. *Journal of Bacteriology, 181*(4), 1110-1117. Retrieved from https://www.ncbi.nlm.nih.gov/pubmed/9973335

McEwan, G., Groner, M., Cohen, A., Imsland, A., Revie, C. (2019). Modelling sea lice control by lumpfish on Atlantic salmon farms: interactions with mate limitation, temperature and treatment rules. *Diseases of Aquatic Organisms, 133*(1), 69-82. Retrieved from https://www.int-res.com/abstracts/dao/v133/n1/p69-82/

Milton, D., Hardman, A., Camara, M., Chhabra, S., Bycroft, B., Stewart, G., Williams, P. (1997). Quorum sensing in *Vibrio anguillarum*: characterization of the *vanI*/*vanR* locus and identification of the autoinducer N-(3-oxodecanoyl)-L-homoserine lactone. *Journal of*

Bacteriology, 179(9), 3004-3012. Retrieved from https://www.ncbi.nlm.nih.gov/pubmed/9139920

Myhr, E., Larsen, J., Lillehaug, A., Gudding, R., Heum, M., Håstein, T. (1991). Characterization of *Vibrio anguillarum* and closely related species isolated from farmed fish in Norway. *Applied and Environmental Microbiology, 57*(9), 2750-2757. Retrieved from https://www.ncbi.nlm.nih.gov/pubmed/1768147

Naka, H., & Crosa, J. (2011). Genetic Determinants of virulence in the marine fish pathogen *Vibrio anguillarum*. *Fish Pathology, 46*, 1-10. doi:10.3147/jsfp.46.1

Naka, H., Lopez, C., Crosa, J. (2010). Role of the pJM1 plasmid-encoded transport proteins FatB, C and D in ferric anguibactin uptake in the fish pathogen *Vibrio anguillarum*. *Environmental Microbiology Reports, 2*(1), 104-111. doi:10.1111/j.1758-2229.2009.00110.x

Naka H., Dias G., Thompson C., Dubay C., Thompson F., Crosa J. (2011). Complete genome sequence of the marine fish pathogen *Vibrio anguillarum* harboring the pJM1 virulence plasmid and genomic comparison with other virulent strains of *V. anguillarum* and *V. ordalii*. *Infection and Immunity, 79*(7), 2889-2900. doi:10.1128/IAI.05138-11

Pedersen, K., Grisez, L., van Houdt, R., Tiainen, T., Ollevier, F., Larsen, J. (1999). Extended serotyping scheme for *Vibrio anguillarum* with the definition and characterization of seven provisional O-serogroups. *Current Microbiology, 38*(3), 183-189. Retrieved from https://www.ncbi.nlm.nih.gov/pubmed/9922470

Powell A., Treasurer C., Pooley A., Keay R., Imsland A., Garcia de Leaniz, C. (2017). Use of lumpfish for sea-lice control in salmon farming:challenges and opportunities. *Reviews in Aquaculture, 0*, 1-20. doi:doi: 10.1111/raq.12194

Pruzzo C., Huq A., Colwell R., Donelli G. (2005). *Pathogenic Vibrio Species in the Marine and Estuarine Environment.* In Belkin S., Colwell, R. *Oceans and Health: Pathogens in the Marine Environment* (pp. 217-252). Springer, Boston, MA.

Ramasamy P, Sujatha Rani J., Gunasekaran D. (2018). Assessment of antibiotic sensitivity and pathogenicity of *Vibrio* spp. and *Aeromonas* spp. from aquaculture enviroment. *MOJ Ecology & Enviromental Science, 3*(3), 128-136. doi:10.15406/mojes.2018.03.00077

Rasmussen, B., Grotkjær, T., Alvise, P., Yin, G., Zhang, F., Bunk, B., Spröer, C., Bentzon-Tilia, M., Gram, L. (2016). *Vibrio anguillarum* is genetically and phenotypically unaffected by Long-Term continuous exposure to the antibacterial compound tropodithietic acid. *Applied and Environmental Microbiology, 82*(15), 4802. doi:10.1128/AEM.01047-16

Rock, J., & Nelson, D. (2006). Identification and characterization of a hemolysin gene cluster in *Vibrio anguillarum*. *Infection and Immunity, 74*(5), 2777-2786. doi:10.1128/iai.74.5.2777-2786.2006

Saitou, N., & Nei, M. (1987). The neighbor-joining method: a new method for reconstructing phylogenetic trees. *Molecular Biology and Evolution, 4*(4), 406-425. doi:10.1093/oxfordjournals.molbev.a040454

Sambrook, J., and Russell, W. (2001). *Molecular Cloning; A Laboratory Manual*., 3rd ed. Cold Spring Harbor, NY. Cold Spring Harbor Press.

Sayer, M., and Davenport, J. 1996. Hypometabolism in torpid goldsinny wrasse subject to rapid reductions in seawater temperature. *Journal of Fish Biology*, 49:64–75.

Sørensen, U., & Larsen, J. (1986). Serotyping of *Vibrio anguillarum*. *Applied and Environmental Microbiology, 51*(3), 593-597. Retrieved from https://www.ncbi.nlm.nih.gov/pubmed/3963811

Steinum, T., Karatas, S., Martinussen, N., Meirelles, P., Thompson, F., Colquhoun, D. (2016). Multilocus sequence analysis of close relatives *Vibrio anguillarum* and *Vibrio ordalii*. *Applied Environmental Microbiology, 82*(18), 5496-5504. doi:10.1128/AEM.00620-16

Teru, Y., Hikima, J., Kono, T., Sakai, M., Takano, T., Hawke, J., Takeyama, H., Aoki, T. (2017). Whole-genome sequence of *Photobacterium damselae* subsp. *piscicida* strain 91-197, isolated from hybrid striped bass (*Morone sp.*) in the United States. *Genome Announcements, 5*(29). doi:10.1128/genomeA.00600-17

Vaidya, G., Lohman, D., Meier, R. (2011). SequenceMatrix: concatenation software for the fast assembly of multi-gene datasets with character set and codon information. *27*(2), 171-180. doi:doi:10.1111/j.1096-0031.2010.00329.x

Villarreal-Chiu, J., Quinn, J., McGrath, J. (2012). The genes and enzymes of phosphonate metabolism by bacteria, and their distribution in the marine environment. *Frontiers in Microbiology, 3*, 19-19. doi:10.3389/fmicb.2012.00019

Weber, B., Chen, C., Milton, D. (2010). Colonization of fish skin is vital for *Vibrio anguillarum* to cause disease. *Environmental Microbiology Reports, 2*(1), 133-139. doi:10.1111/j.1758-2229.2009.00120.x

Weber, B., Hasic, M., Chen, C., Wai, S., Milton, D. (2009). Type VI secretion modulates quorum sensing and stress response in *Vibrio anguillarum. Environmental Microbiology, 11*(12), 3018-3028. doi:10.1111/j.1462-2920.2009.02005.x

Whittaker, B., Consuegra, S., Garcia de Leaniz, C. (2018). Genetic and phenotypic differentiation of lumpfish (*Cyclopterus lumpus*) across the North Atlantic: implications for conservation and aquaculture. *PeerJ, 6*, e5974. doi:10.7717/peerj.5974

Wood, E. (1983). Molecular Cloning. A Laboratory Manual. *Biochem Educ.*, *11*.

3. CHAPTER 3: *Aeromonas salmonicida* Infection Kinetics and Protective Immune Response to Vaccination in Sablefish (*Anoplopoma fimbria*).

The research described in Chapter 3 has been published in *Fish and Shellfish Immunology* as:

Ignacio Vasquez[1], Trung Cao[1], Ahmed Hossain[1], Katherinne Valderrama[1], Hajarooba Gnanagobal[1], My Dang[1], Robine H. J. Leeuwis[2], Michael Ness[5], Briony Campbell[6], Robert Gendron[5], Kenneth Kao[5], Jillian Westcott[4], A. Kurt Gamperl[2], Javier Santander[1*]. (2020). *Aeromonas salmonicida* Infection Kinetics and Protective Immune Response to Vaccination in Sablefish (*Anoplopoma fimbria*). Fish & Shellfish Immunology, 104, pp 557-556

3.1 Abstract

Effective vaccine programs against *Aeromonas salmonicida* have been identified as a high priority area for sablefish (*Anoplopoma fimbria*) aquaculture. In this study, we established an *A. salmonicida* infection model in sablefish to evaluate the efficacy of commercial vaccines and an autogenous vaccine preparation. Groups of 40 fish were intraperitoneally (ip) injected with different doses of *A. salmonicida* J410 isolated from infected sablefish to calculate the median lethal dose (LD_{50}). Samples of blood, head kidney, spleen, brain and liver were also collected at different time points to determine infection kinetics. The LD_{50} was estimated as ~$3x10^5$ CFU/dose. To evaluate the immune protection provided by an autogenous vaccine and two commercial vaccines in a common garden experimental design, 140 fish were PIT-tagged, vaccinated and distributed equally into 4 tanks (35 fish for each group, including a control group). Blood samples were taken every 2 weeks to evaluate IgM titers. At 10 weeks post-immunization, all groups were ip challenged with 100 times the calculated LD_{50} for *A. salmonicida* J410. *A. salmonicida* was detected after 5 days post-infection (dpi) in all collected tissues. At 30 days post-challenge the relative percentage survival (RPS) with respect to the control group was calculated for each vaccine. The RPS for the bacterin mix was 65.22%, for Forte Micro 4® vaccine was 56.52% and for Alpha Ject Micro 4® was 30.43%, and these RPS values were reflected by *A. salmonicida* tissue colonization levels at 10 days post-challenge. Total IgM titers peaked at 6 to 8 weeks post-immunization, where the autogenous vaccine group showed the highest IgM titers, and these values were consistent with the RPS data. Also, we determined that the *A. salmonicida* A-layer binds to immunoglobulins F(ab)´ in a non-specific fashion,

interfering with immune assays and potentially vaccine efficacy. Our results indicate that vaccine design influences sablefish immunity and provide a guide for future sablefish vaccine programs.

3.2 Introduction

The sablefish (*Anoplopoma fimbria*), also referred to as "Black cod", was originally described by Pallas in 1814 (Amaoka, 1984; FAO, 2019). Wild sablefish are found in the Pacific Ocean as far north as the Bering Sea and as far south as Japan and California, with adult sablefish living on the continental shelf and slope at depths of approximately 1,500 meters (FAO, 2019). The sablefish is considered one of the most valuable fish species on Canada's west coast, with a value of US$12.25 per lb (Wiedenhoft, 2017). In addition, there is currently an emerging aquaculture industry for this species in the North Pacific region, with more than 74% of Canada's farmed sablefish exported to Japan. Other important markets include the United States and the United Kingdom (Amaoka, 1984; FAO, 2019; Luening, 2013). Also, sablefish farming is attracting interest in South Korea (Kim et al., 2017) and the USA (Arkoosh et al., 2018; Wiedenhoft, 2017). The decrease in wild sablefish stocks (DFO, 2016), increasing consumer demand (Sonu, 2014) and market value (Luening, 2013), have established sablefish as an emergent aquaculture species.

The development of protocols and techniques for sablefish aquaculture has been on-going since 1984 (Gores & Prentice, 1984), and this species has significant potential for future growth as an aquaculture species. For example, sablefish have one of the fastest industrial growth rates of all teleost species (Kendall & Matarese, 1987), and juveniles

grown in marine net pens can reach commercial size (3-4 kg) in 2 years (Gores & Prentice, 1984). However, during the period in marine net pens the fish are exposed to infectious diseases (Krkošek, 2017). *A. salmonicida* is the most common pathogen isolated from cultured sablefish in British Columbia, Canada (Arkoosh et al., 2018), but *Vibrio anguillarum* outbreaks have also been reported (Liu et al., 2005), both having negative impacts on production costs.

A. salmonicida, one of the oldest marine pathogens known, is a Gram-negative pathogen that causes furunculosis in different cultured fish species (Austin B. & Austin D., 2012; Cipriano & Bullock, 2001), including sablefish (Arkoosh et al., 2018). Effective vaccine programs against *A. salmonicida* are a high priority area for the sablefish aquaculture industry. Vaccination is an important management strategy that reduces disease outbreaks and minimizes the use of antibiotics (Mahoney et al., 2007; Santander et al., 2012; Shoemaker et al., 2009). Currently, there are no effective commercial vaccines specifically developed for sablefish. Only two commercial vaccines are being used in the sablefish industry: 1) Alpha Ject Micro 4®, used in the prevention of furunculosis caused by *Aeromonas salmonicida*, vibriosis caused by *Listonella* (*Vibrio*) *anguillarum* serotypes O1 and O2, and cold water vibriosis caused by *Vibrio salmonicida*, was developed for Atlantic salmon, about 15 g or larger, manufactured by PharmaQ, Overhalla, Norway and distributed by Zoetis Canada Inc., Quebec, Canada (PharmaQ, 2020), and 2) Forte Micro 4®, used in the prevention of furunculosis, vibriosis, and cold water vibriosis, was developed for salmonids, about 10 g or larger, and manufactured by Elanco Canada Limited, P.E.I., Canada (Elanco, 2020). Recently, an autogenous polyvalent vaccine was successfully evaluated against *A. salmonicida* in sablefish in the USA, and it was reported

that this autogenous bacterin preparation injected intraperitoneally was more effective than bath vaccination (Arkoosh et al., 2018). However, Canadian regulations do not allow the importation of autogenous vaccines (FAO, 2009), and current vaccines available in Canada against *A. salmonicida* have not been evaluated in sablefish.

In this study, an *A. salmonicida* infection model was established in cultured sablefish, and we used this model to compare the immune protective response provided by an *A. salmonicida* autogenous monovalent vaccine preparation (bacterin mixture) and two polyvalent commercial vaccines (Alpha Ject Micro 4®, PharmaQ and Forte Micro 4® , Elanco) against an atypical *A. salmonicida* challenge.

3.3 Materials and Methods

3.3.1 Bacterial strains, media, and reagents.

A. salmonicida J409, J410 and J411 strains were isolated from infected cultured sablefish and identified using standard phenotypic tests (Sambrook & Russell, 2001), 16S gene sequencing (Roger et al., 2012), and whole genome sequencing using established protocols (Valderrama et al., 2017a). Additionally, *A. salmonicida* typical isolates J223 ($VapA^+$) and J227 ($VapA^-$, A-layer mutant) were utilized as controls (lab collection). *A. salmonicida* strains were routinely grown in Trypticase Soy Broth (TSB) media (Difco, Franklin Lakes, NJ) from a single colony at 15ºC with aeration (180 rpm) in an orbital shaker, according to previous descriptions (Valderrama et al., 2017b). When required, TSB was supplemented with 1.5% bacto agar (Difco) and 0.02% Congo-red (Sigma-Aldrich, USA). Bacterial growth was monitored by spectrophotometer and by plating to count

colony forming units (CFU/ml) (Leboffe & Pierce, 2015). Bacterial cells were harvested at mid log phase (OD600 nm ~0.6-0.7) by centrifugation (4,200 × *g* for 10 min at 4°C).

3.3.2 Bacterin preparation.

The *A. salmonicida* J409 (Accession number: CP047374-75), J410 (Accession number: CP047376-77), and J411 (Accession number: SUB6785506) strains were grown independently in TSB media supplemented with 100 µM of 2, 2'-dipyridyl at 15ºC with aeration (180 rpm) to induce the expression of immunogenic outer membrane proteins (e.g., iron regulated outer membrane proteins) (Santander et al., 2012) up to an optical density (O.D. 600 nm) of 0.7 (~$1x10^8$ CFU/ml). The bacterial cells were washed three times by centrifugation (4,200 × *g* for 10 min at 4°C) with phosphate buffered saline (PBS; 136 mM NaCl, 2.7 mM KCl, 10.1 mM Na_2HPO_4, 1.5 mM KH_2PO_4 (pH 7.2)) (Sambrook & Russell, 2001) and then fixed with 6% formalin for 3 days at room temperature with gentle agitation. Formalin was removed by centrifugation at 4,200 × *g* for 10 min at 4°C and the bacterin mix was resuspended in PBS. Inactivated cells were dialyzed (Molecular weight cut off 3.5 kDa; Spectra/Por, CA) in 1.0 l of PBS three times at 4ºC with gentle stirring. Cell inactivation was determined by plating in TSB and TSA before and after dialysis. Finally, the three strains were mixed in equal quantities, and the bacterin mix was quantified using flow cytometry and the Bacteria Counting Kit (ThermoFisher, USA) according to the manufacturers' instructions. A BD FACS Aria II flow cytometer (BD Biosciences, CA) and BD FACS Diva v7.0 software were used for bacteria cell quantification. The number of bacterial cells/ml was calculated by dividing the number of signals in the bacterial frame

by the number of signals in the microsphere frame (Appendix XI) as described previously (Eslamloo et al., 2019). The bacterin mix was stored at 4°C at a concentration of $3.5x10^{10}$ CFU/ml until utilization.

3.3.3 Ethics statement.

All animal protocols required for this research were approved by the Institutional Animal Care Committee and the Biosafety Committee at Memorial University of Newfoundland (MUN). Animal assays were conducted under protocols #16-92-KG, #18-01-JS, #18-03-JS, and biohazard license L-01.

3.3.4 Fish origin and holding conditions.

Cultured sablefish juveniles (~ 1 g) were provided by Golden Eagle Sable Fish, British Columbia, Canada. Upon arrival, the fish were acclimated to ~8-10°C in 500 l tanks supplied with 95-110% air saturated and UV treated filtered flow-through seawater, and an ambient photoperiod, at the Cold-Ocean and Deep-Sea Research Facility (CDRF, MUN) for quarantine. Following veterinary clearance, the animals were transferred to the Dr. Joe Brown Aquatic Research Building (JBARB, MUN). Fish were subsequently reared under the previously described conditions. Tank biomass was maintained at < 30 kg m^{-3}, and the fish were fed daily using automatic feeders and a commercial diet (Skretting – Europa; 15 crude protein (55%), crude fat (15%), crude fiber (1.5%), calcium (3%), phosphorus (2%),

sodium (1%), vitamin A (5000 IU/kg), vitamin D (3000 IU/kg) and vitamin E (200 IU/kg)) at 1.5% body weight per day.

3.3.5 Determination of the LD_{50} of A. salmonicida J410 in sablefish.

Sablefish (215.5 $\pm$ 3.2 g) were transferred from the JBARB to the CDRF, separated into six 500 l tanks containing 10 and 30 fish per selected dose (see Appendix XII) and acclimated for 2 weeks under previously described conditions. The median lethal dose 50 (LD_{50}) of *A. salmonicida* J410 was evaluated in these fish according to established protocols (Chakraborty et al., 2019). Briefly, the fish were anesthetized with 40 mg of MS222 (Syndel Laboratories, BC, Canada) per l of sea water and ip infected with 100 µl of 10^4, 10^6, or 10^7 CFU per dose. Three of the six tanks were utilized for monitoring mortality while the remaining three tanks were used to determine *A. salmonicida* tissue colonization and pathogen re-isolation (Appendix XII). The LD_{50} was calculated using the formula: $LD_{50}=10^{a-(PD)}$, where a= $\log_{10}$ (dilution factor of mortality >50%); Proportional Distance $(PD) = \frac{L\%-50\%}{L\%-H\%}$; L%=Dilution point of mortality <50%; H%=Dilution point of mortality >50% (Ramakrishnan, 2016).

3.3.6 Tissue sampling and analysis.

Fish were netted and immediately euthanized with an overdose of MS222 (400 mg/l). Tissue samples sections from liver, spleen, head kidney and brain were aseptically

removed from all groups at 5 and 10 dpi with *A. salmonicida* J410 and placed into sterile homogenizer bags (Nasco Whirl-pak®, USA). Thereafter, they were weighed and homogenized in PBS up to a final volume of 1 ml (weight : volume), serially diluted (1:10) and plate counted onto TSA-Congo red plates. The plates were incubated at 15°C for 5 days to determine the CFU of *A. salmonicida* J410 per g of tissue. Total bacteria were normalized to 1 g of tissue according to the initial weight of the tissue using the following formula: $\mathrm{CFU} * \mathrm{g}^{-1} = \frac{\text{colony forming units (CFU)} * \text{original tissue weight (g)} * 1\ \mathrm{ml}^{-1} * 1\ \mathrm{g}^{-1})}{\text{original tissue weight (g)}}$.

3.3.7 Histopathology.

Tissue sample sections (independent from the previous samples) were fixed in 10% formalin diluted in PBS for three days at room temperature. The formalin was then removed, and the samples were stored in 100% ethanol at 4ºC until in block processing according to established procedures (Chandler & Roberson, 2009). Briefly, fixed tissue samples were dehydrated in alcohol gradients, clarified in xylene, and infiltrated with paraffin wax for subsequent sectioning at 5 μm using and automatic microtome (HM 355S, ThermoFisher, Scientific, USA), and then stained and examined under light microscopy. Sectioned tissues for histology were stained with hematoxylin and eosin, and with Giemsa (Leica Biosystems, Canada), and visualized using a light microscope (Olympus CX21, USA).

3.3.8 Sablefish immunization using a common garden experiment.

Sablefish (125.45 ± 0.5 g) were Passive Integrated Transponder (PIT)-tagged and acclimated for 2 weeks at ~8-10°C before immunization. After this period, independent groups of 35 fish were fasted for 24 h, and ip immunized with 100 µl of the *A. salmonicida* bacterin mix (10^9 CFU/dose; autogenous vaccine), Alpha Ject Micro 4®, Forte Micro 4® or PBS (control group). Alpha Ject Micro 4® (PharmaQ, Norway) is an oil-based vaccine containing *A. salmonicida*, *V. anguillarum* and *Vibrio salmonicida* formalin-killed strains, whereas Forte Micro 4® (Elanco, Canada) is an oil-based vaccine containing formalin-inactivated cultures of *A. salmonicida*, *V. anguillarum* serotypes I and II, *V. ordalii*, and *V. salmonicida* serotype I and II. The immunization of fish with commercial vaccines was conducted following the manufacturers' instructions, and used to evaluate, and compare, the effectiveness of the bacterin mix. Fish were distributed randomly into four different tanks with an equal proportion of each group (Appendix XIII). Fish length and weight were monitored every 2 weeks to determine the specific growth rate (SGR) (Hopkins, 1992) according to the formula: $(\ln(\text{final weight (g)}) - \ln(\text{initial weight (g)}) \times 100)/(\text{time (days)})$. Non-lethal blood samples (1 ml) were taken every 2 weeks from a selected single tank. Each tank was sampled only once during the immunization assay (Appendix XIII).

3.3.9 Challenge of immunized sablefish.

The infection procedures were conducted in the AQ3 biocontainment facility at the CDRF. At 9 weeks post-immunization fish were transferred to the AQ3 biocontainment

facility and acclimated for 1 week under previously described optimal conditions. After this period, sablefish (~200 ± 0.5 g) were ip challenged with 100 times the LD_{50} dose for *A. salmonicida* J410 (10^7 CFU/dose). Mortality was monitored daily. The relative percent survival (RPS) (Amend, 1981) of vaccinated fish was calculated according to the formula: $RPS = \left(1 - \frac{\%\ vaccinated\ mortality}{\%\ control\ mortality}\right) \times 100.$

3.3.10 Sablefish IgM purification.

To produce anti-sablefish IgM and determine the IgM titers of sablefish post-immunization, IgM from sablefish was purified according to previously described protocols for other Teleostei with modifications (Santander et al., 2011). Briefly, IgM was purified from fresh pooled sablefish serum using an immobilized mannan binding protein (MBP) column kit (Pierce™, USA) according to the manufacturer´s instructions, except that 200 ml of serum were used instead of 1 ml. The integrity and purity of the sablefish IgM was evaluated by SDS-PAGE 10% (Sambrook & Russell, 2001), and quantified by DirectUV and the bicinchoninic acid (BCA) standard method (BCA Proteins Assay Kit, Pierce™, USA) using spectrophotometry (Genova-Nano spectrophotometer, Jenway, UK). High quality IgM fractions were pooled and dialyzed against 20 mM Tris-HCl (pH = 8.0) twice at 4°C with gentle agitation using a dialysis cassette (10,000 Da cutoff, Thermo Scientific, USA). After dialysis, the purified sablefish IgM was lyophilized (EdwarDS-Super Modulyo, Boc Ltd, England). Sablefish IgM was resuspended in 20 mM Tris-HCl (pH = 8.0). The final IgM preparation was re-evaluated for integrity using SDS-PAGE

10%. Chicken IgY anti-sablefish IgM antibody was produced, purified, and biotinylated by Somru BioScience Inc. (Charlottetown, PEI, Canada).

3.3.11 Immunohistochemistry.

Immunohistochemistry (IHC) was performed using a Ventana Benchmark Ultra automated immunostainer (Roche, Switzerland) in the Department of Anatomical Pathology, General Hospital, Eastern Health, St. John's NL, on paraffin sections of sablefish head kidney, spleen, brain and human tonsil applied to positively charged slides. Sections were processed on the automated immunostainer using citrate-based (10 mM, pH 6) and tris-based buffer CC1 (Roche, Switzerland) for deparaffinization and antigen retrieval at 100°C for 64 min followed by 32 min of incubation at room temperature with either rabbit monoclonal IgG antibody clone SP67 anti-human CD10 (Roche, Diagnostic 790-4506) or a rabbit IgG (Roche, Diagnostics 790-4795) as negative control using a 1:200 dilution, and detected using Ultraview (Roche, Switzerland) and counterstained with hematoxylin. For anti-*A. salmonicida* and anti-sablefish IgM IHC, we used an anti-VapA *A. salmonicida* rabbit IgG antibody pre-adsorbed with *A. salmonicida* VapA^{-} outer membrane proteins, and an anti-sablefish-IgM chicken IgY antibody custom produced in collaboration with Somru BioScience. Anti-*A. salmonicida* and anti-sablefish-IgM antibodies were applied at a 1:500 dilution using previously described IHC procedures, except that an alkaline phosphatase-conjugated anti-IgY secondary antibody was used at 1:250 dilution to develop the IgM staining reaction (Ahmad et al., 2018).

3.3.12 Confocal microscopy and immune fluorescence visualization.

It has been reported that *A. salmonicida* possesses an A-layer (extracellular membranal protein array) that binds to antibodies (Magnadóttir et al., 2002; Phipps & Kay, 1988). Confocal microscopy was used to evaluate the non-specific binding of different immunoglobulins to the *A. salmonicida* A-layer. *A. salmonicida* strains J409, J410, J411 and J223 expressing the A-layer ($VapA^{+}$) (Valderrama et al., 2019) and J227 (an A-layer mutant ($VapA^{-}$)) were utilized. The strains were grown until logarithmic phase and stained with 5-([4,6-dichlorotriazinyl] amino) fluorescein hydrochloride (DTAF) solution (100 µg in dimethyl sulfoxide (DMSO); Sigma, USA) according to established protocols (Valderrama et al., 2019) and 4′,6-diamidino-2-phenylindole (DAPI; ThermoFisher, USA) according to the manufacturer's instructions. Biotinylated IgY anti-sablefish IgM was labeled with conjugated avidin Texas-Red (Life Technologies, USA) and utilized to assess non-specific binding to the *A. salmonicida* A-layer. Additionally, goat anti-mouse F(ab)´2-FITC labeled IgG (CellLab, USA) was utilized. *A. salmonicida* strains labeled with DTAF, DAPI, and IgY-Texas red or *A. salmonicida* strains labeled with DAPI and IgG-F(ab)´-FITC were visualized with a Nikon AR1 laser scanning confocal microscope.

3.3.13 Direct enzyme linked immunosorbent assay (dELISA).

We verified that high affinity IgY anti-sablefish IgM binds strongly to the *A. salmonicida* A-layer in a non-specific fashion. Therefore, total sablefish IgM titers were evaluated after immunization using dELISA.

The sablefish serum samples were heat treated at 56ºC for 30 min to inactivate the complement and subsequently treated with 100 µl of chloroform (Sigma-Aldrich, USA) for 10 min at room temperature to remove fats. After this period, the samples were centrifuged at 4,000 g for 10 min at room temperature, and the supernatant was transferred to a clean tube and stored at -80ºC until IgM titer determination. Two hundred microliters of pre-treated sablefish serum were serially diluted (1:25) in coating buffer (0.015 mM Na_2CO_3; 0.035 mM $NaHCO_3$; pH 9.8) and added to 96 well plates (Ultra-High Binding Polystyrene Microtiter, ThermoFisher, USA). The plates were incubated at 4°C overnight, washed 3 times with PBS-Tween (PBS-T; 0.1%) and blocked with 150 µl of ChonBlock™ (Chondrex, Inc., WA, USA) for 1 h at 37°C. After this period, the plates were washed 3 times with PBS-T, inoculated with 100 µl of the secondary antibody (IgY anti-sablefish IgM; 1:10,000), and incubated at 37°C for 1 h. Following incubation and washing, 100 µl of streptavidin-HRP (Southern Biotech; 1:10,000) was added, and the plates were incubated at 37°C for 1 h. For visualization and color development, 120 µl of 1X TMB (Invitrogen, Austria) - H_2O_2 (ratio 1:5) were added, and the plates were incubated at room temperature (20-22ºC) for 30 min in darkness. Optical density was determined at 450 nm after adding 50 µl of stop solution (2M H_2SO_4). IgM titers were evaluated in naïve animals (10 fish) and after 2, 4, 6 and 8 weeks post-immunization (8-9 fish at each time point) (Appendix XIII, Supplementary File 3).

The standard curve was developed using established protocols (Hnasko, 2015; Sambrook & Russell, 2001). Briefly, purified sablefish IgM was serially diluted in coating buffer to 50, 25, 12.5, 6.25, 3.125 and 1.563 µg/ml and incubated overnight at 4ºC. Each

concentration was evaluated in triplicate (Supplementary File 3). After incubation and washing, 100 µl of IgY anti-sablefish IgM (1:10,000) was added and incubated at 37°C for 1 h. Following incubation and washing, 100 µl of Streptavidin-HRP (Southern Biotech, USA) (1:10,000) was added and incubated at 37°C for 1 h. For visualization and color development 120 µl of 1X TMB (Invitrogen, Austria) - H_2O_2 (ratio 1:5) was added and incubated at room temperature (20-22ºC) for 30 min in darkness. Optical density was determined at 450 nm after adding 50 µl of stop solution (2M H_2SO_4). The obtained values were normalized using a natural logarithm standard curve of knowns concentrations.

3.3.14 Statistical analysis.

All data are displayed as means ± standard error (SE). Assumptions of normality and homogeneity were tested for variances. For the survival curves, one-way ANOVA analysis was used followed by Tukey's post-hoc tests to determine significant differences between treatment groups ($p<0.05$). The Kaplan-Meier estimator was used to obtain survival fractions after the challenges, and the Log-rank test was used to identify differences between treatments groups. For ELISA IgM titers, a two-way ANOVA multi-comparison analysis was performed to determine significant differences between treatments. All statistical analyses were performed using GraphPad Prism 7.0 (GraphPad Software, La Jolla, California, USA).

3.4 Results

3.4.1 LD_{50} determination and A. salmonicida infection kinetics in sablefish.

Three different groups of 30 fish were ip injected with three different doses of *A. salmonicida* J410 (10^4, 10^6 and 10^7 CFU/dose) (see Appendix XI) to determine the LD_{50}. After 5 dpi, clinical signs of furunculosis and internal petechial hemorrhaging was observed (Fig. 3-1B). Mortality began within 7-10 dpi, reaching 97% in the fish infected with the 10^7 CFU/dose, and 94% in the fish infected with 10^6 CFU/dose after 30 days. In contrast, the fish infected with the lowest dose tested (10^4 CFU /dose) showed 7% mortality (Fig. 3-1A) in the absence of furunculosis clinical signs. Using this data, the LD_{50} for *A. salmonicida* J410 in sablefish was determined as ~$3x10^5$ CFU/dose (Table 3-1).

Three different groups of 10 fish each were injected with three different doses of *A. salmonicida* J410 (10^4, 10^6 and 10^7 CFU/dose) to determine the bacterial colonization at 5 and 10 dpi in different tissues (Appendix XI). We did not detect bacteria in the spleen at 5 dpi in sablefish injected with the lowest dose (10^4 CFU/dose) (Fig. 3-1C). However, one of five fish injected with the lowest dose of *A. salmonicida* presented bacteria in the head kidney, bacteremia was observed in three of five fish sampled, and all the fish sampled presented meningoencephalitis and liver colonization (Fig. 3-1C). Fish injected with 10^6 and 10^7 CFU/dose showed bacterial colonization in all tissues sampled at 5 dpi (Fig. 3-1C). At 10 dpi all the tissues sampled showed bacterial colonization (Fig. 3-1D).

3.4.2 Expression of A. salmonicida, IgM and CD10 in A. salmonicida infected sablefish tissues.

To explore the distribution of *A. salmonicida* IgM and CD10 in *A. salmonicida* infected tissues, we performed IHC analyses of sablefish tissue sections collected at 0 and 10 dpi. Giemsa histological staining revealed pathological changes in several tissues at 10 dpi, including general tissue disorganization and cellular dysplasia in the head kidney, spleen, and brain, and hemorrhaging in the head kidney and spleen (Fig. 3-2). IHC revealed that by 10 dpi the expression of *A. salmonicida* and IgM was in general increased in the head kidney, spleen, and brain. Interestingly, the expression of CD10 appeared to decrease within infection in spleen and brain but increased slightly in the head kidney (Fig. 3-2).

3.4.3 Vaccine challenge.

One hundred and forty fish were challenged 8 weeks post-immunization with 100 times the LD_{50} dose ($1x10^7$ CFU/dose) of the bacterin mix. Mortality began within 8-10 days post-challenge. PBS (mock immunized) fish showed 76.67% mortality (Fig. 3-3A). Based on these results, the relative percentage survival (RPS) for the three vaccine treatments was determined. Alpha Ject Micro 4® conferred an RPS of 30.43%, Forte Micro 4® conferred an RPS of 56.52% and the autogenous bacterin mix conferred an RPS of 65.22% (Fig. 3-3A and Table 3-1).

Bacterial loads were determined after 10 days post-challenge. *A. salmonicida* was detected in all tissues in mock immunized (control) fish, and in most of the tissue samples from Alpha Ject Micro 4® and Forte Micro 4® immunized fish (Fig. 3-3B). Fish immunized

with Alpha Ject Micro 4® and Forte Micro 4® showed similar bacterial loads (Fig. 3-3B). In contrast, only one fish immunized with the *A. salmonicida* bacterin mix showed bacterial colonization in the liver, head kidney and brain (Fig. 3-3B), and only two fish showed *A. salmonicida* colonization in the spleen and blood (Fig. 3-3B).

3.4.4. IgM titers in immunized sablefish.

Sablefish immunoglobulin M (IgM) was purified by an immobilized mannan binding protein (MBP) column from 200 ml of fresh serum. Following purification, the sablefish IgM was concentrated by lyophilization, and we obtained 3,573 µg/ml of IgM. The purified sablefish IgM was visualized by SDS-PAGE 10% under reducing conditions, and displayed a heavy (~75 kDa) and a light chain (~24 kDa) (Fig. 3-5A), similar to other fish IgM (Magnadottir, 1998; Mashoof & Criscitiello, 2016).

An indirect ELISA against the whole *A. salmonicida* cell was initially utilized to determine the IgM titers. However, we determined that *A. salmonicida* binds to the secondary IgY chicken antibody, and additionally to goat IgG F(ab)´, in a non-specific fashion (Fig. 3-4A). Using an *A. salmonicida* A-layer mutant strain we determined that this Ig non-specific binding is dependent on the A-layer. These results indicate that the *A. salmonicida* A-layer interferes with the determination of *A. salmonicida* specific IgM titers (Fig. 3-4A). Therefore, we determined the total plasma IgM titers using direct ELISA.

Table 3-1. Summary table for the infection and vaccination model for sablefish (*Anoplopoma fimbria*)

Treatment	Fish N°	Weight (g)		SGR	IP infection (CFU/dose)	IP challenge (CFU/dose)	% Mortality	RPS %	Total IgM[a] (mg/ml)	
		Initial	Final						6 wpi	8 wpi
***A. salmonicida* J410 infection**										
				-	$1x10^4$	-	6.67	-	-	-
	30	215.5 ± 3.2		-	$1\text{-}x10^6$	-	93.33	-	-	-
				-	$1x10^7$	-	96.67	-	-	-
Calculated LD_{50} dose					$\sim 3.5x10^5$					
Vaccine trial for *A. salmonicida* J410 challenge										
Alpha Ject®	30	135.4	368.0	4.71	-	$1x10^7$	53.3	30.43	0.911*	0.415
Forte Micro®	30	134.3	307.8	4.71	-	$1x10^7$	33.3	56.52	0.605	0.520
Bacterin Mix	30	144.3	317.6	4.78	-	$1x10^7$	26.6	65.22	1.734*	0.827*

[a]Total IgM (mg/ml) average value at 6- and 8-weeks post-immunization
*Tukey's multiple comparison test significance ($p<0.0001$) as compared to control group

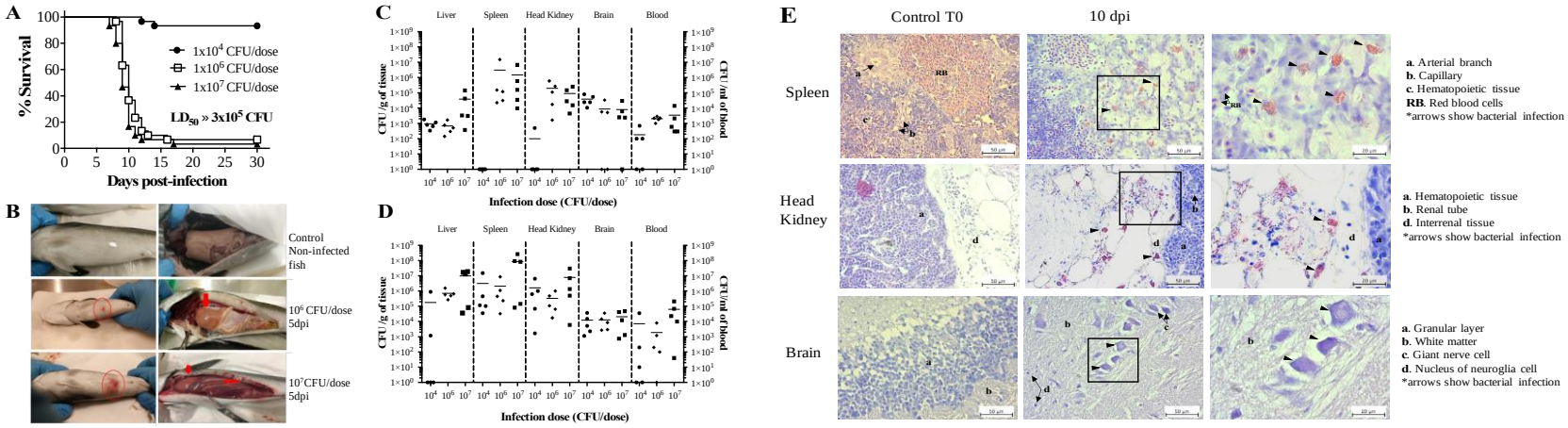

Figure 3-1. ***A. salmonicida*** **infection assay. A.** Sablefish survival (%) after ip infection with 10^4 CFU/dose (black circle), 10^6 CFU/dose (white square), and 10^7 CFU/dose (black triangle). The latter two groups were significantly different from the 10^4 CFU/dose group at $p<0.0001$. **B.** *A. salmonicida* furunculosis clinical signs were detected at 5 dpi. Circles and arrows show skin furunculosis, internal hemorrhage and liver as the primary organ for infection at 10^6 and 10^7 CFU/dose. No signs of infection were detected in the group infected with 10^4 CFU/dose. **C.** *A. salmonicida* J410 tissue colonization (liver, spleen, head kidney, brain, and blood) after 5 dpi (n= 5). **D.** Tissue colonization after 10 dpi. **E.** Histopathology of spleen head kidney and brain after 10 dpi, arrows indicate bacterial infection and/or inside of eukaryotic cell. Scale bars for control and 10 dpi are 50 µm, close-up view scale bars are 20 µm. In **C** and **D**, the bar indicates the average.

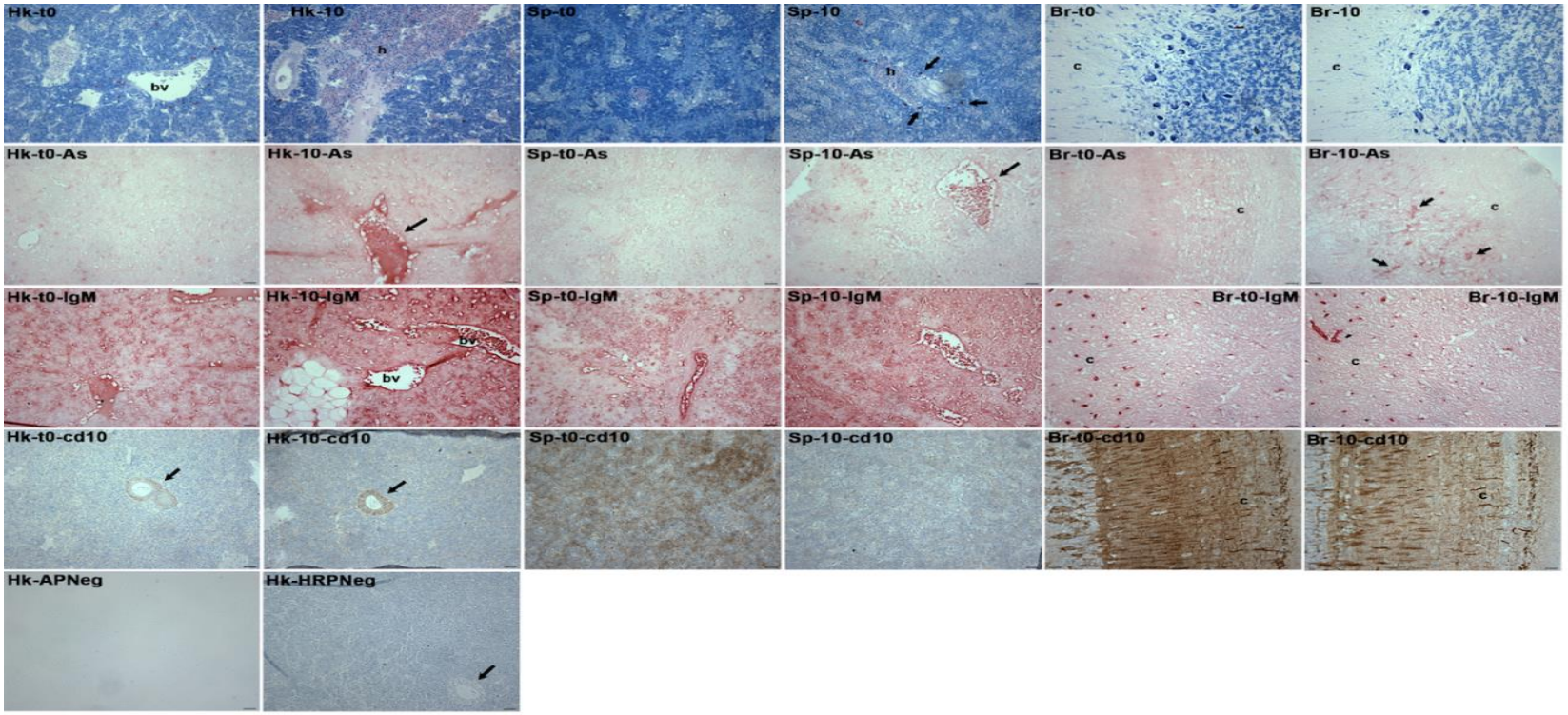

Figure 3-2. Detection of *A. salmonicida,* IgM and CD10 in *A. salmonicida* infected sablefish tissues. Giemsa histological staining revealed pathological changes in several tissues occurring by 10 dpi including general tissue disorganization and cellular dysplasia in head kidney, spleen, brain and hemorrhaging in the head kidney and spleen (top row). By 10 dpi (10), expression of (As) [see arrows indicating *A. salmonicida*- reactive vasculature] and IgM was in general increased in head kidney (Hk), spleen (Sp) and brain (Br) compared to time zero (T0) as shown in figure. Interestingly, expression of $CD10^{+}$ appeared to decrease with infection in spleen and brain but increase slightly in the head kidney. Expression of CD10 also appeared to follow nerve body tracks in the cerebral cortical grey matter (**c**). Representative negative controls performed for the alkaline phosphatase-reacted antibodies (anti- *A. salmonicida* and anti-IgM; Hk-APNeg) and the horseradish peroxidase reacted anti-CD10 (Hk-HRPNeg) are shown at bottom. Head kidney renal tubules are indicated by arrows in Hk-t0-cd10, Hk-10-cd10 and Hk-HRPNeg. Bv, blood vessel; h, hemorrhage; c, cerebral cortex. Magnification X200. Scale bars in the bottom right corners of each panel are 50 µm

We developed a standard curve using different concentrations (50, 25, 12.5, 6.25, 3.125, and 1.563 mg/ml) of purified sablefish IgM (Supplementary File 3). IgM concentrations were standardized using natural logarithm (ln). The linear regression equation was determined to be $y = 0.03417 * \ln(x) + 0.04260$ with an $r^2 = 0.8756$ ($p < 0.0001$) (Fig. 3-5B). Total IgM was measured from non-lethal blood samples at 2, 4, 6, and 8 weeks post-immunization. Also, total IgM was quantified from non-immunized fish prior to vaccination (T0, n=10). IgM titers in naïve sablefish (125.45 g) were estimated to be 0.097 mg/ml (Fig. 3-5C, Supplementary File 3). At 2 weeks post-immunization all the groups showed an increase in the IgM titer (control: 0.331 mg/ml; Alpha Ject Micro 4®: 0.270 mg/ml; Forte Micro 4®: 0.238 mg/ml; bacterin mix: 0.203 mg/ml) (Fig. 3-5C, Supplementary File 3). At 4 weeks post-immunization the PBS control (0.200 mg/ml), Alpha Ject Micro 4® (0.216 mg/ml), and Forte Micro 4® (0.255 mg/ml) immunized groups had similar IgM titers. However, the bacterin mix immunized group had a significantly higher IgM titer (0.423 mg/ml) (Fig. 3-5C, Supplementary File 3). At 6 weeks post-immunization all the immunized fish, with exception of the mock immunized group (0.068 mg/ml), showed an increase in the IgM titers (Fig. 3-5C). The Alpha Ject Micro 4® and Forte Micro 4® immunized groups had an increase on IgM titers of 0.911 mg/ml and 0.606 mg/ml, respectively, whereas the bacterin mix immunized group showed the highest IgM titers (1.734 mg/ml). This difference was significant as compared to the Forte Micro 4®, the Alpha Ject Micro 4® and to the control group at 6 weeks post-immunization (Fig. 3-5C). At 8 weeks post-immunization we observed a reduction in the IgM titers in all treatments (Alpha Ject Micro 4®: 0.415 mg/ml; Forte Micro 4®: 0.520 mg/ml; Bacterin mix: 0.827 mg/ml) but not in the control group (0.064 mg/ml), which showed stable IgM

titers during the whole experiment, and only the bacterin mix group had a significant difference compared to the control group (Fig. 3-5C).

3.5 Discussion

A. salmonicida has been described as causing chronic disease in different fish species like Atlantic salmon (*Salmo salar*) and common carp (*Cyprinus carpio*), and can be transmitted to other species or between wild and farmed fish in open sea net pens (Krkošek, 2017; Skrodenytė-Arbačiauskienė et al., 2012). In this study, we evaluated the virulence of an atypical *A. salmonicida* J410 strain isolated from infected cultured sablefish at marine net pens in Kyuquot Sound, British Columbia. We selected *A. salmonicida* J410 as a model of study based on its phenotypic characteristics, genomic analysis, and its easy growth *in vitro* (Vasquez *et al.*, manuscript under preparation). Although, we found that *A. salmonicida* J410 has low virulence in sablefish (LD_{50}: ~$3x10^5$ CFU/dose; Table 3-1), as compared to *A. salmonicida* J223 in rainbow trout (*Oncorhynchus mykiss*; LD_{50}: $5.7x10^2$ CFU/dose) (Valderrama et al., 2017b), it has a high morbidity rate. Further, *A. salmonicida* J410 did not kill 100% of infected sablefish (Figs. 3-1A and 3-2A) despite remaining in the internal tissues (Fig. 3-1E). Perhaps, the lower virulence of *A. salmonicida* J410 in contrast to other isolates is related to its persistence in the fish tissues.

We observed that *A. salmonicida* J410 first colonized the liver and brain at the lowest doses tested (Fig. 3-1C). These results suggest that the liver and the brain are the primary target organs of *A. salmonicida* J410 in sablefish. We also observed bacteremia at 5 dpi (Fig. 3-1C). Intracellular infection of erythrocytes by *A. salmonicida* has been

described in Atlantic salmon *in vitro* and *in vivo* (Valderrama et al., 2019). Also, colonization of the brain by *A. salmonicida* has been reported in rainbow trout (Bartkova et al., 2017). It appears that *A. salmonicida* can cross the fish blood-brain barrier, and according to the current knowledge and our data, it is possible that infected erythrocytes could serve as a mechanism of transport for *A. salmonicida* to reach different organs, including the brain. The protection conferred by the blood-brain barrier against infectious diseases in fish is not well understood. Several bacterial pathogens have been reported to colonize the fish brain, and perhaps the blood-brain barrier does not confer protection against infectious agents in teleost since encephalitis seems common during bacterial infections (Patterson et al., 2012; Pressley et al., 2005; Starliper, 2011; van Leeuwen et al., 2014).

Immunohistochemistry revealed that *A. salmonicida* detection increased in the head kidney, spleen, and brain by 10 dpi. This is related to the *A. salmonicida* tissue colonization results (Fig. 3-1). CD10 is known as a marker of hematopoietic progenitor cells in mammalian bone marrow (Hollander et al., 1988) and is present in sablefish (Fig. 3-2), and IgM is expressed by B lymphocytes in fish (Parra et al., 2013). The general increase in IgM in the tissues, and decrease of CD10 expression in spleen and brain, could suggest that naïve B cells became plasma cells, and that the decrease of CD10 in the head kidney was related to B cell proliferation (Fig. 3-2) in response to the infection.

Clinical signs of furunculosis were not evident at 5 dpi in fish inoculated with the lowest dose (10^4 CFU/dose) in contrast to fish infected with the higher doses (10^6 and -10^7 CFU/dose), which showed evident furunculosis clinical signs (Fig. 3-1B). These results

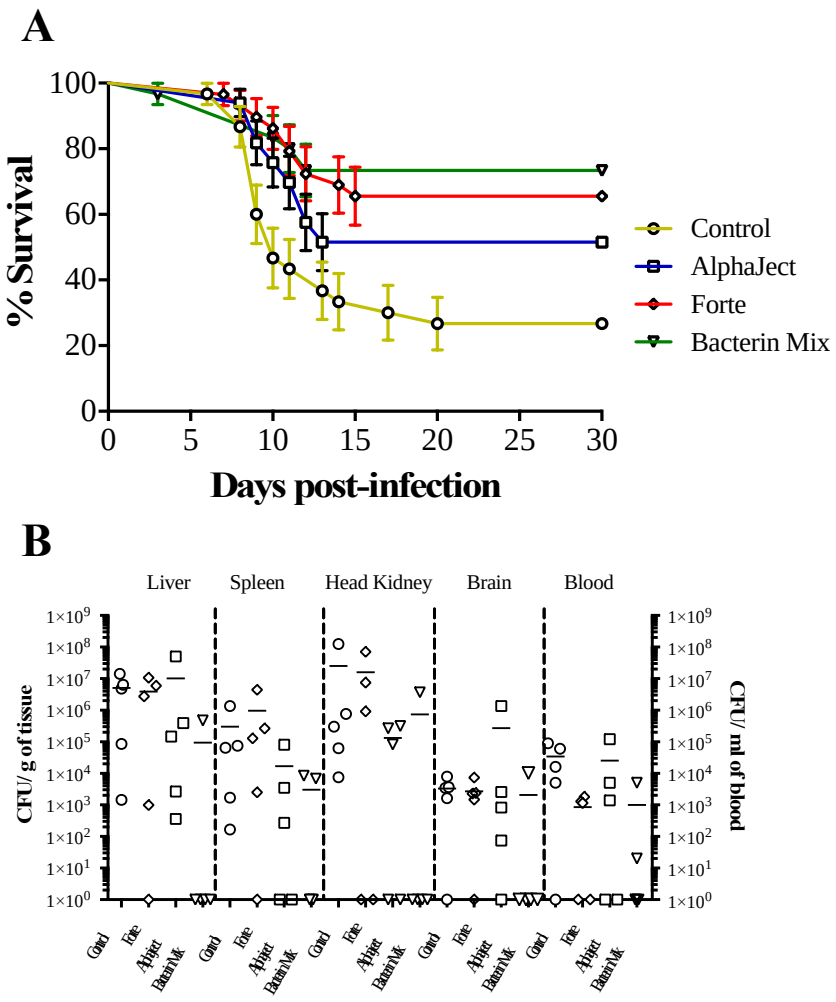

Figure 3-3. Challenge of immunized sablefish. A. Cumulative survival (%) of vaccinated sablefish after intraperitoneal (ip) challenge with 10^7 CFU/dose (100x LD_{50}) of *A. salmonicida* J410. Fish were immunized with phosphate saline buffer (PBS 1X) (yellow line); Alpha Ject Micro 4® (PharmaQ) (blue line); Forte Micro 4® (Elanco) (red line); or bacterin mix (autogenous vaccine; green line). Significant differences were calculated between the control group and the vaccinated groups ($p<0.0001$). **B.** *A. salmonicida* J410 tissue colonization after 10 days post-challenge. White circle (Control); black diamond (Alpha Ject Micro 4®); white square (Forte Micro 4®) and black-down triangle (bacterin mix). The bar indicates the average value.

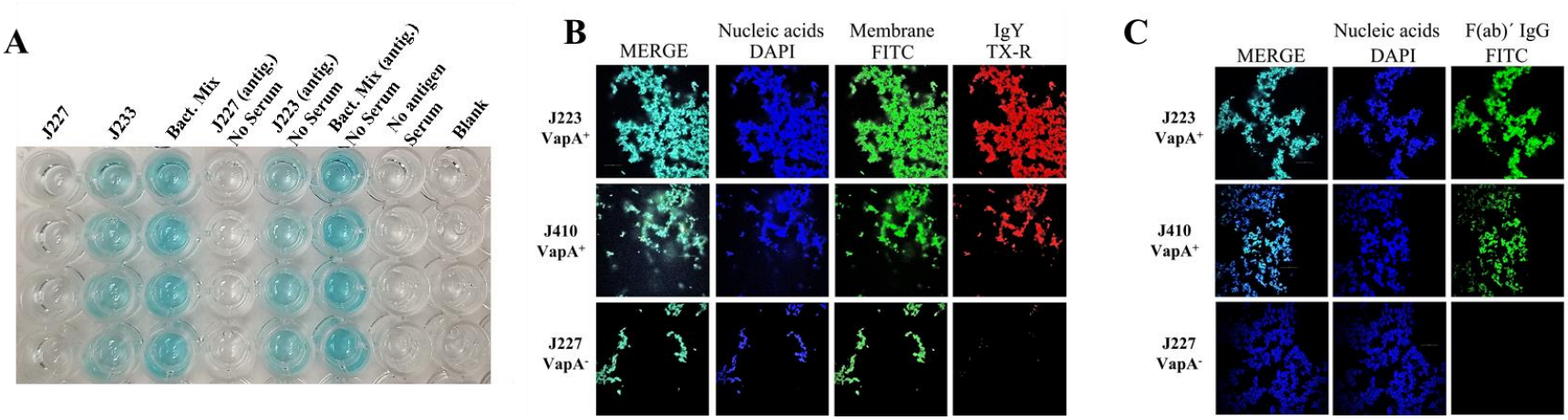

Figure 3-4. Non-specific binding of immunoglobulins to *A. salmonicida* VapA protein. **A**. Indirect ELISA evaluation. Presence of *A. salmonicida* VapA^{+} strains caused a non-specific binding of the secondary antibody IgY-biotinylated. This is not influenced by pre-incubation with sablefish serum from immunized or non-fish. **B.** Confocal microscopy of *A. salmonicida* J223 VapA^{+}; *A. salmonicida* J410 VapA^{+} and *A. salmonicida* J227 VapA^{-} strains labelled with 4′,6-diamidino-2-phenylindole (DAPI), 5-(4,6-dichlorotriazinyl) amino fluorescein (DTAF), and chicken IgY anti-sablefish IgM-avidin Texas-Red. **C.** Confocal Microscopy of *A. salmonicida* J223 VapA^{+}; *A. salmonicida* J410 VapA^{+} and *A. salmonicida* J227 VapA^{-} strains labelled with DAPI and goat F(ab')2 anti-rabbit IgG (H+L)-FITC.

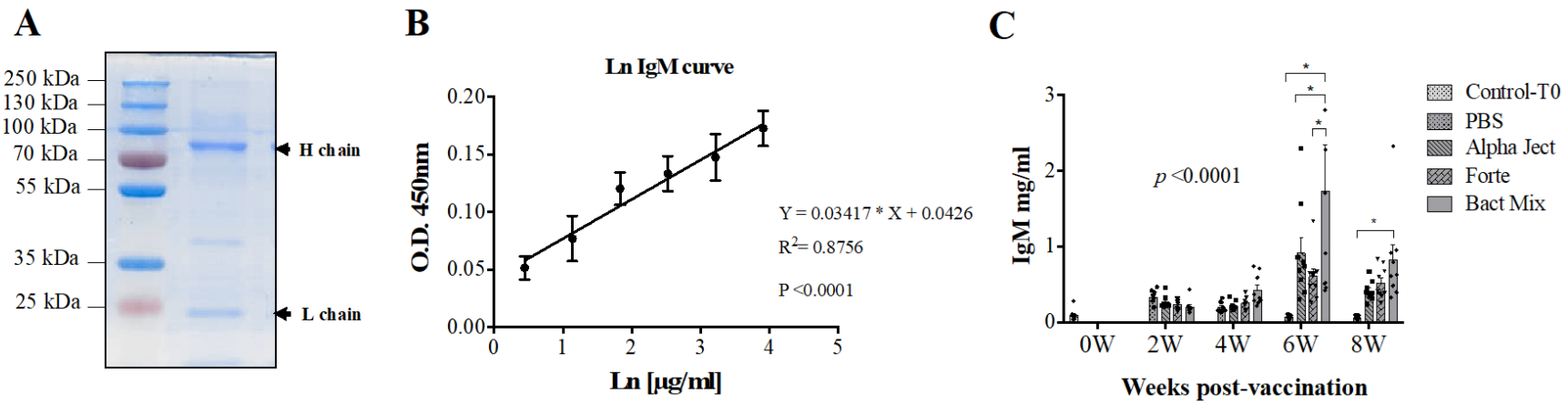

Figure 3-5. Post-challenge IgM levels in sablefish as quantified by dELISA. A. SDS-PAGE 10% of purified sablefish IgM stained with Coomassie Blue (arrows show different chain structures). **B.** Standard curve for purified IgM of known concentrations (100; 50; 25, 12.5; 6.25; 3.125; 1.56 µg/ml); concentrations were standardized to natural logarithm (ln) using a linear regression [Y=0.03417*ln(X)+0.0426] that had an R^2= 0.8756 and a *P* value < 0.0001. **C.** Total IgM quantification by dELISA in serum samples collected at 2, 4, 6, and 8 weeks post-vaccination from PBS (mock), Alpha Ject 4®, Forte Micro 4®, and bacterin mix immunized groups. Values from pre-immunization; time zero (T0) (n=10) are also shown. An asterisk indicates significant differences as compared to all groups. Statistical differences were determined using GraphPad Prism 7.4.

indicate that *A. salmonicida* infection in sablefish is dose-dependent and suggests that *A. salmonicida* strain J410 causes more of a chronic type of infection (Fig. 3-1A).

Enhanced expression of iron regulated outer membrane proteins (IROMPs) has been previously described as a strategy for vaccine development in teleosts (Hirst & Ellis, 1994; Santander et al., 2012). Here, we developed an autogenous vaccine using three atypical *A. salmonicida* strains (J409, J410, and J411) grown under iron-limited conditions to up-regulate the expression of IROMPs and increase vaccine coverage. The RPS of the autogenous vaccine preparation was 64%, and although this was the highest RPS among the evaluated vaccines, this vaccine preparation did not reach the desired RPS of 70% (Midtlyng, 2016). Previously, an injectable autogenous vaccine against atypical *A. salmonicida* was evaluated by Arkoosh *et al*. (2018) in sablefish, and they obtained an RPS of 81.7% (Arkoosh et al., 2018). However, in contrast to our expreriments, the vaccinated animals were challenged with $8.4x10^5$ CFU/dose, similar to our calculated LD_{50} for atypical *A. salmonicida*. Additionally, in the study of Arkoosh *et al*. (2018), the non-immunized control group had 45% survival, which is very close to the LD_{50} calculated in this study (~$3x10^5$ CFU/dose). This suggests that similar results would be obtained with a higher challenge dose, as we determined in our assays (Fig. 3-2A).

The RPS for Alpha Ject Micro 4® was previously determined to be 100% in Atlantic salmon (Romstad et al., 2014), and 58.3% for Forte Micro 4® in Arctic charr (*Salvelinus alpinus*) (Braden et al., 2019). However, the RPS in sablefish at 30 days post-challenge was only ~30% for Alpha Ject Micro 4®, which is almost 1/3 of the reported RPS in Atlantic salmon (Romstad et al., 2014). The RPS in sablefish was ~57% for Forte Micro 4® (Table 3-1), which is consistent with the observed RPS in Arctic charr (Braden et al., 2019).

Post-challenge bacterial load analysis showed that all non-immunized fish had high bacterial colonization in all tested tissues (Fig. 3-2B). Fish groups vaccinated with commercial vaccines showed high bacterial colonization, similar to the non-immunized fish group (Fig. 3-2B). Also, bacterial load was detected in a few fish vaccinated with the autogenous vaccine, suggesting that the vaccine design has room for improvement (Fig. 3-2B).

Nevertheless, it is evident that bacterin-based vaccines against atypical *A. salmonicida* are not optimal. This could be due to the bacterin preparations containing several non-protective immune dominant antigens or immune suppressors, like VapA (A-layer unique component), which attract antibodies such as rabbit IgG and human IgM in a non-specific fashion (Phipps & Kay, 2019). Here, we showed that VapA binds to the antigen-binding fragment F(ab)´ of the antibodies in a non-specific fashion (Fig. 3-3C). This suggests that *A. salmonicida* VapA might be used to enhance phagocytosis mediated opsonization (Strømsheim et al., 1994) and that its efficacy as an immune protective antigen is controversial. For instance, VapA could be playing a role similar as the surface M protein in *Streptococcus pyogenes*, which is a well characterized immunoglobulin-binding protein with highly conserved domains among serotypes (Cunningham, 2000; Hollingshead et al.,1993).

Previous studies have demonstrated that total IgM titers, as well as antigen-specific IgM titers, correlate with vaccine efficacy in rainbow trout (Costa et al., 2012), Atlantic salmon (*Salmo salar*) (Caruffo et al., 2016; Kamil et al., 2011), brown trout (*Salmo trutta*) (Hordvik, 2015; Kamil et al., 2011), coho salmon (*Oncorhynchus kisutch*) (Hordvik, 2015), chinook salmon (*Oncorhynchus tshwytscha*) (Lulijwa et al., 2019), Arctic charr (*Salvelinus alpinus*) (Brown et al., 2020), Nile tilapia (*Oreochromis niloticus*) (Yin et al., 2019), yellow catfish (*Pelteobagrus fulvidraco*) (Xu et al., 2019), Atlantic cod (*Gadus morhua*) (Mikkelsen et al., 2011) and lumpfish

(*Cyclopterus lumpus*) (Rønneseth et al., 2015) against bacteria *A. salmonicida* (Brown, 2020), *Vibrio anguillarum* (Mikkelsen et al., 2011) *Yersinia ruckeri* (Chettri et al., 2019), *Streptococcus iniae* (Costa et al., 2012), *Streptococcus agalactiae* (Yin et al., 2019), *Flavobacterium columnare* (Xu et al., 2019) and viruses (Brown et al., 2020; Castro et al., 2013). Here, we showed that total IgM levels reflected the vaccine's RPS in sablefish. Additionally, we determined that the serum of naïve sablefish of 125.45 g fish contains ~75 µg/ml (Fig. 3-5C), which is low compared to other fish species. For instance, IgM titers in Atlantic salmon of 2-8 kg are 0.8-1.3 mg/ml (Havarstein et al., 1988), and in rainbow trout of 20 g are 0.67 ± 0.66 mg/ml (Sanchez et al., 1993). To our current knowledge, IgM titers for fish of similar size to the sablefish used in this study are between 2.1-9.1 mg/ml of serum (Hordvik, 2015). Nonetheless, the values for serum IgM that we obtained using the ELISA assay were comparable with the IgM titers that we obtained during purification, i.e., we obtained 3.5 mg/ml of sablefish IgM from 150 to 200 ml of serum.

Sablefish vaccinated with the autogenous vaccine (bacterin mix) preparation had higher IgM titers as compared to the commercial vaccines (Fig. 3-5C). Total IgM titers peaked at 6 weeks post-immunization (wpi) and were significantly higher (by 25 and 3 times) as compared to the control group and the Forte Micro 4® vaccinated group, respectively (Fig. 3-5C, Table 3-1). At 8 weeks post-vaccination, the bacterin mix immunized group again showed the highest IgM titers, these 12 times higher as compared to control fish (Fig. 3-5C, Table 3-1), which fits with their high RPS observed in this study. Forte Micro 4® showed higher IgM titers than Alpha Ject Micro 4® at 8 wpi, however the difference was not significant.

The autogenous vaccine mix triggered superior immune protection as compared to currently available commercial vaccines, and our results agree with previous studies where IgM titers against *A. salmonicida* bacterin showed a peak between 6 and 12 weeks post-immunization

in Atlantic salmon (Strømsheim et al., 1994) and in wolffish (*Anarhichas minor*) immunized with atypical *A. salmonicida* bacterin mixed with an oil-adjuvant (Grøntvedt et al., 2004). However, 100% immune protection was not achieved in our study, and this indicates that vaccine design plays an important role in efficacy. For instance, to improve the vaccine efficacy of the bacterin mix, immune dominant and not immunoprotected antigens could be removed. Also, modern adjuvants can improve the immunogenicity of vaccines (Di Pasquale et al., 2015; Leroux-Roels, 2010). The commercial vaccines evaluated in this study are polyvalent. This adds a complexity to the antigenic balance between immune protective antigens and may impact vaccine efficacy in sablefish.

3.6 Conclusions

In conclusion, we developed an infection model for sablefish, including determining the LD_{50} dose for atypical *A. salmonicida*. Atypical *A. salmonicida* J410 does not cause an acute infection in sablefish. Rather it causes a chronic type of infection that involves initial colonization of the hematopoietic tissues and the brain. The monovalent autogenous vaccine mix using three *A. salmonicida* strains provided better protection than two polyvalent commercial vaccines. Sablefish IgM titers peaked at 6 weeks post-vaccination. Vaccine immune protection was associated with the IgM titers, where the autogenous vaccinated fish had the highest RPS and IgM titers. The *A. salmonicida* A-layer binds to immunoglobulins in a non-specific fashion, raising the question about its utility as an immune protective antigen. Although this study provides novel insights about sablefish vaccinology for the prevention of furunculosis, further research is required to develop an effective cross-protective vaccine for this species.

3.7 References

Ahmad, N., Ammar, A., Storr, S., Green, A., Rakha, E., Ellis, I., Martin, S. (2018). IL-6 and IL-10 are associated with good prognosis in early stage invasive breast cancer patients. *Cancer Immunology, Immunotherapy, 67*(4), 537-549. doi:10.1007/s00262-017-2106-8

Amaoka, K. (1984). The Fishes of the Japanese Archipelago. *H. Masuda; K. Amaoka; C. Araga; T. Uyeno; T. Yoshino (eds.). Tokai Univ. Press.*(Anoplopomatidae), 320.

Amend, D. (1981). Potency testing of fish vaccines. *Developments in biological standardization.* (49) 447-454.

Arkoosh, M., Dietrich, J., Rew, M., Olson, W., Young, G., Goetz, F. (2018). Exploring the efficacy of vaccine techniques in juvenile sablefish, *Anoplopoma fimbria*. *Aquaculture Research, 49*(1), 205-216. doi:10.1111/are.13449

Austin, B., & Austin D. (2012). *Bacterial Fish Pathogens* (5th ed.). Disease of Farmed and Wild Fish: Springer Netherlands. XXIV, 654. doi:10.1007/978-94-007-4884-2.

Bartkova, S., Kokotovic, B., Dalsgaard, I. (2017). Infection routes of *Aeromonas salmonicida* in rainbow trout monitored in vivo by real-time bioluminescence imaging. *Journal of Fish Diseases 40*(1) 73-82. doi:10.1111/jfd.12491

Braden, L., Whyte, S., Brown, A., Iderstine, C., Letendre, C., Groman, D., Lewis, J., Purcell, S., Hori, T., Fast, M. (2019). Vaccine-induced protection against furunculosis involves pre-emptive priming of humoral immunity in Arctic Charr, *Frontier in Immunology 10*, 120-120. doi:10.3389/fimmu.2019.00120

Brown, A., Whyte, S., Braden, L., Groman, D., Purcell, S., Fast, M. (2020). Vaccination strategy is an important determinant in immunological outcome and survival in Arctic charr (*Salvelinus alpinus)* when challenged with atypical *Aeromonas salmonicida*. *Aquaculture, 518*, 734838. doi:https://doi.org/10.1016/j.aquaculture.2019.734838

Caruffo, M., Maturana, C., Kambalapally, S., Larenas, J., Tobar, J. (2016). Protective oral vaccination against infectious salmon anaemia virus in *Salmo salar*. *Fish & Shellfish Immunology, 54*, 54-59. doi:https://doi.org/10.1016/j.fsi.2016.03.009

Castro, R., Jouneau, L., Pham, H., Bouchez, O., Giudicelli, V., Lefranc, M., Quillet, E., Benmansour, A., Cazals, F., Six, A., Fillatreau, S., Sunyer, O., Boudinot, P. (2013). Teleost fish mount complex clonal IgM and IgT responses in spleen upon systemic viral infection. *Fish & Shellfish Immunology, 34*(6), 1643-1644. doi:https://doi.org/10.1016/j.fsi.2013.03.029

Chakraborty, S., Cao, T., Hossain, A., Gnanagobal, H., Vasquez, I., Boyce, D., Santander, J. (2019). Vibrogen-2 vaccine trial in lumpfish (*Cyclopterus lumpus*) against *Vibrio anguillarum. Journal of Fish Diseases, 42*(7), 1057-1064. doi:10.1111/jfd.13010

Chandler, D., & Robenson, R. (2009). Bioimaging : current concepts in light and electron microscopy. *Jones and Bartlett Publishers, Sudbury, Mass*.

Chettri, J., Al-Jubury, A., Hansen, M., Lihme, A., Dalsgaard, I., Buchmann, K., Heegaard, P. (2019). Protective effect of in-feed specific IgM towards *Yersinia ruckeri* in rainbow trout. *Fish & Shellfish Immunology, 93*, 934-939. doi:https://doi.org/10.1016/j.fsi.2019.08.024

Cipriano, R., & Bullock, G. (2001). Furunculosis and other diseases caused by *Aeromonas salmonicida. Fish Disease Leaflet*. U.S. Fish and Wildlife Service. *66* 33p. Retrieved from http://pubs.er.usgs.gov/publication/fdl66

Costa, G., Hillary, D., Priti, K., Bromage, E. (2012). A holistic view of the dynamisms of teleost IgM: A case study of *Streptococcus iniae* vaccinated rainbow trout (*Oncorhynchus mykiss*). *Developmental & Comparative Immunology, 36*(2), 298-305. doi:https://doi.org/10.1016/j.dci.2011.04.011

Cunningham, M. (2000). Pathogenesis of group A streptococcal infections. *Clinical microbiology reviews, 13*(3), 470-511. doi:10.1128/cmr.13.3.470-511.2000

Department of Fisheries and Oceans Canada, (DFO). (2017). Value Added | Fisheries and Oceans Canada. Retrieved from http://www.dfo-mpo.gc.ca/stats/aqua/aqua-val-eng.htm

Department of Fisheries and Oceans Canada, (DFO). (2016). British Columbia Seafood Industry-year in review. Retrieved from https://www2.gov.bc.ca/assets/gov/farming-natural-resources-and-industry/agriculture-and-seafood/statistics/industry-and-sector-profiles/sector-reports/british_columbias_fisheries_and_aquaculture_sector_2016_edition.pdf

Di Pasquale, A., Preiss, S., Tavares Da Silva, F., Garçon, N. (2015). Vaccine Adjuvants: from 1920 to 2015 and Beyond. *Vaccines, 3*(2), 320-343. doi:10.3390/vaccines3020320

Elanco Canada Ltd. (2020). Forte micro. Retrieved from https://www.drugs.com/vet/forte-micro-can.html

Eslamloo, K., Surendra, K., Caballero-Solares, A., Gnanagobal, H., Santander, J., Rise, M. (2019). Profiling the transcriptome response of Atlantic salmon head kidney to formalin-killed *Renibacterium salmoninarum. Fish & Shellfish Immunology* (98) 937-949. doi:https://doi.org/10.1016/j.fsi.2019.11.057

Food and Agriculture Organization of the United Nations, (FAO). (2009). *How to feed the world 2050*. Retrieved from http://www.fao.org/fileadmin/templates/wsfs/docs/expert_paper/How_to_Feed_the_World_in_2050.pdf

Food and Agriculture Organization of the United Nations, (FAO). (2019). *Fisheries and Aquaculture Department, Species Fact Sheets*. Retrieved from http://www.fao.org/fishery/species/3341/en

Gores, K., & Prentice, E. (1984). Growth of sablefish (*Anoplopoma fimbria*) in marine net-pens. *Aquaculture, 36*(4), 379-386. doi:10.1016/0044-8486(84)90330-2

Grøntvedt, R., Lund, V., Espelid, S. (2004). Atypical furunculosis in spotted wolffish (*Anarhichas minor O.*) juveniles: bath vaccination and challenge. *Aquaculture, 232*(1), 69-80. doi:https://doi.org/10.1016/j.aquaculture.2003.06.001

Havarstein, L., Aasjord, P., Ness, S., Endresen, C. (1988). Purification and partial characterization of an IgM-like serum immunoglobulin from Atlantic salmon (*Salmo salar*). *Developmental & Comparative Immunology, 12*(4), 773-785. doi:10.1016/0145-305x(88)90052-3

Hirst, I., & Ellis, A. (1994). Iron-regulated outer membrane proteins of *Aeromonas salmonicida* are important protective antigens in Atlantic salmon against furunculosis. *Fish & Shellfish Immunology, 4*(1), 29-45. doi:https://doi.org/10.1006/fsim.1994.1004

Hnasko R., 2015. *ELISA, Methods and Protocols*. 1st ed. Springer, NY. Humana Press. X, 216p. doi: 10.1007/978-1-4939-2742-5.

Hollander, Z., Shah, V., Civin, C., Loken, M. (1988). Assessment of proliferation during maturation of the B lymphoid lineage in normal human bone marrow. *Blood, 71*(2), 528-531. doi:10.1182/blood.V71.2.528.528

Hollingshead, S., Readdy, T., Yung, D., Bessen, D. (1993). Structural heterogeneity of the emm gene cluster in group A streptococci. *Molecular Microbiology, 8*(4), 707-717. doi:10.1111/j.1365-2958.1993.tb01614.x

Hopkins, K. (1992). Reporting fish growth: A review of the basics. *Journal of the World Aquaculture Society, 23*(3), 173-179. doi:10.1111/j.1749-7345.1992.tb00766.x

Hordvik, I. (2015). Immunoglobulin isotypes in Atlantic salmon, *Salmo salar*. *Biomolecules, 5*(1), 166-177. doi:10.3390/biom5010166

Kamil, A., Falk, K., Sharma, A., Raae, A., Berven, F., Koppang, E., Hordvik, I. (2011). A monoclonal antibody distinguishes between two IgM heavy chain isotypes in Atlantic salmon and brown trout: Protein characterization, 3D modeling and epitope mapping. *Molecular Immunology, 48*(15), 1859-1867. doi:https://doi.org/10.1016/j.molimm.2011.05.005

Kendall, A., & Matarese A. (1987). Biology of eggs, larvae and epipelagic juvinales of sablefish, *Anoplopoma fimbria*, in relation to their potential use in management. *Marine Fisheries Review*. Retrieved from https://spo.nmfs.noaa.gov/sites/default/files/pdf-content/MFR/mfr491/mfr4911.pdf

Kim, J., Park, H., Hwang, I., Han, J., Kim, D., Oh, Ch., Lee, J., Kang, J. (2017). Alterations of growth performance, hematological parameters, and plasma constituents in the sablefish, *Anoplopoma*

fimbria depending on ammonia concentrations. *Fisheries and Aquatic Sciences, 20*(1), 4. doi:10.1186/s41240-017-0049-9

Krkošek, M. (2017). Population biology of infectious diseases shared by wild and farmed fish. *Canadian Journal of Fisheries and Aquatic Sciences, 74*(4), 620-628. doi:10.1139/cjfas-2016-0379

Leboffe, M., & Pierce, B. (2015). *Microbiology: laboratory theory & application*. 4th ed. Morton Publishing Company, USA. ISBN:1617314188, 9781617314186, 896p.

Leroux-Roels, G. (2010). Unmet needs in modern vaccinology: adjuvants to improve the immune response. *Vaccine, 28 Suppl 3*, C25-36. doi:10.1016/j.vaccine.2010.07.021

Ling, X., Dong, W., Zhang, Y., Hu, J., Liu, J., Zhao, X. (2019). A recombinant adenovirus targeting typical *Aeromonas salmonicida* induces an antibody-mediated adaptive immune response after immunization of rainbow trout. *Microbial Pathogens, 133*, 103559. doi:10.1016/j.micpath.2019.103559

Liu Y., Volpe J., Sumaila U.R. (2005). Ecological and economic impact assessment of sablefish aquaculture in British Columbia, *13*(3). doi:http://dx.doi.org/10.14288/1.0074787

Lulijwa, R., Alfaro, A. C., Merien, F., Burdass, M., Venter, L., Young, T. (2019). *In vitro* immune response of chinook salmon (*Oncorhynchus tshawytscha*) peripheral blood mononuclear cells stimulated by bacterial lipopolysaccharide. *Fish & Shellfish Immunology, 94*, 190-198. doi:https://doi.org/10.1016/j.fsi.2019.09.003

Magnadottir, B. (1998). Comparison of immunoglobulin (IgM) from four fish species. *Buvisindi, 12*.

Magnadóttir, B., Bambir, S., Gudmundsdóttir, B., Pilström, L., Helgason, S. (2002). Atypical *Aeromonas salmonicida* infection in naturally and experimentally infected cod, *Gadus morhua L. Journal of Fish Diseases, 25*(10), 583-597. doi:10.1046/j.1365-2761.2002.00407.x

Mahoney, R., Krattiger, A., Clemens, J., Curtiss, R., 3rd. (2007). The introduction of new vaccines into developing countries. IV: Global Access Strategies. *Vaccine, 25*(20), 4003-4011. doi:10.1016/j.vaccine.2007.02.047

Mashoof, S., & Criscitiello, M. (2016). Fish Immunoglobulins. *Biology (Basel), 5*(4). doi:10.3390/biology5040045

Michel, C., Dorson, M., Faivre, B. (1991). Opsonizing activity of anti-*Aeromonas salmonicida* antibodies after inactivation of complement in rainbow trout. *Annal Recherches Veterinaries, 22*(1), 51-58.

Mikkelsen, H., Lund, V., Larsen, R., Seppola, M. (2011). Vibriosis vaccines based on various sero-subgroups of *Vibrio anguillarum* O2 induce specific protection in Atlantic cod (*Gadus morhua L.*) juveniles. *Fish & Shellfish Immunology, 30*(1), 330-339. doi:https://doi.org/10.1016/j.fsi.2010.11.007

Midtlyng, P. (2016). *Methods for measuring efficacy, safety and potency of fish vaccines*, In: Adams A. (eds) *Fish Vaccines*. Birkhäuser Advances in Infectious Diseases. Springer, Basel 119-141pp.

Parra, D., Takizawa, F., Sunyer, J. (2013). Evolution of B cell immunity. *Annual Review Animal Bioscience, 1*, 65-97. doi:10.1146/annurev-animal-031412-103651

Patterson, H., Saralahti, A., Parikka, M., Dramsi, S., Trieu-Cuot, P., Poyart, C., Rounioja, S., Ramet, M. (2012). Adult zebrafish model of bacterial meningitis in *Streptococcus agalactiae* infection. *Dev Comp Immunol, 38*(3), 447-455. doi:10.1016/j.dci.2012.07.007

PharmaQ. (2020). Alpha Ject micro 4. Retrieved from https://www.drugs.com/vet/alpha-ject-micro-4-can.html

Phipps, B., & Kay, W. (1988). Immunoglobulin binding by the regular surface array of *Aeromonas salmonicida*. *Journal of Biological Chemistry, 263*(19), 9298-9303.

Pressley, M., Phelan, P., Witten, P., Mellon, M., Kim, C. (2005). Pathogenesis and inflammatory response to Edwardsiella tarda infection in the zebrafish. *Developmental & Comparative Immunology, 29*(6), 501-513. doi:https://doi.org/10.1016/j.dci.2004.10.007

Ramakrishnan, M. (2016). Determination of 50% endpoint titer using a simple formula. *World journal of virology, 5*(2), 85-86. doi:10.5501/wjv.v5.i2.85

Roger, F., Lamy, B., Jumas-Bilak, E., Kodjo, A. (2012). Ribosomal Multi-operon diversity: An original perspective on the genus *Aeromonas. PLoS ONE, 7*(9), e46268. doi:10.1371/journal.pone.0046268

Romstad, A., Reitan, L., Midtlyng, P., Gravningen, K., Emilsen, V., Evensen, O. (2014). Comparision of a serological potency assay for furunculosis vaccines (*Aeromonas salmonicida* subsp. *salmonicida*) to intraperitoneal challenge in Atlantic salmon (*Salmo salar* L.). *Biologicals, 42*(2), 86-90. doi:10.1016/j.biologicals.2013.11.007

Rønneseth, A., Ghebretnsae, D., Wergeland, H., Haugland, G. (2015). Functional characterization of IgM+ B cells and adaptive immunity in lumpfish (*Cyclopterus lumpus L.*). *Developmental & Comparative Immunology, 52*(2), 132-143. doi:https://doi.org/10.1016/j.dci.2015.05.010

Sambrook, J., and Russell, W. (2001). *Molecular Cloning; A Laboratory Manual*. 3rd ed. Cold Spring Harbor, NY. Cold Spring Harbor Press.

Sanchez, C., Babin, M., Tomillo, J., Ubeira, F., Dominguez, J. (1993). Quantification of low levels of rainbow trout immunoglobulin by enzyme immunoassay using two monoclonal antibodies. *Veterinary Immunology & Immunopathology, 36*(1), 65-74. doi:10.1016/0165-2427(93)90006-p

Santander, J., Golden, G., Wanda, S., Curtiss, R., 3rd. (2012). Fur-regulated iron uptake system of *Edwardsiella ictaluri* and its influence on pathogenesis and immunogenicity in the catfish host. *Infection & Immunity, 80*(8), 2689-2703. doi:10.1128/iai.00013-12

Santander, J., Mitra, A., Curtiss, R. (2011). Phenotype, virulence and immunogenicity of *Edwardsiella ictaluri* cyclic adenosine 3′,5′-monophosphate receptor protein (Crp) mutants in catfish host. *Fish & Shellfish Immunology, 31*(6), 1142-1153. doi:https://doi.org/10.1016/j.fsi.2011.10.009

Shoemaker, C., Klesius, P., Evans, J., Arias, C. (2009). Use of modified live vaccines in aquaculture. *Journal of the World Aquaculture Society, 40*(5), 573-585. doi:10.1111/j.1749-7345.2009.00279.x

Skrodenytė-Arbačiauskienė, V., Kazlauskienė, N., Vosylienė, M., Virbickas, T. (2012). *Aeromonas salmonicida* infected fish transfer disease to healthy fish via water. *Central European Journal of Biology, 7*(5), 878-885. doi:10.2478/s11535-012-0066-8

Sonu, S. (2014). Supply and Market for Sablefish in Japan. *NOAA technical memoramdum.* Retrieved from https://www.st.nmfs.noaa.gov/Assets/commercial/market-news/sablefishSupplyMarket2014.pdf

Starliper, C. (2011). Bacterial coldwater disease of fishes caused by *Flavobacterium psychrophilum*. *Journal of Advanced Research, 2*(2), 97-108. doi:https://doi.org/10.1016/j.jare.2010.04.001

Strømsheim, A., Eide, D., Fjalestad, K., Larsen, H., Røed, K. (1994). Genetic variation in the humoral immune response in Atlantic salmon (*Salmo salar*) against *Aeromonas salmonicida* A-layer. *Veterinary Immunology and Immunopathology, 41*(3), 341-352. doi:https://doi.org/10.1016/0165-2427(94)90106-6

Valderrama, K., Saravia, M., Santander, J. (2017a). Phenotype of *Aeromonas salmonicida* sp. *salmonicida* cyclic adenosine 3',5'-monophosphate receptor protein (Crp) mutants and its virulence in rainbow trout (*Oncorhynchus mykiss*). *Journal of Fish Diseases, 40*(12), 1849-1856. doi:10.1111/jfd.12658

Valderrama, K., Soto-Davila, M., Segovia, C., Vasquez, I., Dang, M., Santander, J. (2019). *Aeromonas salmonicida* infects Atlantic salmon (*Salmo salar*) erythrocytes. *Journal of Fish Diseases, 42*(11), 1601-1608. doi:10.1111/jfd.13077

Valderrama, K., Soto-Davila, M., Santander, J. (2017b). Draft Genome Sequence of the Type Strain *Aeromonas salmonicida* subsp. *salmonicida* ATCC 33658. *Genome announcements, 5*(40), e01064-01017. doi:10.1128/genomeA.01064-17

van Leeuwen, L., van der Kuip, M., Youssef, S., de Bruin, A., Bitter, W., van Furth, A., van der Sar, A. (2014). Modeling tuberculous meningitis in zebrafish using *Mycobacterium marinum*. *Diseases Models & Mechanisms, 7*(9). doi:10.1242/dmm.015453

Wiedenhoft, H. (2017). Advances in US sablefish aquaculture. *Aquaculture North America*. Retrieved from https://www.aquaculturenorthamerica.com/advances-in-us-sablefish-aquaculture-hits-snag-1584/

Xu J., Zhang X., Luo Y., Wan X., Yao Y., Zhang L., Yu Y., Ai T., Wang Q., Xu Z. (2019). IgM and IgD heavy chains of yellow catfish (*Pelteobagrus fulvidraco*): Molecular cloning, characterization and expression analysis in response to bacterial infection. *Fish & Shellfish Immunology, 84*, 233-243. doi:https://doi.org/10.1016/j.fsi.2018.10.012

Yin X., Liangliang M., Shengli F., Liting W., Kailiang H., Hairong W., Xia B., Xiufang W., Zheng G., Anli W., Jianmin Y. (2019). Expression and characterization of Nile tilapia (*Oreochromis niloticus*) secretory and membrane-bound IgM in response to bacterial infection. *Aquaculture, 508*, 214-222. doi:https://doi.org/10.1016/j.aquaculture.2019.03.058

4. SUMMARY

In this thesis, the general objective was to analyze the genome and determine the virulence of *V. anguillarum* and *A. salmonicida* isolated from *C. lumpus* and *A. fimbria*, respectively. Additionally, this study determined the effectiveness of an autogenous vaccine design against *A. salmonicida* infection and evaluated the immune response in cultured sablefish.

In Chapter 2, the results related to *V. anguillarum* J360 virulence and the comparative genome analysis, showed that this pathogenic bacterium isolated from an outbreak in cultured lumpfish is a *V. anguillarum* serotype O2, which is highly virulent in lumpfish, capable of killing 100% of naïve population within 10 days after infection, and causing classic vibriosis clinical signs. Comparative genomics analysis showed that *V. anguillarum* J360 possesses a larger genome size compared to others *V. anguillarum* strains. Virulence-associated genes were identified in both chromosomes (i.e. hemolysins, iron uptake and transports, lipases, gelatinases, etc.), but a virulence plasmid was not detected in contrast to *V. anguillarum* strains isolated from the Pacific coast. This suggest that *V. anguillarum* J360 could be even more virulent if a virulence plasmid is acquired. Also, *V. anguillarum* J360 was shown to be closely related to *V. anguillarum* VIB43, an Atlantic isolate. However, differences in their genome organization were identified, indicating that translocation and insertion events caused by insertion sequences elements (ISs) are driving the evolution of *V. anguillarum* J360. Also, these results suggest that both strains share a common ancestor, and that their evolution relies on environmental conditions and host adaptation. Further analysis would be necessary to answer the question if the ISs are the responsible for the variability in terms of serotypes and if they drive the pathogenesis of this marine bacteria.

In the Chapter 3 in this thesis, I developed an infection model for atypical *A. salmonicida* in sablefish, calculated the LD_{50} for this pathogen, and evaluate the immune response and survival

of sablefish injected with an autogenous vaccine and two commercial vaccines. Atypical *A. salmonicida* J410 is a strain isolated from cultured sablefish from Golden Eagle Sable Fish, BC, Canada, that does not cause acute infection. Rather it causes a chronic type of infection and target the hematopoietic tissues and brain as primary organs of infection. The monovalent autogenous vaccine preparation provided better protection than the commercial vaccines and induced the highest sablefish IgM titers. Additionally, the atypical *A. salmonicida* A-layer was shown to binds to immunoglobulins in a non-specific fashion, suggesting that VapA protein should not be utilized as an immune protective antigen and that protocols for IgM titers determination should be reconsidered and modified to direct ELISA method.

In conclusion, this thesis provides novel insights about the virulence and the genome of a *V. anguillarum* strain isolated from lumpfish (*C. lumpus*) that can be used for further vaccine development. For instance, the expression of virulence factors during bacterin preparation (i.e. iron homeostasis and transport associated proteins, active hemolysin activity, etc.) can improve the vaccine efficacy and trigger a stronger adaptive immune response. Also, the genome analysis results showed common virulence factors among several *Vibrio* strains that could be used as antigens in the development of a multivalent DNA vaccine or live-attenuated vaccine design.

Regarding to vaccine development for the sablefish (*A. fimbria*) aquaculture industry, I have developed an infection model for atypical *A. salmonicida* that can be used as a model for vaccine testing, including autogenous vaccines and commercial vaccines currently being used in the industry. The significances of this study are reflected in the current production of this autogenous vaccine in the sablefish industry for field test purposes.

5. APPENDICES

Appendix I. Housekeeping genes used for MLSA.

Housekeeping Gene and Size	Description	*V. anguillarum* Gene Locus Tags
16S rRNA (1,544 bp)	ribosomal RNA subunit	VAA_r008; VANGB10 (233624..235167); N175_01225; CMV05_00360; CK207_00110; CEQ50_00475; CG015_01435; B5S57_08110; CEA93_00375; CEJ46_00360; CLI14_00110; PL14_00290; CEG15_00290; A8140_00610; AL536_07795; AL464_04065; VS_r0045
ftsZ (1,148 bp)	cell-division protein	VAA_RS03925; VANGNB10_cI2165c; N175_04065; CMV05_12545; CK207_12375; CEQ50_11740; CG015_11710; B5S57_08595; CEA93_11805; CEJ46_11435; CLI14_02890; PL14_10850; CEG15_10675; A8140_02565; AL536_17830; AL464_01670; VS_0454
gapA (1,443 bp)	glyceraldehyde-3-phosphate dehydrogenase	VAA_RS09935; VANGNB10_cI0936c; N175_15935; CMV05_17185; CK207_05935; CEQ50_05455; CG015_05975; B5S57_15270; CEA93_05315; CEJ46_05345; CLI14_09005; PL14_04780; CEG15_04820; A8140_10660; AL536_01340; AL464_04430; VS_0932
gyrB (2,418 bp)	gyrase beta subunit	VAA_RS01005; VANGNB10_cI0013; N175_01055; CMV05_00065; CK207_15105; CEQ50_00155; CG015_01215; B5S57_05625; CEA93_00065; CEJ46_00065; CLI14_14270; PL14_00020; CEG15_00065; A8140_00300; AL536_11690; AL464_14755; VS_0013
mreB (1,044 bp)	rod shape-determining protein	VAA_RS13485; VANGNB10_cI0292; N175_13945; CMV05_01690; CK207_01990; CEQ50_02110; CG015_02870; B5S57_18600; CEA93_01790; CEJ46_01640; CLI14_12555; PL14_01680; CEG15_01650; A8140_13375; AL536_18720; AL464_05080; VS_0341
pyrH (732 bp)	uridine monophosphate (UMP) kinase or uridylate kinase	VAA_RS10055; VANGNB10_cI2045c; N175_04705; CMV05_11900; CK207_11775; CEQ50_11105; CG015_11100; B5S57_09200; CEA93_11190; CEJ46_10830; CLI14_03495; PL14_10250; CEG15_10075; A8140_11485; AL536_09140; AL464_07985; VS_2351
recA (1,047 bp)	recombinase A	VAA_RS12550; VANGNB10_cI0448; N175_12945; CMV05_02370; CK207_02730; CEQ50_02830; CG015_03445; B5S57_17775; CEA93_02675; CEJ46_02620; CLI14_11580; PL14_02240; CEG15_02305; A8140_10030; AL536_18120; AL464_06820; VS_2596

rpoA (993 bp)	RNA polymerase alpha subunit	VAA_RS03025; VANGNB10_cI2326c; N175_03130; CMV05_13510; CK207_13280; CEQ50_12630; CG015_12595; B5S57_07715; CEA93_12685; CEJ46_12320; CLI14_01985; PL14_11715; CEG15_11560; A8140_01855; AL536_22115; AL464_02385; VS_2807
topA (2,631 bp)	DNA topoisomerase I	VAA_RS09170; VANGNB10_cI1085; N175_09445; CMV05_00315; CK207_00385; CEQ50_06215; CG015_06725; B5S57_14500; CEA93_06085; CEJ46_06100; CLI14_08235; PL14_05545; CEG15_05570; A8140_00570; AL536_12085; AL464_14115; VS_1081

Appendix II. Enzymatic profile of *V. anguillarum* J360 using the API ZYM system

Enzymatic Assay for:	**Reaction**
Alkaline phosphatase	+
Esterase (C_4)	+
Esterase lipase (C_8)	+
Lipase (C_{14})	+
Leucine arylamidase	+
Valine arylamidase	+
Cystine arylamidase	+
Trypsin	-
α-Chymotrypsin	-
Acid phosphatase	+
Naphthol-AS-BI-Phosphohydrolase	-
α-Galactosidase	-
β-Galactosidase	-
β-Glucoronidase	-
α-Glucosidase	-
N-Acetyl-β-glucosaminidase	-
α-Mannosidase	-
α-Fucosidase	-

Appendix III. Biochemical profile of *V. anguillarum* J360 using API20NE

Biochemical Assay for:	**Reaction**
Reduction of nitrates to nitrites	+
Indole production	+
Glucose fermentation	+
Urease	+
β-Galactosidase	+
Hydrolysis of:	
Arginine	+
Esculin	+
Gelatin	+
Assimilation of:	
D-Glucose	+
L-Arabinose	+
D-Mannose	+
D-Mannitol	+
N-acetyl-glucosamine	+
D-Maltose	+
Potassium gluconate	+
Capric acid	-
Adipic acid	-
Malic acid	+
Trisodium citrate	+
Phenylacetic acid	-
Code	7777745
Result	Possible *V. fluvialis*

Appendix IV. Biochemical profile of *V. anguillarum* J360 using API20E

Biochemical Assay for:	**Reaction**
β-Galactosidase	+
Indole production	-
Acetoin production	+
Citrate utilization	+
H_2S production	-
Urease	+
Hydrolysis of:	
L-Arginine	+
L-Lysine	+
L-Ornithine	-
L-Tryptophan	-
Gelatin	+
Assimilation of:	
D-Glucose	+
D-Mannitol	-
Inositol	-
D-Sorbitol	-
L-Rhamnose	-
D-Saccharose	-
D-Melibiose	-
D-Amygdaline	-
L-Arabinose	-

Appendix V. Evolutionary taxa relationship of *V. anguillarum* chromosome-I and chromosome-II.

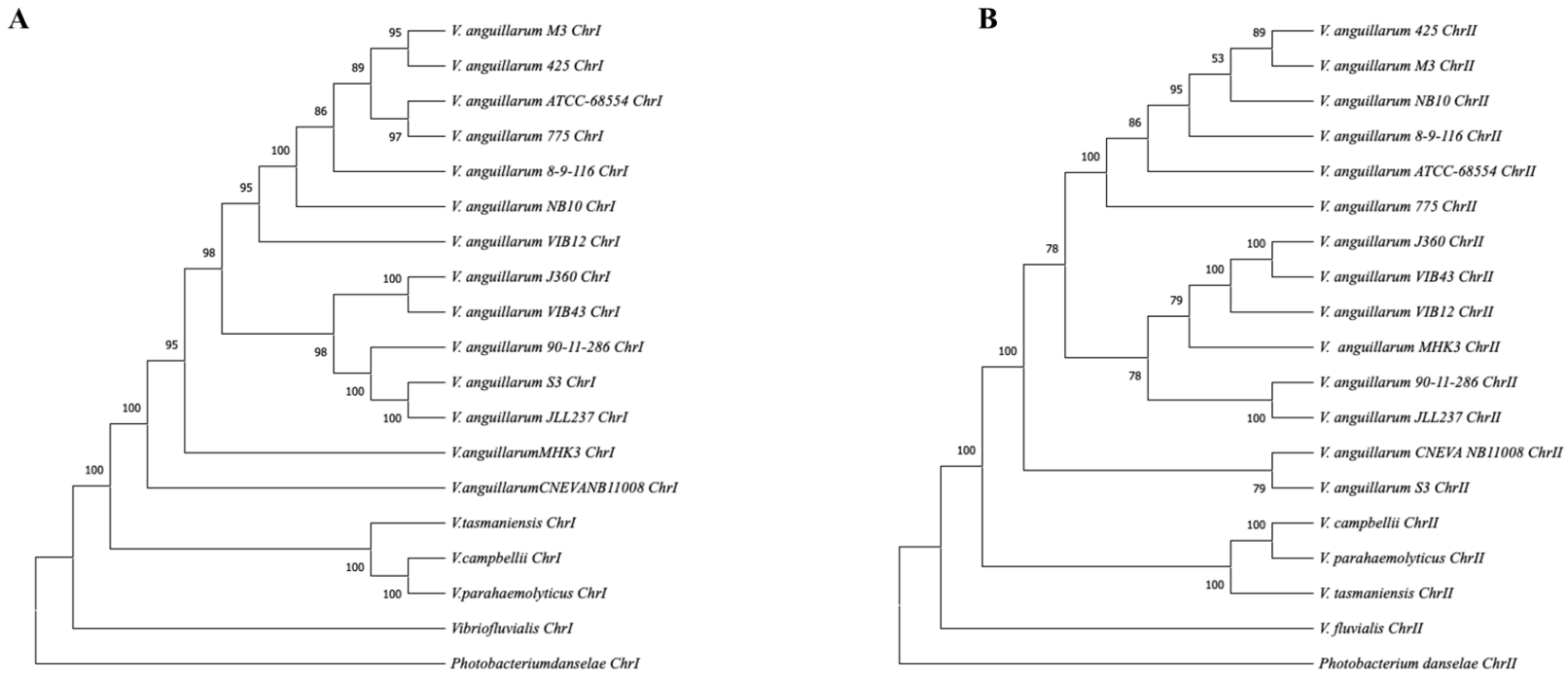

A. *V. anguillarum* chromosome-I evolutionary relationships; **B.** *V. anguillarum* chromosome-I evolutionary relationships. Evolutionary history was calculated using Neighbor-Joining method with a bootstrap consensus tree (500 replicates). Evolutionary distances were computed using the Jukes-Cantor method. and are in the units of the number of base substitutions per site. Ambiguous positions were removed for each sequence pair (pairwise deletion option). There was a total of 1,322,945 positions in the final dataset for chromosome-I and 310,515 positions in the final dataset of chromosome-II. Evolutionary analyses were conducted in MEGA X.

Appendix VI. Average nucleotide identity (ANI) comparison of *V. anguillarum* whole genome alignment.

A

		1	2	3	4	5	6	7	8	9	10	11	12	13	14	15	16	17	18	19
V. anguillarum J360_ChrI	1	100.00	83.09	0.00	83.73	83.97	83.77	98.55	98.54	98.53	98.50	98.52	98.49	98.49	98.50	98.60	99.95	98.52	98.71	98.50
Photobacterium danselae_ChrI	2	3.27	100.00	0.00	83.17	83.56	83.68	83.12	83.15	83.10	83.03	82.99	83.06	83.12	83.06	83.21	83.09	83.01	83.13	82.98
Vibrio fluvialis_ChrI	3	0.13	0.03	100.00	0.00	0.00	0.00	0.00	0.00	0.00	0.00	0.00	0.00	0.00	0.00	0.00	0.00	0.00	0.00	0.00
V. tasmaniensis__ChrI	4	6.77	4.41	0.38	100.00	84.05	83.88	83.64	83.74	83.58	83.66	83.72	83.73	83.61	83.73	83.70	83.73	83.73	83.69	83.74
V. campbellii_ChrI	5	7.67	4.91	0.43	17.37	100.00	85.80	83.97	83.89	84.08	83.91	83.90	83.92	83.99	83.93	84.06	83.97	83.93	84.11	83.94
V. parahaemolyticus_ChrI	6	8.44	4.89	0.42	15.19	50.56	100.00	83.78	83.90	83.84	83.69	83.70	83.69	83.87	83.72	83.77	83.77	83.71	83.77	83.72
V. anguillarum MHK3_ChrI	7	83.68	3.46	0.90	7.39	7.87	8.95	100.00	98.67	98.63	98.66	98.65	98.64	98.57	98.62	98.77	98.48	98.64	98.68	98.66
V. anguillarum S3_ChrI	8	82.61	3.37	0.19	7.15	7.85	8.61	89.41	100.00	98.68	98.53	98.55	98.57	98.90	98.56	98.65	98.48	98.55	98.65	98.55
V. anguillarum 90-11-286_ChrI	9	83.56	3.40	0.13	7.30	7.70	8.62	87.38	89.00	100.00	98.68	98.69	98.68	99.17	98.68	98.55	98.52	98.69	98.68	98.67
V. anguillarum M3_ChrI	10	81.40	3.45	0.15	7.04	7.60	8.78	86.85	87.29	85.93	100.00	99.84	99.89	98.55	99.88	98.67	98.46	99.91	98.65	99.84
V. anguillarum ATCC-68554_ChrI	11	81.95	3.53	0.25	7.05	7.73	8.89	87.36	88.02	86.53	98.24	100.00	99.94	98.59	99.94	98.74	98.50	99.92	98.69	99.93
V. anguillarum NB10_ChrI	12	81.75	3.49	0.25	6.99	7.59	8.81	87.12	87.79	86.37	96.11	96.66	100.00	98.63	99.95	98.78	98.52	99.94	98.70	99.94
V. anguillarum JLL237_ChrI	13	82.51	3.32	0.13	7.20	7.54	8.39	86.96	89.61	90.47	86.42	86.94	86.31	100.00	98.64	98.56	98.49	98.64	98.60	98.59
V. anguillarum 8-9-116_ChrI	14	82.00	3.48	0.25	6.98	7.65	8.82	87.42	88.02	86.55	96.01	96.78	98.82	86.46	100.00	98.78	98.53	99.94	98.71	99.93
V. anguillarum CNEVA NB11008_ChrI	15	82.02	3.44	0.29	7.08	7.49	8.66	88.07	85.40	85.07	85.61	85.92	85.43	84.32	85.62	100.00	98.54	98.72	98.70	98.67
V. anguillarum VIB43_ChrI	16	94.24	3.30	0.13	6.84	7.73	8.53	84.65	83.95	84.02	82.32	82.71	82.38	83.21	82.73	82.99	100.00	98.56	98.67	98.53
V. anguillarum 425_ChrI	17	81.45	3.46	0.25	6.95	7.60	8.76	86.94	87.54	86.05	94.56	95.28	97.22	85.96	97.56	85.24	82.11	100.00	98.69	99.91
V. anguillarum VIB12_ChrI	18	79.72	3.26	0.14	6.80	7.19	8.37	81.50	81.30	80.10	80.77	81.14	80.46	80.84	80.62	80.41	80.89	80.26	100.00	98.69
V. anguillarum 775_ChrI	19	82.06	3.54	0.25	7.03	7.66	8.86	87.38	87.90	86.51	98.59	99.12	96.48	86.65	96.35	86.36	82.70	95.09	81.51	100.00

B

		1	2	3	4	5	6	7	8	9	10	11	12	13	14	15	16	17	18	19
NZ_CP034673	1	100.00	0.00	0.00	0.00	0.00	0.00	98.49	98.58	98.36	98.37	98.38	98.44	98.39	98.43	98.38	99.93	98.40	98.48	98.44
Photobacterium danselae_ChrII	2	0.12	100.00	0.00	0.00	0.00	0.00	0.00	0.00	0.00	0.00	0.00	0.00	0.00	0.00	0.00	0.00	0.00	0.00	0.00
Vibrio fluvialis_ChrII	3	0.17	0.00	100.00	0.00	0.00	0.00	0.00	0.00	0.00	0.00	0.00	0.00	0.00	0.00	0.00	0.00	0.00	0.00	0.00
V. tasmaniensis_ChrII	4	0.20	0.02	0.00	100.00	83.96	84.02	0.00	0.00	0.00	0.00	0.00	0.00	0.00	0.00	0.00	0.00	0.00	0.00	0.00
V. campbellii_ChrII	5	0.33	0.36	0.16	3.68	100.00	83.96	0.00	0.00	0.00	0.00	0.00	0.00	0.00	0.00	0.00	0.00	0.00	0.00	0.00
V. parahaemolyticus_ChrII	6	0.71	0.21	0.33	2.77	21.02	100.00	0.00	0.00	0.00	0.00	0.00	0.00	0.00	0.00	0.00	0.00	0.00	0.00	0.00
V. anguillarum MHK3_ChrII	7	73.07	0.00	0.16	0.18	0.53	0.76	100.00	98.29	98.27	98.33	98.33	98.38	98.29	98.37	98.50	98.44	98.36	98.39	98.39
V. anguillarum S3_ChrII	8	71.71	0.00	0.13	0.30	0.54	0.71	73.37	100.00	99.06	98.39	98.45	98.45	99.09	98.44	98.45	98.61	98.42	98.43	98.46
V. anguillarum 90-11-286_ChrII	9	71.84	0.00	0.18	0.26	0.59	0.63	70.68	78.25	100.00	98.35	98.37	98.35	99.93	98.35	98.44	98.38	98.36	98.30	98.41
V. anguillarum M3_ChrII	10	75.76	0.00	0.15	0.27	0.66	0.89	82.09	77.88	75.76	100.00	99.76	99.76	98.34	99.82	98.42	98.34	99.81	98.41	99.78
V. anguillarum ATCC-68554_ChrII	11	72.43	0.00	0.15	0.19	0.65	0.87	78.43	74.55	72.65	94.32	100.00	99.85	98.35	99.86	98.44	98.36	99.86	98.39	99.85
V. anguillarum NB10_ChrII	12	68.84	0.00	0.13	0.24	0.60	0.80	74.84	70.64	68.79	89.13	87.75	100.00	98.39	99.87	98.47	98.40	99.84	98.46	99.82
V. anguillarum JLL237_ChrII	13	75.42	0.00	0.19	0.28	0.69	0.68	74.73	79.22	89.31	78.45	74.97	71.41	100.00	98.37	98.39	98.39	98.36	98.31	98.39
V. anguillarum 8-9-116_ChrII	14	67.93	0.00	0.15	0.24	0.58	0.80	73.91	69.82	68.10	87.01	86.27	96.03	70.91	100.00	98.48	98.40	99.86	98.45	99.82
V. anguillarum CNEVA NB11008_ChrII	15	76.23	0.06	0.18	0.27	0.66	0.78	79.65	77.40	74.92	82.11	77.95	74.88	78.80	74.21	100.00	98.45	98.45	98.49	98.49
V. anguillarum VIB43_ChrII	16	90.41	0.04	0.17	0.20	0.38	0.73	72.86	72.12	72.61	76.35	72.68	69.54	75.76	68.87	76.55	100.00	98.40	98.50	98.43
V. anguillarum 425_ChrII	17	68.01	0.00	0.14	0.25	0.60	0.73	73.95	69.97	68.03	86.50	85.60	89.64	70.80	89.22	73.90	68.75	100.00	98.37	99.79
V. anguillarum VIB12_ChrII	18	71.29	0.00	0.16	0.24	0.48	0.63	70.33	69.83	70.28	74.63	71.38	67.72	73.51	67.25	74.38	72.38	67.49	100.00	98.46
V. anguillarum 775_ChrII	19	75.78	0.00	0.15	0.27	0.66	0.89	82.10	77.91	75.78	98.76	93.95	89.28	78.75	87.31	81.98	76.47	86.97	75.68	100.00

A. *V. anguillarum* chromosome-I; **B.** *V. anguillarum* chromosome-II. Identity percentage parameters for annotated genes were set up as minimum similarity of 0.8 and minimum length 0.8. Analyses were conducted in CLC Genomic Workbench v20 (CLC Bio). ANIs tables indicate that *V. anguillarum* J360 and *V. anguillarum* VIB43 possess about 99.95% of identity within chromosome-I and 99.93% within chromosome -II.

Appendix VII. Phylogenetic analysis of *V. anguillarum* using Multi-Locus Sequence Analysis (MLSA).

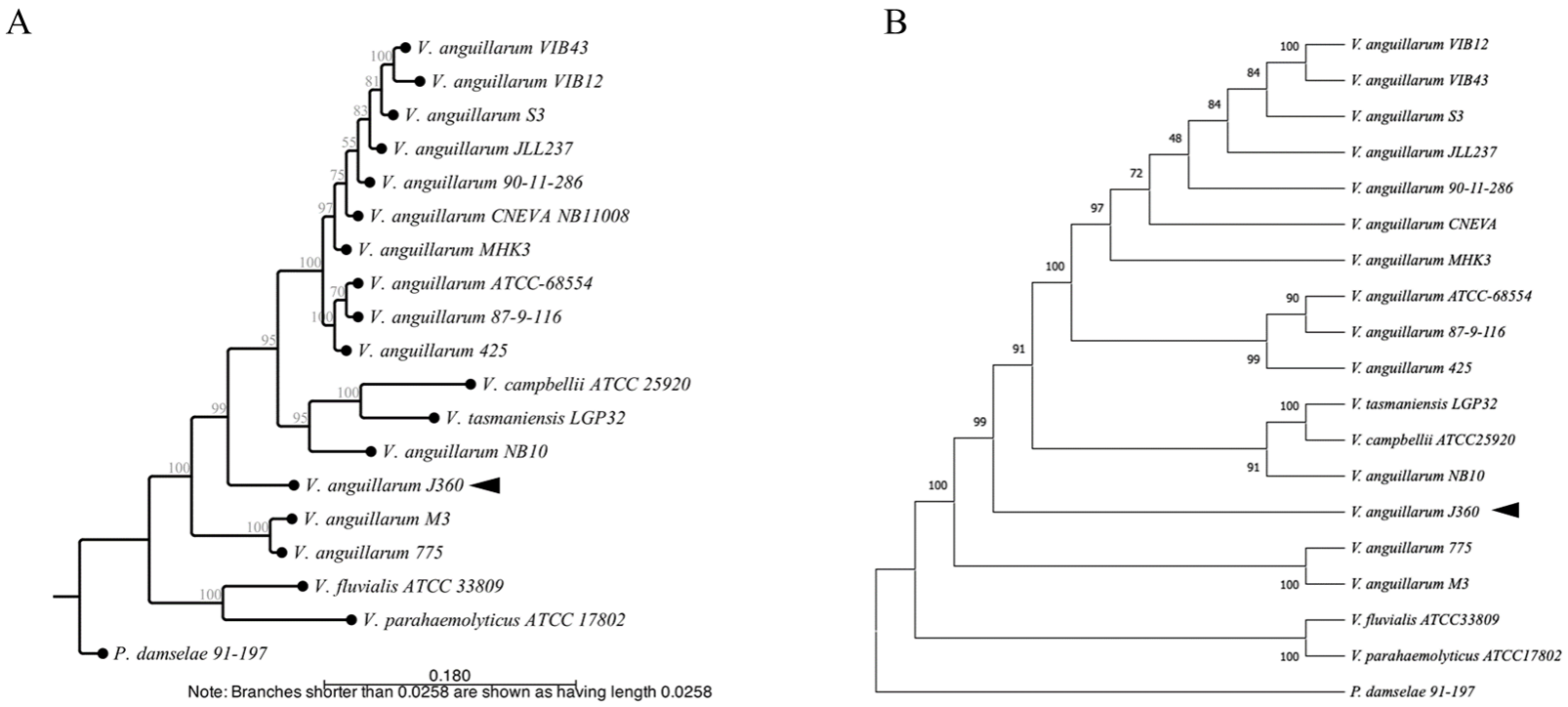

A. Phylogenetic analysis conducted in CLC Workbench v20 (CLC Bio). **B.** Phylogenetic analysis conducted in MEGAX. The evolutionary distance was calculated using the Neighbor-Joining method with a bootstrap consensus from 500 replicates. Evolutionary distance was computed using Jukes-Cantor method. All ambiguous positions were removed for each sequence pair (pairwise deletion option). The analysis involved 9 loci (16S rRNA, *fstZ*, *gapA*, *gyrB*, *mreB*, *pyrH*, *recA*, *rpoA*, *topA*) from the complete genomes of 18 *Vibrio* species and *Ph. damselae* 91-197 as an outgroup.

Appendix VIII. Comparative whole genome alignment between *V. anguillarum* J360 and *V. anguillarum* VIB43.

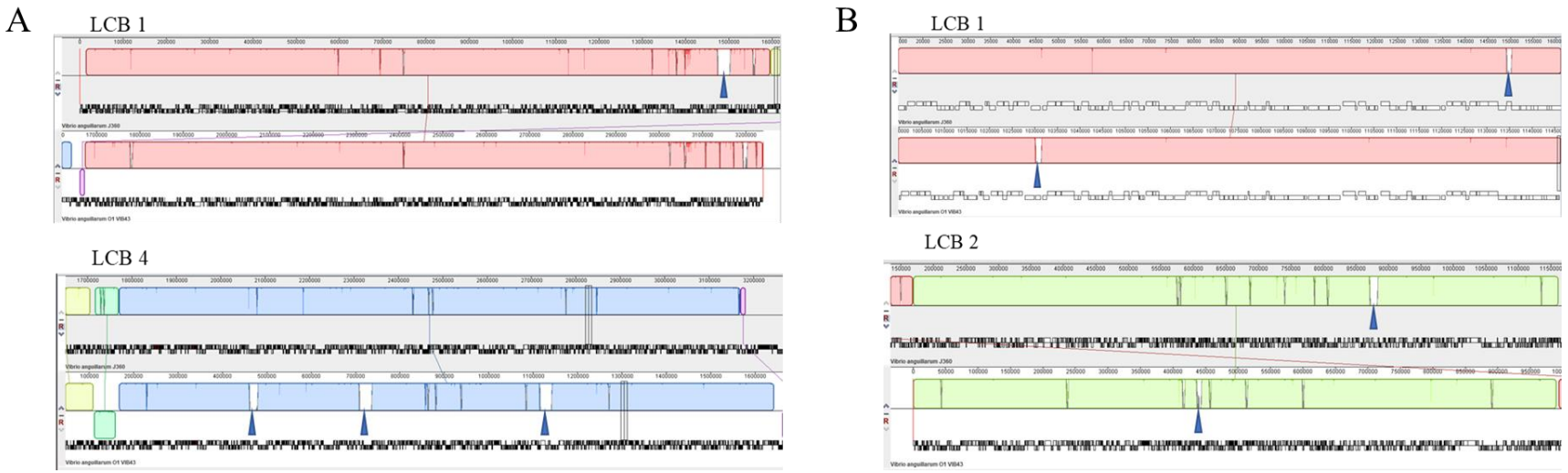

A. LCBs-1 and -3 of chromosome-I. **B.** LCBs-1 and -2 of chromosome-II. Solid arrows represent genome gaps (GGs).

Appendix IX. Comparative analysis of *V. anguillarum* J360 large plasmid pVaJ360-I.

A

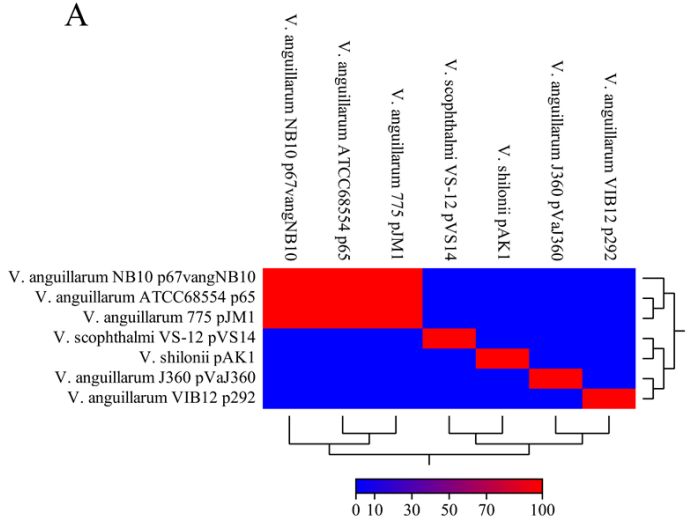

B

	1	2	3	4	5	6	7
V. scophthalmi VS-12 pVS14	1	100.00	0.00	0.00	0.00	0.00	0.00	0.00
V. shilonii pAK1	2	0.00	100.00	0.00	0.00	0.00	0.00	0.00
V. anguillarum J360 pVaJ360	3	0.00	0.00	100.00	0.00	0.00	0.00	0.00
V. anguillarum ATCC68554 p65	4	0.00	0.00	0.00	100.00	0.00	100.00	100.00
V. anguillarum VIB12 p292	5	0.00	0.00	0.00	0.00	100.00	0.00	0.00
V. anguillarum NB10 p67vangNB10	6	0.00	0.00	0.00	93.94	0.00	100.00	99.99
V. anguillarum 775 pJM1	7	0.00	0.00	0.00	64.65	0.00	64.36	100.00

A. Heat map visualization of aligned sequences identity for large plasmid pVaJ360-I. **B.** Average nucleotide identity (ANI) comparison of pVaJ360-I. Identity percentage parameters for annotated genes were set up as minimum similarity of 0.8 and minimum length 0.8. Analyses were conducted in CLC Genomic Workbench v20 (CLC Bio). Analysis involved 5 *V. anguillarum* large plasmids: pJM1 (AY312585), p67 (LK021128), p65 (CP023210), p15 (CP023056) and pVaJ360-I. Analysis was conducted using CLC Workbench v20 (CLC Bio). ANI table and heat map indicate that large plasmid pVaJ360 do not possess percentage of identity within pJM1 or pJM1-like virulent plasmids.

Appendix X. *V. anguillarum* VIB43 genomic islands (GIs).

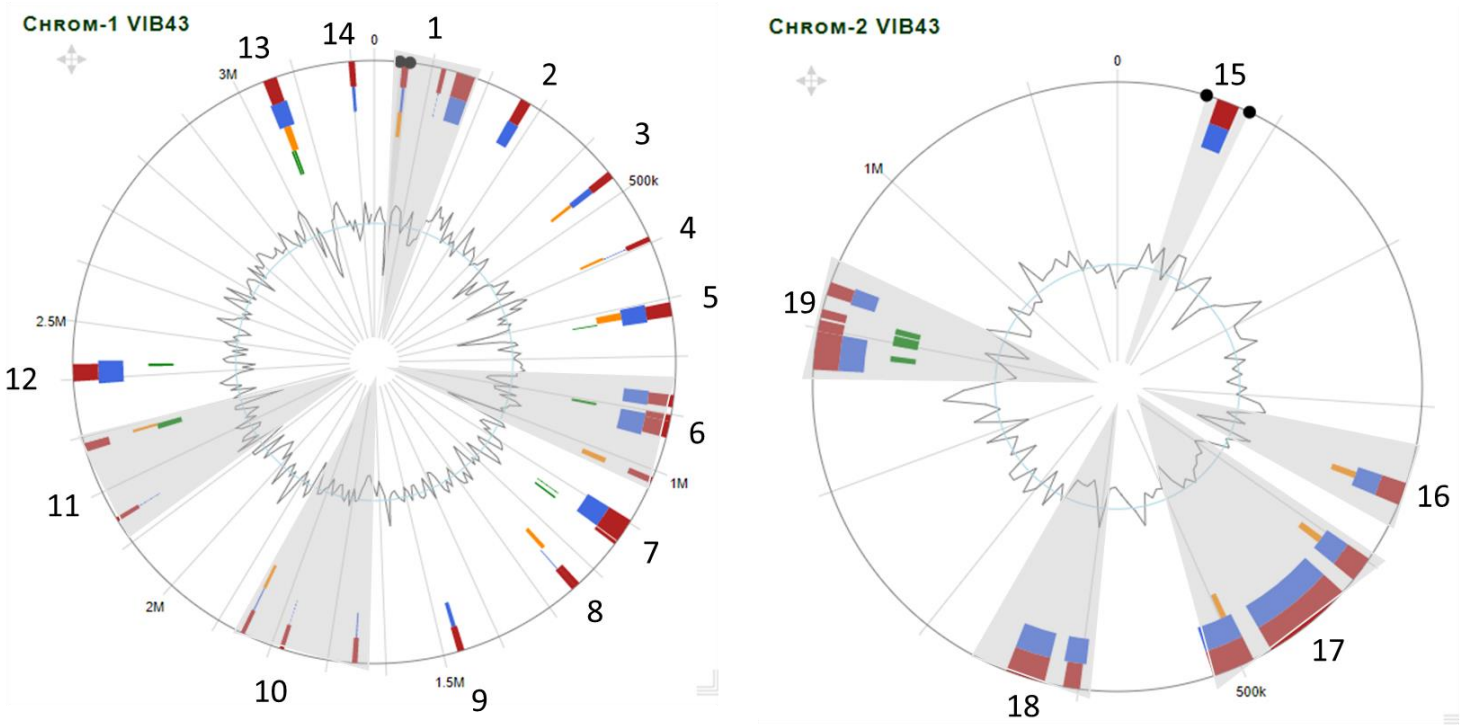

Genomic islands (GIs) detected in chromosome-I and in chromosome-II. Red bars represent GIs detected using 3 different packages; blue bars represent the GIs detected with the SIGI-HMM package; orange bars represent the GIs detected with the IslandPath-DIMOB package; green bars represent the GIs detected with the IslandPick package.

Appendix XI. Flow cytometry based bacterial cell-counting.

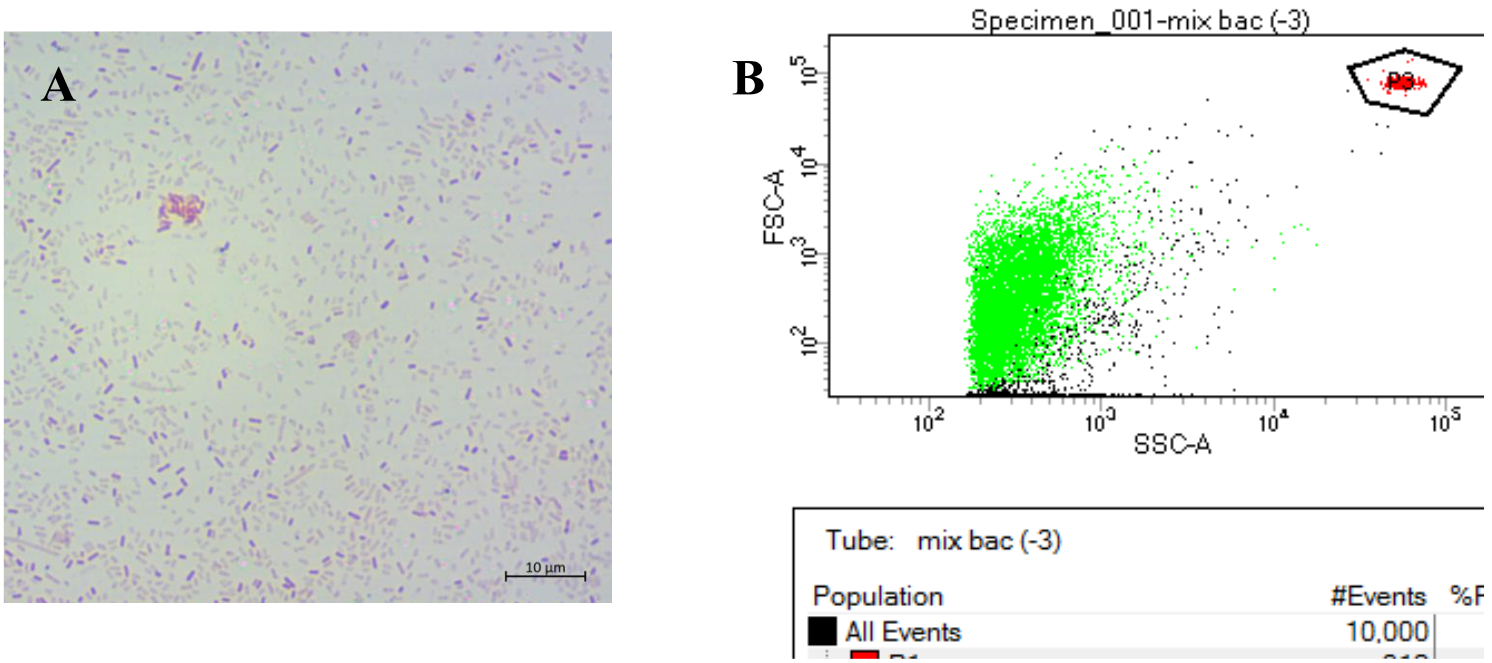

A. Characterization of *A. salmonicida* bacterin by Gram staining. **B.** Flow cytometry enumeration of *A. salmonicida* bacterin mix using Bacterial Cell-counting Kit. Plot shows Forward Scattering (FSC) vs Green Fluorescence units (FITC). ***P1***: red signal for microsphere particles frame; ***P2***: green signal represents formalin-killed *A. salmonicida* stained with SYTO BC bacterial stain.

Appendix XII. *A. salmonicida* LD_{50} experimental design

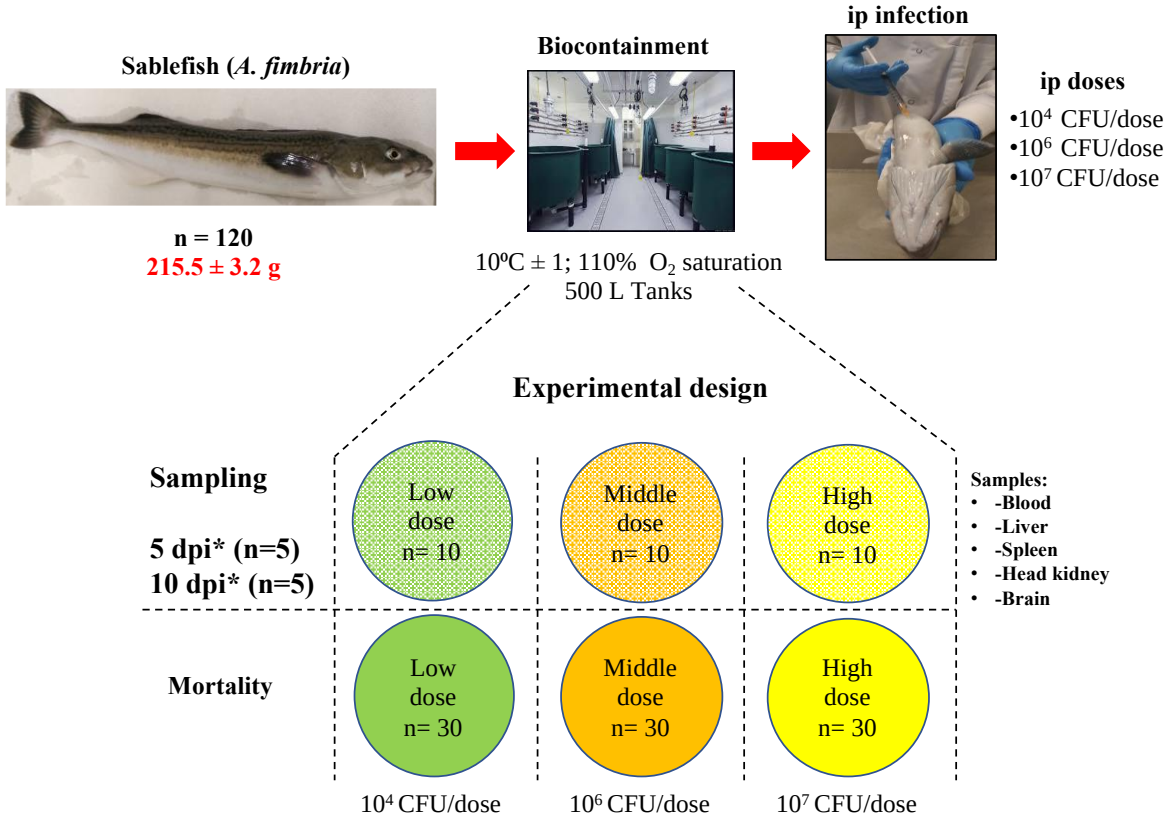

One hundred and twenty sablefish with an average weight of ~215.5 ± 3.2 g were used to calculate the lethal dose 50 (LD_{50}). Additionally, three tanks with 10 fish each were used for sampling blood, liver, spleen, head kidney and brain at 5 and 10- days post-infection. Six fish were utilized to obtain pre-infection samples. *dpi: days post-infection.

Appendix XIII. *A. fimbria* immunization common garden experimental design

Immunization and non-lethal blood sample

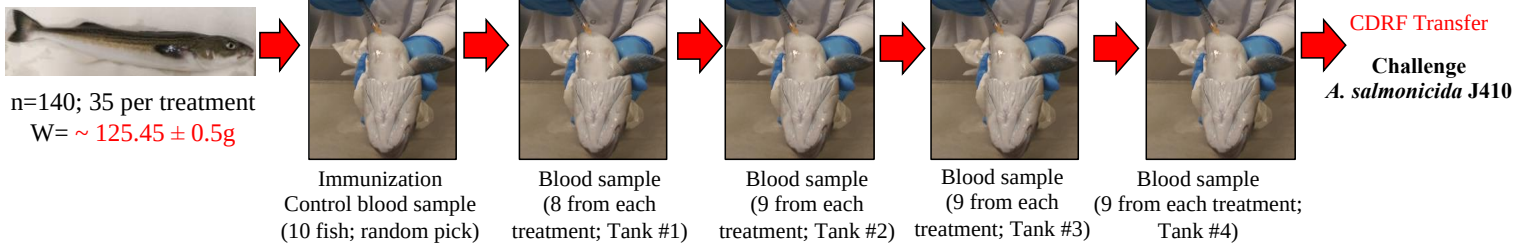

500 l tanks; 10ºC ± 1
110 % O_2 saturation

Single immunization

A. Forte Vaccine = 35 fish
B. AlphaJect Vaccine = 35 fish
C. Bacterin Mix = 35 fish
D. PBS control = 35

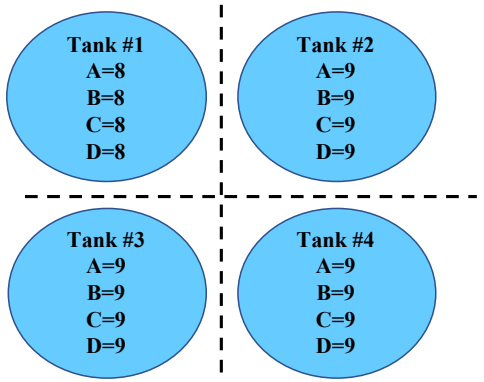

One hundred and forty sablefish with an average weight of ~125.5 ± 0.5 g were injected with 100 µl of each vaccine (bacterin mix; Alpha Ject Micro 4®, PharmaQ; Forte Micro 4®, Elanco), and PBS as a control. Four tanks were set up, Tank #1 with 32 fish (8 fish per treatment) and Tanks #2,3 and 4 with 35 fish each (9 fish per treatment). Blood samples were taken pre-immunization time, and every 2 weeks after immunization.